Master's Thesis

System-Level Seismic Risk Assessment of Bridge Transportation Networks

Hye-Young Tak

Department of Urban and Environmental Engineering
(Disaster Management Engineering)

Graduate School of UNIST

2019

System-Level Seismic Risk Assessment of Bridge Transportation Networks

Hye-Young Tak

Department of Urban and Environmental Engineering

(Disaster Management Engineering)

Graduate School of UNIST

System-Level Seismic Risk Assessment of Bridge

Transportation Networks

A thesis submitted to the Graduate School of UNIST
in partial fulfillment of the requirements for the degree of
Master of Science

Hye-Young Tak

07. 09. 2019

Approved by

_____

Advisor

Young Joo Lee

System-Level Seismic Risk Assessment of Bridge Transportation Networks

Hye-Young Tak

This certifies that the thesis of Hye-Young Tak is approved.

07/09/2019

_____

Advisor: Young Joo Lee

Department of Urban and Environmental Engineering

Ulsan National Institute of Science and Technology (UNIST)

_____

Thesis Committee Member: Sung-Han Sim

Department of Urban and Environmental Engineering

Ulsan National Institute of Science and Technology (UNIST)

_____

Thesis Committee Member: Byungmin Kim

Department of Urban and Environmental Engineering

Ulsan National Institute of Science and Technology (UNIST)

ABSTRACT

Seismic risk assessment has recently emerged as an important issue for infrastructure systems because of their vulnerability to seismic hazards. Earthquakes can have significant impacts on transportation networks such as bridge collapse and the resulting disconnections in a network. One of the main concerns is the accurate estimation of the seismic risk caused by the physical damage of bridges and the reduced performance of the associated transportation network. This requires estimating the performance of a bridge transportation network at the system level. Moreover, it is necessary to deal with various possible earthquake scenarios and the associated damage states of component bridges considering the uncertainty of earthquake locations and magnitudes.

To perform the seismic risk assessment of a bridge transportation network, system reliability is required. It is a challenging task for several reasons. First, the seismic risk itself contains a great deal of uncertainty, which comprises location, magnitude, and the resulting intensity of possible earthquakes in a target network. Second, the system performance of a bridge transportation network after the seismic event needs to be estimated accurately, especially for realistic and complex networks. Third, the seismic risk assessment employing system reliability may increase the computational costs and can be time-consuming tasks, because it requires dealing with various possible earthquake scenarios and the resulting seismic fragility of component bridges. Fourth, a precise performance measure of the system needs to be introduced.

In this study, a new method is proposed to assess the system-level seismic risk of bridge transportation networks considering earthquake uncertainty. In addition, a new performance measure is developed to help risk-informed decision-making regarding seismic hazard mitigation and disaster management. For the tasks, first of all, a matrix-based system reliability framework is developed, which performs the estimation of a bridge transportation network subjected to earthquakes. Probabilistic seismic hazard analysis (PSHA) is introduced to enable the seismic fragility estimation of the component bridges, considering the uncertainty of earthquake locations and magnitudes. This is systemically used to carry out a post-hazard bridge network flow analysis by employing the matrix-based framework. Secondly, two different network performance measures are used to quantify the network performance after a seismic event. Maximum flow capacity was originally used for a bridge transportation network, however the numerical example using this measure is further developed for applications to more accurate system performance analysis using total system travel time (TSTT). Finally, a new method for system-level seismic risk assessment is proposed to carry out a bridge network flow analysis based on TSTT by employing the matrix-based system reliability (MSR) method. In the proposed method, the artificial neuron network (ANN) is introduced to approximate the network performance, which can reduce the computational cost of network analysis.

The proposed method can provide statistical moments of the network performance and component importance measures, which can be used by decision-makers to reduce the seismic risk of a target area. The proposed method is tested by application to a numerical example of an actual transportation network in South Korea. In the seismic risk assessment of the example, PSHA is successfully integrated with the matrix-based framework to perform system reliability analysis in a computationally efficient manner.

Keywords: seismic risk, bridge transportation network, system reliability, probabilistic seismic hazard analysis, artificial neural network

TABLE OF CONTENTS

List of Figures

List of Tables

1. Introduction

Natural disasters have serious impacts on infrastructure systems, including transportation, electricity, gas and water distribution networks, etc., causing structural damage and massive economic losses in both commercial and residential activities. Because these systems are structurally complicated, interdependent and interconnected, the damage to any component infrastructure will cascade into another resulting in widespread failure or disruption of human activities. In particular, earthquakes are one of the natural disasters that can cause significant physical damage and disconnection of transportation networks. Damage to transportation system is a major concern, as it imposes an extra burden on other lifelines (Applied Technology Council 2004, Nicholson and Dalziell 2003). One of the most significant impacts of earthquakes is the disconnection of bridge transportation networks, which can impede post-hazard emergency responses, such as the movement of emergency vehicles. This is because bridges are one of the most critical components of transportation networks, acting as "bottlenecks": the structural failure of a bridge can interfere with traffic flow and decrease network performance (Furtado 2015). Hence, it is essential to assess the seismic risk of a bridge transportation system and accurately predict the post-hazard performance.

The objective of seismic risk assessment is to obtain useful information for risk-informed decision-making regarding seismic hazard mitigation and disaster management. Seismic risk assessment of critical infrastructure systems has been conducted extensively. Nuti et al. (2010) proposed a methodology for the reliability assessment of electric power, water and road systems, not considering the interdependence between the networks, whereas Poljnašek et al. (2012) proposed a method for gas and electricity transmission networks considering the increased vulnerability due to interdependency. Dueñas-Osorio et al. (2007) evaluated seismic responses considering the interdependency of the water and power networks in Shelby County, Tennessee 56 area, and proposed a method to apply mitigation action efficiently. With regard to transportation networks, Kiremidjian et al. (2007) evaluated the risk posed by earthquakes to a transportation system in terms of direct loss caused by damage to bridges in the San Francisco Bay area. Moreover, various studies have proposed post-earthquake flow models for evaluating the impact of seismic events and the functionality of the networks (Chang et al. 2010, Eisenberg et al. 2017)

Most infrastructure systems are composed of a number of components, and their reliability is predicted by overall system states or the probability that the system does not fail. Therefore, to perform the seismic risk assessment of a bridge transportation network, system reliability analysis is required to predict the post-hazard flow capacity of the network after a seismic event. However, predicting both the disconnection probabilities in the network and the uncertain traffic flow capacity are challenging tasks due to the following reasons. First, the seismic risk itself contains a great deal of uncertainty, namely, location, magnitude, and the resulting intensity of possible earthquakes in target networks. Second, conceptualizing and quantifying system performance measures in uncertain events is not easy, because

their determination depends on various specifications of the system under different situations. An appropriate performance measure can quantify the ability of the network more accurately, especially for realistic and complex bridge transportation networks. While numerous performance measures have been proposed for such quantification, these definitions are sometimes inconsistent and few attempts to review all literature (Faturechi and Miller-Hooks 2014). Third, quantifying these uncertainties and accurately estimating the performance of system reliability may increase computational costs and can be time-consuming tasks to deal with in possible earthquake scenarios and the resulting seismic fragility of the component bridges.

The characterization of uncertainty, accuracy, and efficiency motivated the research reported in this thesis, which focuses on proposing a new method of system-level seismic risk assessment. First, to assess the seismic hazard, the uncertainty of earthquake locations and magnitudes is analyzed probabilistically, which is also referred to as probabilistic seismic hazard analysis (PSHA) (Kramer 1996). Cornell (1968) firstly introduced the concept of PSHA, and McGuire (2004, 2007) summarized the early development of PSHA and provided probabilistic estimation of losses from earthquakes along with information on practical estimation of the input parameters. PSHA aims to quantify the uncertainties and produce a desired description of them as explicit probability distributions (Baker 2008). This mathematical analysis helps to quantify the uncertainties in an earthquake event.

Post-hazard network performance analysis is also important because the analysis results are necessary to make effective plans for emergency evacuations, rescue, and recovery. Performance measure typically have target value which defines the acceptable conditions for a network. For example, Murray-Tuite (2006) proposed quantitative measures for transportation system adaptability, mobility, and recovery based on simulation method for computation. Faturechi and Miller-Hooks (2014) provided a comprehensive framework for conceptualizing, categorizing and quantifying system performance measures, especially numerical-transportation-related example. Moreover, The Analysis Procedures Manual (Oregon department of transportation 2018), or APM, provides the current methodologies, and procedures for conducting analysis of transportation plans and projects. In this manual, transportation analysis performance measure, as also referred to as measures of effectiveness (MOEs), are quantitative estimates on the performance of a transportation network. In traffic engineering, there are commonly used performance measures such as volume to capacity ratio, level of service, vehicle delay, travel time, and capacity.

To deal with the uncertainties associated with earthquakes and infrastructure response, a few sampling-based approaches was often used (Ellingwood and Kinali 2009). However, this may increase the computational costs and can be time-consuming tasks to deal with in possible component failure scenarios. To overcome these challenges, a few non-sampling-based approaches have been developed. Li and He (2002) proposed a recursive decomposition algorithm for seismic reliability evaluation to compute the probabilities of disconnections in a network, while Kang et al. (2008) and Kang and Song

(2008) proposed a new non-sampling-based system reliability analysis method, namely the matrix-based system reliability (MSR) method. The matrix-based framework of the MSR method enables rapid calculation of multiple probability scenarios and separation of network and vulnerability analyses. Employing the MSR method, Lee et al. (2011) estimated the post-hazard flow capacity of a bridge transportation network considering ten seismically vulnerable bridge. The MSR method was successfully applied for evaluating the system reliability within a network. Lastly, this thesis further develops original numerical example such that it can account for network performance capacity more accurately according to change in maximum flow capacity into total system travel time (TSTT). Since the evaluation of TSTT requires function to calculate this measure and thousands of network states as input data, a different approach based on a *surrogate model* or *meta-model* is used. Numerous engineering problems have benefited from such models, particularly when difficulties are found in the construction or application of a mathematical model, and likewise when considering optimization procedures (Pina et al. 2013). Surrogate models can be constructed to provide approximate results through function using only some of the input data, thus not requiring detailed knowledge of the dynamic parameters of the system (Pina et al 2008 and Ford et al. 2011). The ANN is one of the widely used as surrogate model and advantages of learning algorithms to approximate discrete or continuous target values. The merit of this model is useful to several applications such as classification, clustering, pattern recognition, function approximation, optimization, signal processing, and robotics (Widrow et al. 1993). For example, among many approaches and attempts available for surrogate model, the ANN has been successfully applied in many fields (Basheer and Hajmeer 2000, Ben-Nakhi and Mahmoud 2004, Sung 1998, Pina et al. 2013, and Melo et al. 2014).

This thesis is organized into two steps. In the first step, a new framework for seismic risk assessment is proposed by employing PSHA with the MSR method, which consists of three small steps as follows: 1) seismic fragility estimation of the bridges based on PSHA; 2) system-level performance estimation using the matrix-based framework of the MSR method; and 3) seismic risk assessment based on the total probability theorem. PSHA enables the seismic fragility estimation of the components considering the uncertainty of earthquake events. Moreover, MSR method helps to conduct efficient calculations for seismic risk assessment and system reliability. In the second step, the proposed framework is further developed for more accurate assessment of network performance by introducing an advanced performance measure of bridge transportation networks and ANN-based surrogated model. In the further developed method, the matrix-based seismic risk assessment using ANN model enables the system performance estimation with only partial real data. The method in both steps is systemically used to carry out a post-hazard bridge network flow analysis employing the matrix-based framework.

The proposed method offers insights into seismic risk assessment and system reliability and provides statistical moments of the network performance, critical earthquake scenarios and component importance measures, which can be useful for decision-makers to reduce the seismic risk of a target

area. In summary, the seismic risk assessment employing PSHA are successfully integrated with the matrix-based framework to perform system reliability analysis in a computationally efficient manner.

2. Theoretical Background

2.1. Probabilistic seismic hazard analysis (PSHA)

The main concern of seismic hazard analysis is to ensure that structural damage is assigned a desired level of performance and intensity. However, the estimation of ground motion intensity corresponding to hazards is a challenging task due to the uncertainty in seismic hazards and structural damage, as well as the complex nature of the network performance in the area. PSHA aims to consider the uncertainties with respect to the size, location, and resulting intensity of the earthquake, and combine them to produce the description of a possible earthquake event that may occur in an area of interest. In PSHA, a seismic hazard is defined as a physical phenomenon, such as ground shaking or failure caused by an earthquake, which can have serious effects on human activities (Kramer 1996).

The main goal of seismic hazard analysis is to refine the understanding of earthquake magnitudes and the corresponding intensity of ground shaking. Particularly, PSHA allows a better insight into earthquake generation and seismic effects on a region by quantifying the uncertainties and estimating the distribution of earthquake occurrences (Sánchez-Silva et al. 2005). The resulting intensity is calculated by the ground motion prediction model (GMPE), also referred to as the *seismic attenuation model*. This prediction model is generally developed using statistical regression on the observation from various data of observed and cumulated ground motion intensities. For the precise estimation of the risk caused by a seismic event in a particular area, the seismic hazard should be analyzed probabilistically, by considering uncertainties in earthquake locations and magnitudes. The approach presented in this thesis is based on the concepts as exemplified in the study of Baker (2008). PSHA comprises five steps as follows:

1. Identification of all earthquake sources through means of observation of past locations and geological evidence
2. Quantification of the distribution of earthquake magnitudes (the rates at which earthquakes of various magnitudes are expected to occur)
3. Characterization of the source-to-site distances corresponding to possible earthquake events
4. Calculation of the resulting intensity using ground motion prediction model as a function of earthquake magnitude, distance, etc.
5. Combination of uncertainties in earthquake magnitude, location, and ground motion intensity, using the total probability theorem.

In the proposed method, the uncertainties of earthquake locations and magnitudes are determined using PSHA based on past earthquake records. The locations in cities with the most severe damage were assumed to be the epicenters of past earthquakes in related studies (Lee et al. 1976, Usami 1979, Poirier and Taher, 1980, and Lee and Yang, 2006). Rather than considering all earthquake sources capable of producing damages to the structure, for the sake of simplicity, this thesis focuses uniquely on the

epicenters of past earthquakes at sites of interest for the seismic risk assessment. Meanwhile, to account for the uncertainty in earthquake magnitudes, a series of modeling procedures is required. In this study, one such modeling procedure is briefly introduced, whereas more details on PSHA are provided in Baker (2008).

2.1.1. Earthquake magnitude uncertainty modeling

To account for the uncertainty in earthquake magnitudes, as the first step, the occurrence rate of earthquakes in a target region is assumed to follow the Gutenberg-Richter (G-R) recurrence law (Gutenberg and Richter 1944) given by

$$\log \lambda_m = a - bm \tag{1}$$

where m is the specific earthquake magnitude of interest, λ_m is the occurrence rate of earthquakes with magnitudes greater than m, and a and b are the constants which are referred to as G-R recurrence parameters and can be determined from past earthquake records. When the minimum and maximum magnitudes are determined using Equation (1), the cumulative distribution function (CDF) of the earthquake magnitude can be derived as (Baker 2008)

$$F_M(m) = P(M \leq m | m_{min} \leq M \leq m_{max}) = \frac{1 - 10^{-b(m-m_{min})}}{1 - 10^{-b(m_{max}-m_{min})}} \tag{2}$$

where $F(\cdot)$ denotes the CDF of a random variable, M is the earthquake magnitude, and m_{min} and m_{max} are the minimum and maximum of the earthquake magnitude, respectively. By differentiating Equation (2), the probability density function (PDF) can be obtained as

$$f_M(m) = \frac{b\ln(10)10^{-b(m-m_{min})}}{1 - 10^{-b(m_{max}-m_{min})}} \tag{3}$$

where $f(\cdot)$ denotes the PDF of a random variable. This bounded PDF is termed the *bounded Gutenberg-Richter recurrence law* (Baker 2008), and it can be obtained based on the frequency of past earthquakes with varying magnitudes.

Once the bounded PDF is obtained, to generate possible earthquake scenarios with varying magnitudes as an input of seismic risk assessment, the continuous distribution of earthquake magnitudes needs to be converted into a discrete set of magnitudes of interest. The probabilities of occurrence, according to this discrete set of magnitudes, represent only a partial distribution of the magnitude at a site. Subsequently, a normalizing process that divides all of the cumulated values by their sum is required so that the sum of the probability distribution in the partial magnitudes amounts to 1.0.

2.1.2. Seismic attenuation model

After modeling the probability distribution of earthquake magnitudes, the associated distances from the earthquake source to the bridges (i.e., source-to-site distances) of the target transportation network and

the ground motion intensities need to be analyzed. Given the earthquake magnitude and location, the ground motion intensities at different bridges must be analyzed based on a seismic attenuation model. One such representative model is the ground motion prediction equation (GMPE). In this equation, the ground motion intensity is expressed as a function of several parameters including earthquake magnitude, distance, and local site effects (Joyner and Boore 1993). For seismic event i recorded at the site j, the general form of GMPE considering the total variability of the ground motion is given as Emolo et al. (2015)

$$Y_{ij} = \overline{Y_{ij}(M_i, R_{ij}, \xi_{ij})} + \eta_i + \varepsilon_{ij} \qquad (4)$$

where Y_{ij} represents the response variable, such as peak ground acceleration (PGA), peak ground velocity (PGV), and spectral acceleration (SA), which often corresponds to the logarithm (natural or common), M_i is the earthquake magnitude of the event, R_{ij} is the distance between the epicenter of event i and the site j, ξ_{ij} is the geomorphic factor affecting the ground motion, $\overline{Y_{ij}(M_i, R_{ij}, \xi_{ij})}$ is the mean of the response variable, and η_i and ε_{ij} are the inter- and intra-event parameters representing the uncertainty of the ground motion. The parameter η_i represents the uncertainty of the ground motion inherent to the earthquake itself, termed the *Earthquake-to-Earthquake* variability, whereas the parameter ε_{ij} denotes the uncertainty of the ground motion because of the energy paths and geological characteristics, termed the *Site-to-Site* variability (Emolo et al. 2015).

In this study, as in HAZUS-MH (FEMA 2003), the structural vulnerabilities of a bridge are described by the probability conditioned to the ground motion intensity which is expressed in terms of SA. In addition, the GMPE proposed by Emolo et al. (2015) is introduced. The GMPE was derived using statistics of 222 earthquakes recorded at 132 stations in South Korea, employing the nonlinear mixed effects regression analysis. Moreover, the equation includes both fixed and random effects accounting for inter- and intra-event residual values. Using this equation, the mean of the response variable in Equation (4) can be given as

$$\overline{Y_{ij}(M_i, R_{ij}, \xi_{ij})} = \ln (SA_{ij})$$
$$= c_1 + c_2 M_i + c_3 \ln\left[\sqrt{R_{ij}^2 + h^2}\right] + c_4 R_{ij} + c_5 s \qquad (5)$$

where SA_{ij} is the spectral acceleration caused by an earthquake event i at site j, h is the focal depth, c_k ($k = 1,\ldots,5$) are the regression coefficients, and s is the station dummy variable, which assumes a value of -1, 0, or 1. The dummy variable depends on the sign of the mean residual (negative, zero, or positive, respectively), and it is generally chosen by the seismological observatory.

In addition, the inter- and intra-events parameters in Equation (4) can be expressed by the following equations (Goda and Hong 2008, Goda and Arkinson 2009, Sokolov et al., 2010):

$$\eta_i = \frac{\sigma_\eta^2}{\sigma_\eta^2 + \sigma_\varepsilon^2}, \qquad \varepsilon_{ij} = \frac{\sigma_\varepsilon^2}{\sigma_\eta^2 + \sigma_\varepsilon^2}\rho(\Delta_{ij}) \tag{6}$$

where $\sigma_\eta{}^2$ and $\sigma_\varepsilon{}^2$ are the inter- and intra-standard residuals, respectively, Δ_{ij} is the distance between the epicenter of event i and the site j, and $\rho(\Delta_{ij})$ is the spatial correlation equation. For the special correlation equation, in this study, the following equation suggested by Goda and Hong (2008) is introduced:

$$\rho(\Delta_{ij}) = e^{(-0.509\sqrt{\Delta_{ij}})} \tag{7}$$

As described above, PSHA enables the consideration of earthquake uncertainty. For the given location and magnitude of an earthquake, the ground shaking intensity of individual bridges is expressed in terms of SA using the GMPE in Equation (4). Then, the probabilities of several damage states of bridges can be provided by fragility curves. Subsequently, it becomes possible to estimate the performance of the bridge transportation network, which requires system reliability analysis.

2.2. Matrix-based system reliability (MSR) method

The MSR method was recently proposed and successfully applied to evaluate the post-earthquake performance of a bridge transportation network in terms of the disconnection probability (Kang et al. 2008) and maximum flow capacity (Lee et al. 2011). The MSR method conducts a matrix-based framework of system reliability analysis in which two tasks of "system event description" and "probability calculation" are performed separately. This enables efficient evaluations of the post-hazard capacity under possible component scenarios of the system without repeatedly performing deterministic flow capacity analyses.

In this study, a bridge transportation network is considered, consisting of n_b bridges, each of which has n_d distinct damage states. Under the assumption that component bridges are statistically independent, there is a total of $(n_d)^{n_b}$ damage scenarios, which are mutually exclusive and collectively exhaustive (MECE) events. Due to their mutual exclusiveness, the probability of the system event E_{sys}, i.e., $P(E_{sys})$ is the sum of the probabilities that belong to the system event. Therefore, $P(E_{sys})$ can be easily computed by the inner product of the two vectors, namely the probability and event vectors (Kang et al. 2008 and Lee et al. 2011)

Let $P_{i(j)}$, $i = 1, \ldots, n_b, j = 1, \ldots, n_d$, indicate the probability that the ith bridge enters the jth damage state. Then, the probability of dealing with multiple damage states can be expressed by the following sequential matrix calculations,

$$\mathbf{p} = \begin{bmatrix} P_{(1,1,\ldots,1)} \\ P_{(2,1,\ldots,1)} \\ \vdots \\ P_{(d_1,d_2,\ldots d_{n_b})} \\ \vdots \\ P_{(n_d,n_d,\ldots n_d)} \end{bmatrix} = \begin{bmatrix} P_{1,(1)} \times P_{2,(1)} \times \ldots \times P_{n_b,(1)} \\ P_{1,(2)} \times P_{2,(1)} \times \ldots \times P_{n_b,(1)} \\ \vdots \\ P_{1,(d_1)} \times P_{2,(d_2)} \times \ldots \times P_{n_b,(d_{n_b})} \\ \vdots \\ P_{1,(n_d)} \times P_{2,(n_d)} \times \ldots \times P_{n_b,(n_d)} \end{bmatrix} \tag{8}$$

where $\mathbf{p}$ denotes the probability vector for all possible damage scenario of the system, d_i is the damage state of the ith bridge (where $i = 1, \ldots, n_b$), and $P(\ldots)$ denotes the probability of a damage state system with the numbers in the subscript. The subscript signifies the component damage states. For example the second row, $P_{(2,1,\ldots,1)}$ depicts that all of the components are in the first damage state, except for the first component, which is in the second damage state.

To carry out a post-hazard flow analysis employing the MSR method, a certain corresponding quantity can be estimated using the matrix-based framework. Therefore, a new column vector $\mathbf{q}$, termed the "quantity vector", is constructed, which has same size as $\mathbf{p}$ in Equation (8). For all damage states of the system, the quantities are generalized to

$$\mathbf{q} = \begin{bmatrix} Q_{(1,1,\ldots,1)} \\ Q_{(2,1,\ldots,1)} \\ \vdots \\ Q_{(d_1, d_2, \ldots d_{n_b})} \\ \vdots \\ Q_{(n_d, n_d, \ldots n_d)} \end{bmatrix} = \begin{bmatrix} f(q_{1,(1)}, q_{2(1)}, \ldots, q_{n_b,(1)}) \\ f(q_{1,(2)}, q_{2,(1)}, \ldots, q_{n_b,(1)}) \\ \vdots \\ f\left(q_{1,(d_1)}, q_{2,(d_2)}, \ldots, q_{n_b,(d_{n_b})}\right) \\ \vdots \\ f(q_{1,(n_d)}, q_{2,(n_d)}, \ldots, q_{n_b,(n_d)}) \end{bmatrix} \tag{9}$$

where $\mathbf{q}$ denotes the quantity vector, $Q(\ldots)$ denotes the performance quantity of the system with damage states as the subscript, and $f(\cdot)$ is the post-earthquake capacity of the network. In this study, the maximum flow capacity, i.e., the maximum number of vehicles that can pass per unit time, is considered as a measure of the network flow capacity (Ahuja et al 1993 and Nojima 1998). For each maximum flow capacity corresponding to the damage states of the network, the MATLAB® version of Boost Graph Library (Boost 2008 and Gleich 2008) is employed.

As results of the probability vector $\mathbf{p}$ in Equation (8) and the quantity vector $\mathbf{q}$ in Equation (9), the statistical parameters such as the mean, variance, and coefficient of variation (c.o.v.) can be obtained as follows:

$$\mu_Q = \mathbf{q}^{\mathbf{T}}\mathbf{p}$$
$$\sigma^2_Q = \mathbf{p}^T(\mathbf{q}.*\mathbf{q}) - \mu_Q^2 \tag{10}$$
$$\delta_Q = \sigma_Q / |\mu_Q|$$

where μ_Q, σ^2_Q and δ_Q are the mean, variance, and c.o.v. of the network flow capacity Q, respectively. In Equation (10), '.*' denotes the element-by-element multiplication.

Furthermore, an importance measure (IM) of components can also be evaluated using a matrix-based formulation. For regional authorities who need to make decisions regarding the allocation of budgets and other resources, it is important to identify the important locations of a transportation network (Park et al. 2015). To evaluate the relative importance of these components, several IMs have been developed in system engineering. In this study, the reduction factor (RF) proposed by Lee et al. (2011) is adopted as a new IM. RF computes the reduction of the expected mean flow capacity by the observed event E_{obs}, e.g., the failure of a bridge, which can quantify the relative importance of

component bridges. The computation of the proposed RF is as follows:

$$RF = 1 - \mu_{Q|E_{obs}}\ /\mu_Q\ = 1 - (\mathbf{q^T\tilde{p}})/(\mathbf{q^Tp}) \qquad (11)$$

where $\mu_{Q|Eobs}$ represents the conditional mean of the flow capacity given an observed event, E_{obs}, and

$\mathbf{\tilde{p}}$ is the probability vector constructed using the conditional probabilities of components given by E_{obs}.

2.3. Artificial neural network (ANN)

The artificial neural network (ANN) has been developed extensively during the past three decades. An ANN is a branch of artificial intelligence techniques, and it represents a computing model whose layered structure is similar to the networked structure of neurons in the human brain with layers of inter-connected nodes.

The ANN is defined by the neurons, topological structure, and learning rules. Analogous to the neurons in the human brain, an artificial neuron consists of inputs, weights, processing units, and outputs (Haykin 1994). A typical ANN is composed three of more layers: one input layer, one output layers, and one or two hidden layers. The input layer consists of a data set, which represents the problem of interest, and the output layer indicates a related response or function result regarding each problem. This approach has the ability to learn from data, and it can be trained to recognize patterns, classify data, and forecast future events. The goal of learning is to achieve a set of weights that will produce an output most resembling the target (Jensen et al. 1999). Therefore, it is important for input layers to match each input to the output.

For the best configuration of the ANN, *training* processes are carried out, to enable the trained network to provide a good approximation of the desired response. During the training process, the constructed ANN iteratively minimizes the mean square error of the data set, adjusting a set of known input-output pairs until the output error falls below an acceptable value.

2.3.1. Artificial neuron and activation function

The neuron is the cell responsible for reception of external inputs, processing of signals, and transmission. Figure 1 shows a simplified artificial model of a neuron, also referred to as the McCulloch-Pitts neuron (Widrow et al. 1994)

Figure 1. Simplified artificial model of a neuron

Each neuron receives a designated number of inputs x_i (where $i = 1, …, N$) and calculates a linear combination of these inputs using weights w_i to produce the w*eighted input z*, that can be expressed by

$$z = \sum_{i=1}^{N} w_i x_i \tag{12}$$

Next, it produces an output y through an activation function $f(z)$, which serves for increasing monotonic behavior over a range of values for z, assuming a constant value outside this range (Pina et al. 2013). Several configurations of adjusting z values were tested, and the continuous log *sigmoid function*, illustrated in Figure 2, is widely used in ANN applications. As the sigmoid function is bounded between 0 and 1, the input data needs to be normalized within the same range. This is because the normalization or scaling process aids in the appropriate preparation for the training data set. This function is expressed by the following equation:

$$y = f(z) = \frac{1}{1 + e^{-z}} \tag{13}$$

Figure 2. Typical sigmoid function

2.3.2. Layers and methods for determining number of hidden neurons

Neural networks consist of several neurons in layers, which can be simply illustrated as in Figure 3. The structure of the network comprises one or more layers between the input and output layers. If the neurons are arranged into layers, then all neurons in the same layer send or receive signals through the specified learning process. In further detail, the input layer receives data, which represents the problem of interest from the user. The output layer represents the targeted response or desired performance of an unknown function. This layer sends the data to the user. The intermediate layer is also referred to as the *hidden layer* that can contain zero or more layers. Figure 3(b) illustrates two-layer networks that are widely used in most ANN applications, with only one hidden layer.

Figure 3. Topology of typical layered neural networks: (a) single layer neural network and (b) multilayer neural network

Here, the determination of the number of neurons in the hidden layer, N_h, is one of the major difficulties in the process of creating the ANNs topology. If N_h is too small, then the network may not be strong enough to fulfill desired requirements. In contrast, too large N_h may cause long training steps and recalling time (Tijanana et al. 2016). In this study, five different methods were applied to choose the number of hidden neurons, as shown in Table 1. N_i and N_o depict the number of input neurons and the number of output neurons, respectively.

Method 1	Li, Chow and Yu, 1995
Equation	$N_h = \dfrac{\sqrt{1 + 8N_i} - 1}{2}$
Method 2	Rules of Thumb by Heaton, 2005
Equation	$(N_i + N_o) \cdot \dfrac{2}{3}$
Method 3	Shibata and Ikeda, 2009
Equation	$N_h = \sqrt{N_i \cdot N_o}$
Method 4	Hunter, Yu, Pukisi Ⅲ, Kolbusz and Wilamowski, 2012
Equation	$N_h = \log_2(N_i + 1) - N_o$

Method 5	Sheela and Deepa, 2013
Equation	$N_h = \dfrac{(4N_i{}^2 + 3)}{N_i{}^2 - 8}$

Table 1. Methods for determining number of hidden neurons

Finally, the network output y_j of the jth hidden neuron can be expressed by combining Equations (12) and (13):

$$y_j = \frac{1}{1 + \exp(-\sum_{i=1}^{N} w_{ij} x_i)} \qquad (14)$$

where w_{ij} is the weight of the input x_i for the jth neuron. The network output y_o can be derived when the optimal N_h are determined through comparison of those methods, similarly to Equation (14):

$$y_o = \sum_{j=1}^{N_h} w_{jo} \frac{1}{1 + \exp(-\sum_{i=1}^{N} w_{ij} x_i)} \qquad (15)$$

where w_{jo} denotes the weight of the contribution of the jth hidden neuron to the network output.

3. Proposed Method

3.1 Matrix-based seismic risk assessment employing PSHA

The objective of a seismic risk assessment is to obtain useful information for risk-informed decision-making regarding seismic hazard mitigation. Seismic risk assessment of critical infrastructure has been conducted extensively, addressing water distribution, electric power, and transportation networks. Various studies have proposed the direct loss of components from the networks based on sampling-based approaches. However, dealing with possible component failure scenarios may a time-consuming task. To overcome this problem, a few non-sampling-based system reliability analysis methods have been developed. The MSR method is one of the approaches proposed by Kang et al. (2008) and Kang and Song (2008).

Most previous studies conducted seismic risk assessments without probabilistic seismic hazard analysis (PSHA). At a fundamental level of seismic risk assessments, there is a consensus regarding a great degree of uncertainty regarding the location, magnitude, and resulting intensity of possible earthquakes, such that a mathematical approach for considering uncertainty in the form of PSHA is necessary. PSHA has the merit of considering earthquake uncertainty, as it is useful for determining the uncertainty of earthquake locations and magnitudes in a target region (Baker 2008). However, employing PSHA in seismic risk assessment is not easy, as it requires dealing with a large number of possible earthquake scenarios and quantifying the performance of a bridge transportation network. This

section proposes a new method that is a matrix-based system-level seismic risk assessment for bridge transportation networks employing PSHA. The MSR method is successfully applied to perform system-level seismic risk assessment. It enables rapid calculation of multiple probability scenarios corresponding to the number of potential earthquake sources.

The main goal of the proposed method is to estimate the performance of a bridge transportation network after a seismic event, considering earthquake uncertainty. For this purpose, PSHA is employed to deal with the uncertainty of earthquake magnitudes and locations in the proposed method. The proposed method introduces the matrix-based framework of the MSR method to evaluate the uncertainty of the performance of a bridge transportation network at the system level, due to uncertain earthquakes.

The MSR method was originally developed to perform system reliability analyses of various structures (Kang et al. 2008, 2012). However, its matrix-based framework provides efficient calculation for the system reliability analysis of lifelines, and it was successfully applied to evaluate the system-level performance of bridge transportation networks (Lee et al. 2011 and Kang et al. 2017). Lee et al. (2011) derived the post-hazard flow capacity considering the structural deterioration of bridges within a network. In previous research, the time-dependent bridge fragilities could be computed efficiently using the MSR method, while the corresponding flow capacities were evaluated using a maximum flow capacity analysis algorithm. The matrix-based framework allowed the separate probability calculation and network flow analysis, which enabled performing extensive parametric studies and time-varying post-hazard flow analyses without repeated network flow analyses. Similarly, in this research, the matrix-based framework of the MSR method is introduced to deal with the earthquake uncertainty.

As mentioned above, by assuming that all components are statistically independent, basic MECE events can be simply computed by use of the matrix calculation proposed in Equation (8). However, many reliability problems of network systems are composed of various components that are statistically inter-dependent. Nevertheless, applying the concept of a *common source random variable* (CSRV), a system event can be described by the combination of component MECE events, which are conditionally independent.

In the proposed method, the earthquake magnitude and various locations are introduced as CSRVs that influence the damage states of individual bridges within the network. When the uncertainty of earthquake magnitudes and locations is characterized by PSHA and defined as CSRVs, applying the total probability theorem, the probability of a system can be expressed as

$$P(E_{sys}) = \iint P(E_{sys}|m,l) f_{M,L}(m,l) \, dm \, dl \qquad (16)$$

where E_{sys} is the system event of interest, M is the earthquake magnitude, L is the earthquake location, and $f_{M,L}(m,l)$ is the joint PDF of the earthquake magnitude and location when $M = m$ and $L = l$. With the conditional PDF, the joint PDF in Equation (16) can be changed to

$$f_{M,L}(m,l) = f_{M|L}(m|l)f_L(l) \tag{17}$$

where $f_L(l)$ is the marginal PDF of the earthquake location and $f_{M|L}(m|l)$ is the marginal PDF of the earthquake magnitude conditioned to $L = l$.

Since the damage states of individual bridges become conditionally statistically independent given the earthquake magnitude and location, the conditional probability vector $\mathbf{p}|(m,l)$ can be constructed using Equations (8), (16), and (17):

$$\mathbf{p}|(m,l) = \begin{bmatrix} P_{(1,1,\ldots,1)}|(m,l) \\ P_{(2,1,\ldots,1)}|(m,l) \\ \vdots \\ P_{(d_1,d_2,\ldots d_{n_b})}|(m,l) \\ \vdots \\ P_{(n_d,n_d,\ldots n_d)}|(m,l) \end{bmatrix}$$

$$= \begin{bmatrix} \left(P_{1,(1)}|(m,l)\right) \times \left(P_{2,(1)}|(m,l)\right) \times \ldots \times \left(P_{n_b,(1)}|(m,l)\right) \\ \left(P_{1,(2)}|(m,l)\right) \times \left(P_{2,(1)}|(m,l)\right) \times \ldots \times \left(P_{n_b,(1)}|(m,l)\right) \\ \vdots \\ \left(P_{1,(d_1)}|(m,l)\right) \times \left(P_{2,(d_2)}|(m,l)\right) \times \ldots \times \left(P_{n_b,(d_{n_b})}|(m,l)\right) \\ \vdots \\ \left(P_{1,(n_d)}|(m,l)\right) \times \left(P_{2,(n_d)}|(m,l)\right) \times \ldots \times \left(P_{n_b,(n_d)}|(m,l)\right) \end{bmatrix} \tag{18}$$

where $P_{(\ldots)}|(m,l)$ represents the conditional probability of a component's damage state with the numbers in the subscript. Unlike the probability vector, the quantity vector $\mathbf{q}$ can remain the same as in Equation (9), because the matrix-based framework of the MSR method enables the separate construction of the probability and quantity vectors.

Hence, applying the total probability theorem, the statistical parameters can be obtained as

$$\mu_Q = \iint \mu_Q(m,l) f_{M,L}(m,l)\,dmdl = \iint \mathbf{q}^{\mathbf{T}}(\mathbf{p}|(m,l))\,dmdl$$

$$\sigma_Q{}^2 = \iint \left(\mathbf{p}|(m,l)\right)^{\mathbf{T}}(\mathbf{q}.* \mathbf{q})\,dmdl - \mu_Q{}^2 \tag{19}$$

$$\delta_Q = \sigma_Q / |\mu_Q|$$

Similarly, the reduction factor RF can be calculated as

$$\mathrm{RF} = \iint \{1 - (\mathbf{q}^{\mathbf{T}}\widetilde{\mathbf{p}}|(m,l))/(\mathbf{q}^{\mathbf{T}}\mathbf{p}|(m,l))\}\,dmdl \tag{20}$$

where $\widetilde{\mathbf{p}}|(m,l)$ is the conditional probability vector which can be constructed using Equation (11).

The proposed method consists of three steps: 1) seismic fragility estimation of the bridges based on PSHA, 2) system-level performance estimation using the matrix-based framework of the MSR method, and 3) seismic risk assessment based on the total probability theorem. In the proposed method, PSHA enables the seismic fragility estimation of the component bridges considering the uncertainty of earthquake locations and magnitudes, and it is systemically used to carry out a post-earthquake bridge

network flow analysis employing the MSR method.

The MSR method provides an efficient framework for seismic risk assessment, which performs separate calculations for the seismic hazard and network flow analyses. PSHA contains the investigation of earthquake generation using several proposed relations provided in Equations (1)–(7), with the aim to obtain the probabilities of structural damage scenarios considering bridge fragilities, given the earthquake magnitude and location. When the corresponding network flow capacities are identified, and the probability vector and quantity vector are constructed, the MSR method enables the calculation of various risk-informed measures and statistical use of the total probability theorem. Figure 4 shows a flow chart of the seismic risk assessment proposed in this research.

Figure 4. Flow chart of proposed seismic risk assessment employing PSHA and MSR method

To initiate the analysis employing the proposed method, it is first necessary to collect input data in the form of information related to the study area. The input data can be classified into three groups: exposure data, hazard data, and structural vulnerability data. The exposure data contains the topology information of the target transportation network, such as the number of nodes and links in the target region. Past earthquake data are likewise necessary to identify the earthquake uncertainty using PSHA. The hazard data contain the mean occurrence rate of earthquakes with varying magnitudes and the seismic attenuation law (i.e., GMPE) with the spatial correlations described in Equations (4)–(7). Lastly, the structural vulnerability data include the determination of damage states in individual bridges. For this task, the fragility curve parameters provided in HAZUS-MH (FEMA 2003) are adopted in this study.

The next step is to perform seismic risk assessment employing PSHA and the matrix-based framework of the MSR method. First, using past earthquake data, earthquake sources are analyzed using the G-R relation law. The purpose of PSHA is to identify uncertainties related to the earthquake itself and calculate the resulting intensity of the ground motion. Therefore, final results comprise the PDF of earthquake magnitude and the probability of the different damage states of the component bridges. After performing the seismic hazard analysis, the proposed approach predicts the post-hazard flow capacity of a transportation network for given magnitudes and locations of earthquake. In this process, the quantity vector $\mathbf{q}$ is constructed for all possible combinations of bridge damage states using the maximum flow capacity analysis. Next, the conditional probability vector $\mathbf{p}|(m,l)$ in Equation (18) is constructed based on the probabilities of bridge damage states.

Lastly, the conditional probability vector construction is repeated for various earthquake scenarios with different earthquake magnitudes (M) and locations (L). Subsequently, the performance of the transportation network can be estimated in terms of the statistical moments of the maximum flow capacity using Equation (19). Moreover, the importance measure of RF can be estimated for all component bridges using Equation (20). Only the tasks marked by the dotted boxes in Figure 4 need to be repeated, whereas the computationally expensive maximum flow capacity analysis does not.

3.2. Numerical example

The proposed method is tested by applying it to an actual transportation network around Pohang city, South Korea. The study area is located in the southeast of the Korean Peninsula, which experienced a 5.4-magnitude earthquake in 2017 (Kang et al. 2019). Although South Korea is known to have relatively low seismic risk, this earthquake and its aftershocks raised lasting concerns, which this study aims to help address.

Figure 5 illustrates the topology of the target network, consisting of 37 nodes (red solid circles) and 46 links (blue lines). It is a network of expressways and national routes in and around Pohang city and includes ten (i.e., $n_b = 10$) relatively long bridges (illustrated in black) in the area. In this example, the objective is to measure the network capability to accommodate an emergency evacuation. Nodes 3 and 30 represent an evacuation area and a downtown area, respectively. Table 2 depicts the locations (i.e., connecting nodes) of the ten bridges, and Table 3 shows their structural information. Table 4 lists the maximum flow capacities of the links (given as the number of passing vehicles per hour). These assumptions enable the performance assessment of this network in terms of the maximum flow capacity using a node-to-node flow analysis.

Figure 5. Network map of the Pohang bridge transportation network

Bridge no.	Connecting nodes
1	(14,16)
2	(19,20)
3	(25,26)
4	(20,21)
5	(29,30)
6	(33,36)
7	(15,23)
8	(28,29)
9	(4,7)
10	(10,12)

Table 2. Locations of the bridges

Bridge no.	Total length (m)	Width (m)	Maximum span length (m)	Type	Year of construction	Design
1	169.7	20.5	25.7	PSCI	1992	Conventional
2	345	7.5	60	Steel box	2006	Seismic
3	455	28	35	PSCI	2009	Seismic
4	300	21	40	PSCI	2011	Seismic
5	25	8	12.5	RC slab	1990	Conventional
6	140	20	50	Steel box	2012	Seismic
7	102	9.5	14.6	RC slab	1992	Conventional
8	125.2	24	26	Steel plate	1975	Conventional
9	480	12.1	60	Steel box	2004	Seismic
10	115	8.3	45	Steel box	2004	Seismic

Table 3. Structural information on the bridges

Flow capacity (number of vehicles per hour)	Link numbers
2200	(2,5), (4,5), (5,6), (6,11), (10,11), (11,14), (14,15), (15,23), (22,23), (23,25), (22,28), (28,29), (29,30), (30,32)
4400	(1,2), (2,3), (2,4), (4,7), (7,10), (13,14), (14,16), (16,17), (17,18), (17,21), (18,19), (19,20), (19,24), (20,21), (21,22), (24,25), (25,26), (26,27), (27,35), (29,31), (31,32), (31,33), (32,34), (33,34), (33,36), (35,36), (35,37)
6520	(8,9), (9,10), (10,12), (12,18), (27,37)

Table 4. Maximum flow capacity of links in the Pohang transportation network

To account for the uncertainty in the seismic damage states of bridges, seismic fragility curves are introduced. Seismic fragility is defined as the conditional probability that the demand of a structure exceeds a specified threshold for a given earthquake intensity (Lee and Moon 2014, Moon et al. 2018, Nguyen and Lee 2018), and seismic fragility curves are often used for setting retrofit and repair priorities of bridges after an unexpected and disastrous event (Lee et al. 2007). In this study, SA, which can be calculated by the GMPE provided in Equation (4), is introduced as the earthquake intensity. In

addition, seismic fragility curves are obtained from HAZUS-MH (FEMA 2003), where bridges are classified by several factors including their length, type, and seismic design methods, and the corresponding seismic fragility curves are provided. Similarly, the seismic fragility curves of the ten bridges considered are determined based on the structural information presented in Table 3.

In this example, five damage states of slight, moderate, extensive, and complete damage are assumed (i.e., $n_d = 5$). The maximum flow capacities of a bridge are assumed to be related to its damage state, as described in Table 4. In the table, 100%, 75%, 50%, 25%, and 0% of original flow capacities represent the remaining traffic capacity of the five damage states. For each combination of bridge damage states in the probability vector, in the MSR method, these flow capacity values are assigned to the corresponding bridges during the maximum flow capacity analysis, so that the quantity vector can be constructed.

Damage states	Description	Flow capacities
No	–	100%
Slight	Any column experiencing minor cracking	75%
Moderate	Any column experiencing moderate cracking	50%
Extensive	Any column degrading without collapse	25%
Complete	Any column collapsing and connection	0%

Table 5. Damage states and associated flow capacities

To identify earthquake uncertainty in the target region, past earthquake data (with magnitude, M_L, greater than or equal to 3.0) was collected from the Korea Meteorological Association (KMA) website (KMA 2019), in the period from January 1st, 1918 to August 22nd, 2018. In total, twenty earthquake records were collected. Table 6 presents the earthquake information, and Figure 6 shows the locations of the twenty earthquakes (named EQ1, EQ2, …, EQ20) and ten bridges (named Bridge 1, Bridge 2, …, Bridge 10). In this example, it is assumed that all past earthquake epicenters have the same likelihood of a repeated earthquake occurrence, and the distances between the epicenters and the bridge locations are calculated based on their location information.

No.	Date	Origin time	Latitude	Longitude	Depth (km)	M_L
1	14 Apr. 1981	11:47	35.90	130.10	7	4.8
2	27 Aug. 1981	21:35	35.80	129.80	7	3.5
3	10 Dec. 1985	21:42	35.80	129.70	7	3.2
4	17 Mar. 1986	11:52	35.90	129.50	7	3.2
5	6 Oct. 1987	7:04	35.90	129.90	7	3.1

6	6 Oct. 1987	23:36	36.20	130.10	7	3.5
7	22 Oct. 1990	18:09	35.90	130.00	7	3.4
8	24 Apr. 1999	1:35	36.00	129.30	7	3.2
9	9 Jul. 2002	4:01	35.90	129.60	7	3.8
10	28 Mar. 2011	13:50	35.97	129.95	7	3.2
11	15 Apr. 2017	11:31	36.11	129.36	7	3.1
12	15 Nov. 2017	14:29	36.11	129.37	7	5.4
13	15 Nov. 2017	14:32	36.10	129.36	8	3.6
14	15 Nov. 2017	15:09	36.09	129.34	8	3.5
15	15 Nov. 2017	16:49	36.12	129.36	10	4.3
16	16 Nov. 2017	9:02	36.12	129.37	8	3.6
17	19 Nov. 2017	23:45	36.12	129.36	9	3.5
18	20 Nov. 2017	6:05	36.14	129.36	12	3.6
19	25 Dec. 2017	16:19	36.11	129.36	10	3.5
20	11 Feb. 2018	5:03	36.08	129.33	9	4.6

Table 6. Earthquake events of magnitude 3.0 and above in the study area
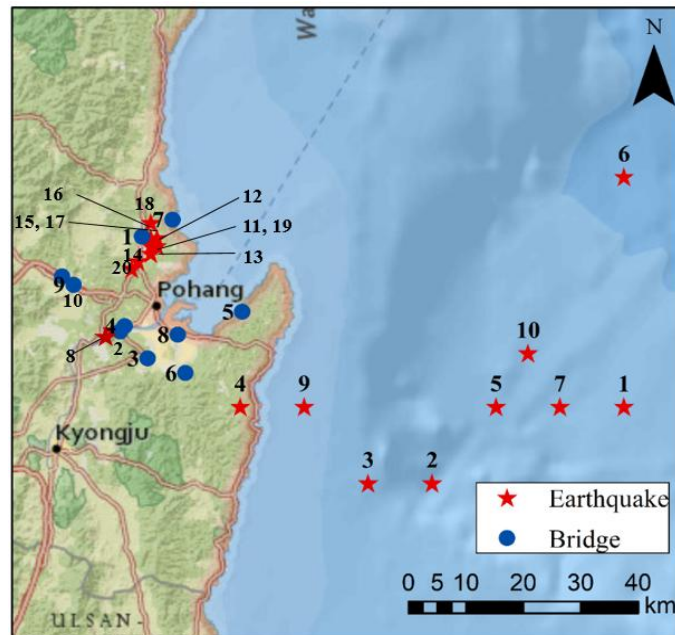

Figure 6. Locations of earthquake epicenters and bridges around Pohang, South Korea

Based on these earthquake records, the earthquake uncertainty is identified using the G-R law given in Equation (1), and the parameters of *a* and *b* are obtained as 2.167 and 0.699, respectively, from the regression analysis. The bounded PDF of the earthquake magnitude can be constructed by Equation (3).

The observations of earthquake magnitudes are shown in Figure 7 (a), along with Gutenberg-Richter recurrence laws fit to the data and Figure 7(b) shows the corresponding discrete occurrence probabilities with varying earthquake magnitudes in the range from 4.5 to 7.5.
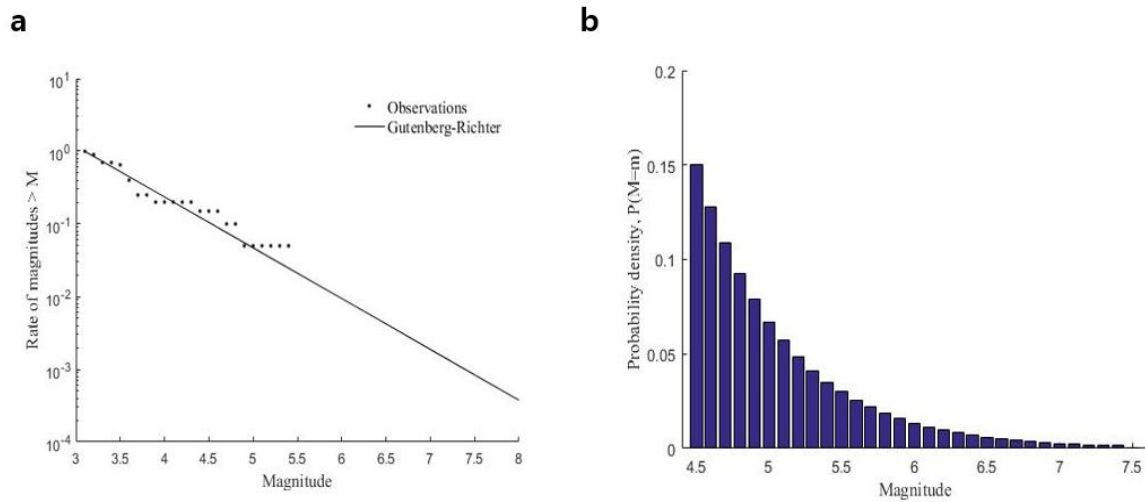

Figure 7. (a) Distribution of observed earthquake magnitude along with G-R recurrence laws fit to the observations and (b) the corresponding occurrence probability

Once the PDF of the earthquake magnitude is constructed, the earthquake intensities at the ten bridge locations are calculated using Equation (4). Primarily, the mean of the response variable can be calculated using Equation (5). For the calculation, the regression coefficients c_k (k = 1, …, 5) are assumed to be −5.15, 0.95, −0.92, 6.8, −0.0003, and 0.208, respectively (Emolo et al. 2015), and the station dummy variable s is assumed to be −1, which was recommended by the seismological observatory (station code: PHA2) of the region.

3.3. Analysis results

3.3.1. Annual expected earthquake frequency (AEEF)

PSHA results are formulated in terms of return periods, which are defined as the reciprocal of the rate of occurrence (Sánchez-Silva et al. 2005). Based on H. Konsuk et al. (2013), the return periods of earthquakes are estimated annually. Consequently, the average recurrence time of given magnitudes can be defined as the number of years between the occurrences of an earthquake in the region. The annual expected earthquake frequency (AEEF) is simply obtained by multiplying each probability, $f_M(m)$ by the ratio of the number of observed earthquake frequencies to the entire time considered. In this study, the number of earthquake frequencies is 20 and the total time is 100 years. The average recurrence period can likewise be calculated using the following equation:

$$Recurrence\ period\ (year) = \frac{1}{AEEF\ (a\ year)} \qquad (21)$$

where *AEEF (a year)* denotes the expected annual earthquake frequencies, given particular probabilities of earthquake magnitudes. For example, the AEEF of a 5.4 magnitude earthquake is 0.001532, and resulting average recurrence period is 653 years. Figure 8 plots the AEEF (left blue y-axis) and return period (right red y-axis) corresponding to the earthquake magnitudes.
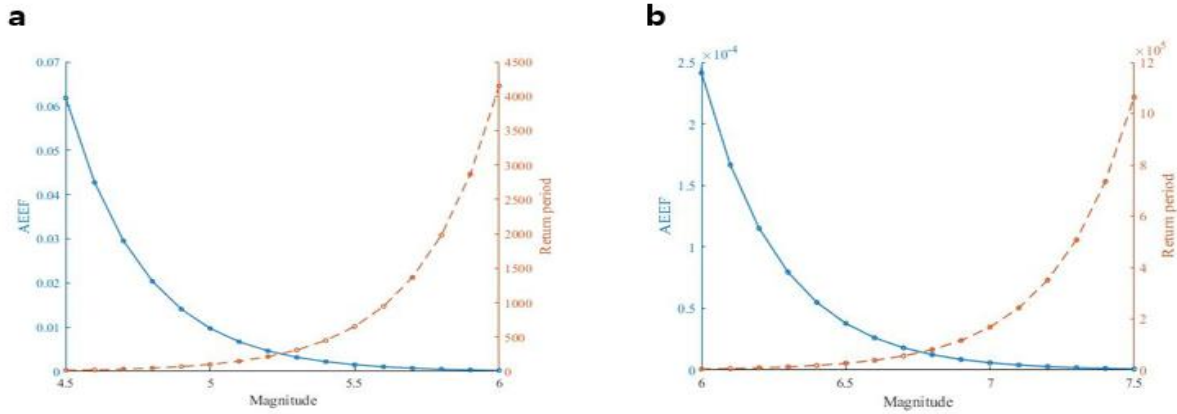

Figure 8. Return periods obtained from annual expected earthquake frequencies (a) Magnitude distribution, given $4.5 \leq M \leq 6.0$ (b) Magnitude distribution, given $6.0 \leq M \leq 7.5$

3.3.2. Evaluation of network performance

For earthquake magnitudes between 4.5 and 7.5, the statistical moments of the flow capacity according to the twenty earthquake sources are obtained by the proposed method. Figure 9 shows the mean of the maximum flow capacity with varying earthquake magnitudes for the twenty earthquake locations presented in Table 6. Results show that the mean flow decreases with increasing earthquake magnitude. When the earthquake magnitudes are relatively small, the mean flow capacity is close to the original maximum flow capacity of the network, 4440, however it decreases with increasing earthquake magnitude. In addition, the rates of decrease are different among the twenty earthquake sources, since the associated site-source distances and focal depths are different.

Figure 9. Mean flow capacity for all earthquake scenarios with varying earthquake magnitudes for (a) EQ 1-5 (b) EQ 6-10 (c) EQ 11-15 (d) EQ 16-20

For a better comparison, Figure 10 presents the mean flow capacities of the twenty earthquake scenarios and their average (colored blue) which depicts the mean flow capacity for uncertain earthquake location (L). The mean flow capacity for uncertain location also decreases as the earthquake magnitude increases. In addition, it is found that, among the twenty earthquake scenarios, EQ 8 is the most critical, followed by EQ 20.

Figure 10. Collected mean flow capacities and their mean values (colored blue) with varying magnitudes

Similarly, the standard deviation and the c.o.v. of the flow capacities of the twenty earthquake scenarios and their average (illustrated in blue) for uncertain earthquake location can be calculated and are presented in Figures 11 and 12, respectively. Generally, the standard deviation increases with increasing earthquake magnitude. In some scenarios, however, the standard deviation decreases after certain magnitude. Figure 12 shows that the c.o.v., i.e., a standardized measure of dispersion, increases with increasing magnitude. This means that a stronger seismic event gives rise to more uncertainty regarding the network flow capacity. Furthermore, the mean, standard deviation, and c.o.v. of the network flow capacity for uncertain earthquakes (i.e., uncertain magnitudes and locations of earthquake) can be calculated using Equation (19), the results of which are shown in Table 7.

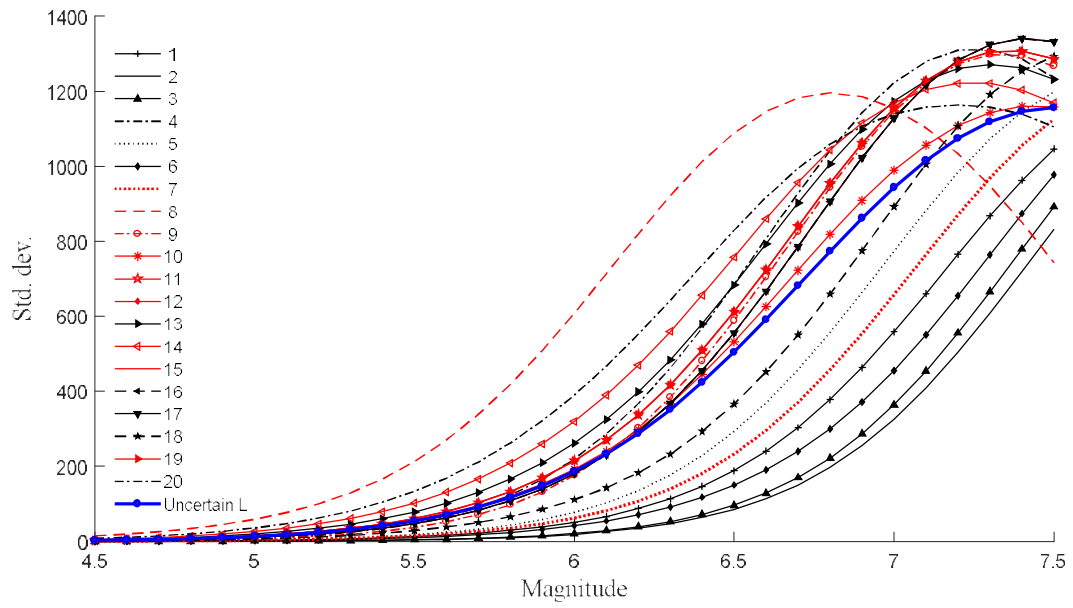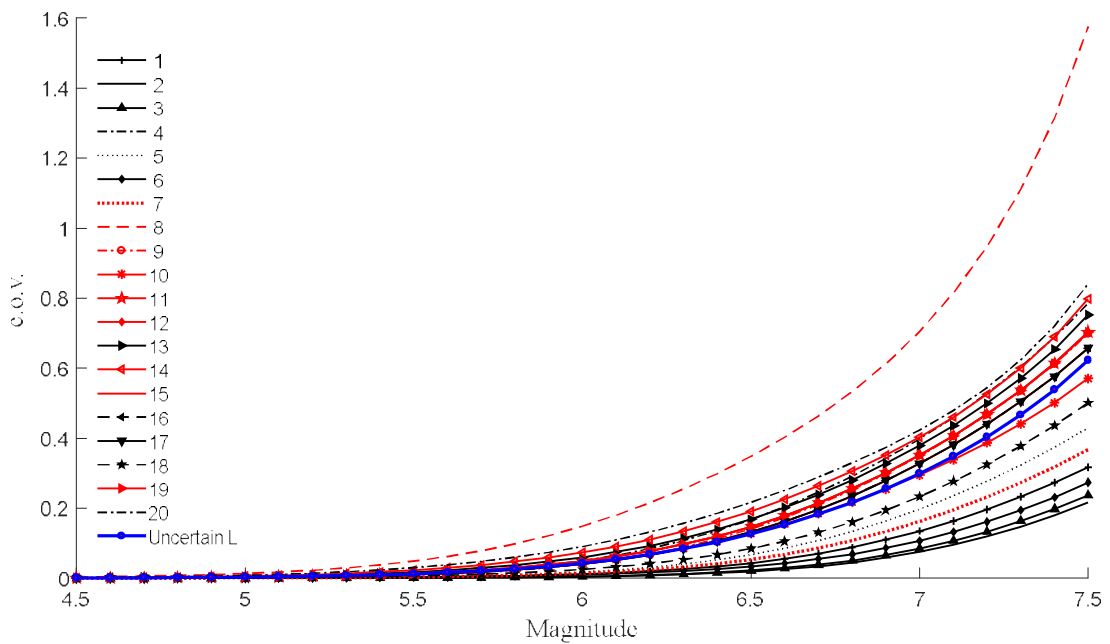Figure 11. Collected standard deviations of flow capacities and their mean values (colored blue) with varying magnitudes

Figure 12. Collected c.o.v.s of flow capacities and their mean values (colored blue) with varying magnitudes

Statistical moments	Results
Mean (μ_Q, number of vehicles per hour)	4076.077
Standard deviation (σ_Q, number of vehicles per hour)	57.263

c.o.v (δ_Q)	0.015

Table 7. Statistical moments of the network flow capacity for uncertain earthquake

It is noteworthy that sampling-based approaches would be inefficient for this sort of parametric study, because network flow analysis should be conducted for all of the individual magnitude values and locations of earthquake. On the contrary, the proposed method makes it possible to perform this parametric study efficiently.

3.3.3. Evaluation of component risk and importance

The first evaluation of component risks involves the construction of the hazard curve shown in Figures 13 and 14. The overall curve has a higher rate of exceedance with smaller-magnitude earthquakes. The hazard curve for SA shows the rates of exceedance with varying of SA levels. In this study, the rate of exceedance is defined as AEEF, for the range of earthquake magnitudes from 4.5 to 7.5. Further, the location of the earthquake is set to the location of EQ 8 (as shown in Figure 6). Subsequently, the earthquake intensities for the magnitudes are computed by the seismic attenuation model in Equation (5). In Figures 13 and 14, Bridge 2 and Bridge 4 have a higher annual rate of exceedance with respect to SA levels than the other bridges, in the case where the earthquake occurs near the location of EQ 8.

In the second evaluation of component risks, the proposed method moreover enables the computation of the reduction factor RF using Equation (20). RF contains the performance measure; hence, the results can be used to investigate the relative importance of bridges in the network. Figure 9 shows RFs of all bridges for the two severe earthquake scenarios (i.e., EQ 8 and EQ 20) and for the uncertain earthquake. Consequently, Bridges 3, 5, 6, 9, and 10 are relatively important in the region under the assumed emergency evacuation scenario from Node 30 to Node 3. For example, $RF_{6, avg.}$, $RF_{6, EQ8}$, and $RF_{6, EQ20}$ for Bridge 6 are 0.5031, 0.5322, and 0.5034, respectively. The values depict that the mean of passing vehicles per hour is reduced by 50.31%, 53.22%, and 50.34%, respectively, if Bridge 6 fails. Bridges 3, 5, 6, 9, and 10 are located at the most critical sites under the assumed emergency evacuation scenario from Node 30 to Node 3.
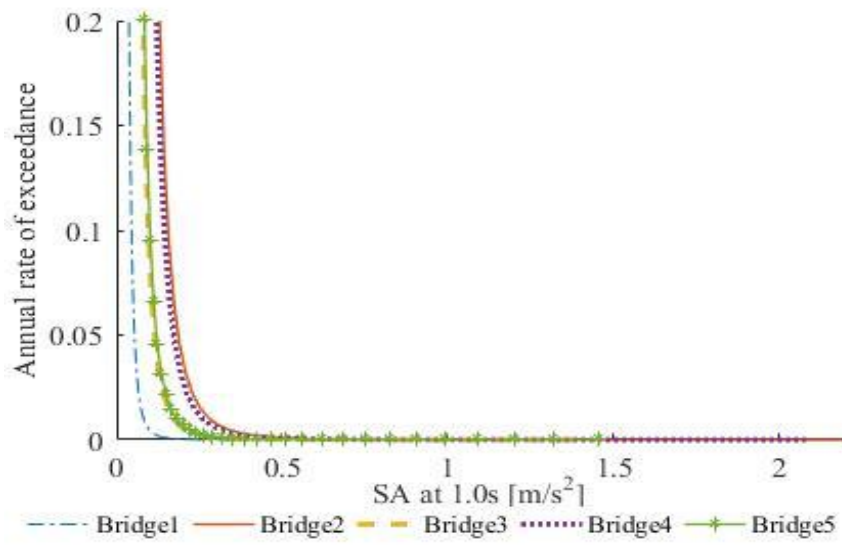
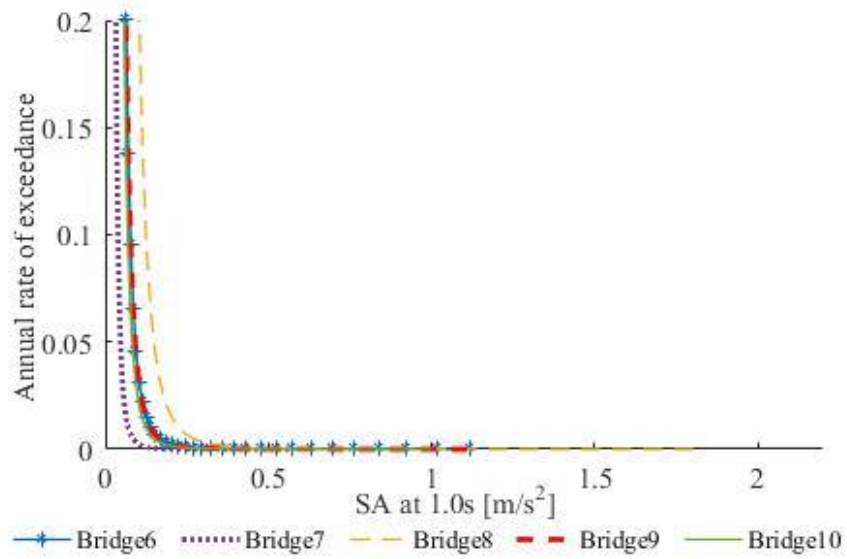Figure 13. Hazard curves for uncertain magnitudes from Bridge 1 to Bridge 5

Figure 14. Hazard curves for uncertain magnitudes from Bridge 6 to Bridge 10
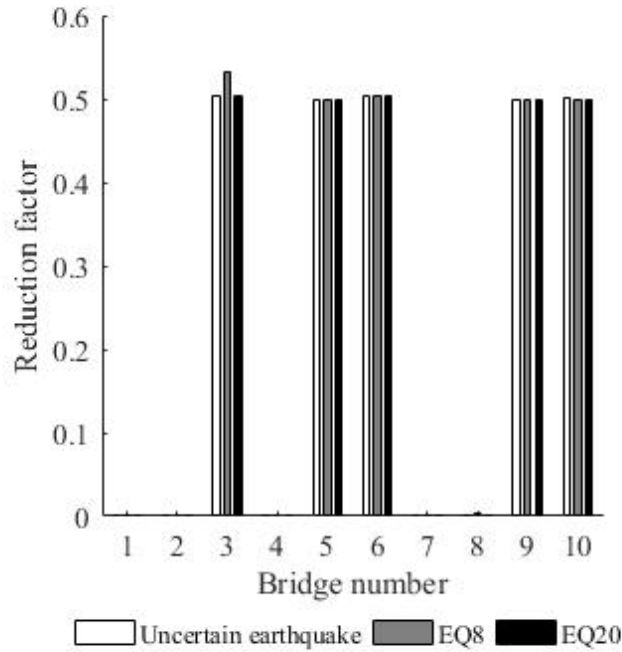
2 8

Figure 15. Reduction factors for EQ 8, EQ 20, and uncertain earthquake

4. Further Development of the Proposed Method

4.1 Matrix-based seismic risk assessment employing ANN-based surrogate model

The goal of further developing the method is to increase accuracy to estimate the performance of a bridge transportation network, as illustrated in Figure 6. To this end, the proposed method in this section introduces a new network performance, where TSTT is compared to the maximum flow capacity. Similarly, the performance of a bridge transportation network that is subjected to earthquakes becomes uncertain, and the further developed method employs the matrix-based framework of the MSR method to evaluate this uncertainty at the system level. Moreover, the ANN model is used for the approximation of TSTT in a partial earthquake scenario and corresponding TSTT values.

As stated in Section 3, all the components are statistically independent as the concept of CSRV events applies. This assumption enables the use of the more efficient matrix calculation. The calculations of the probability of a system and the three statistical parameters are obtained from Equation (16) to (19). The development of the method is two-fold: (1) the performance quantity of the system with damage states is changed from the maximum flow capacity to TSTT, and it is supplied to the quantity vector **q** as a dataset using the ANN model; and (2) a new importance measure is suggested that can account for the relative importance of components under the new performance quantity.

In this thesis, the maximum flow capacity was originally used for a bridge transportation network, but the numerical example using this measure is further developed for applications to achieve more

accurate system performance analysis using TSTT. Under the system condition of maximum flow capacity, no driver can reduce travel costs by shifting to another route, and this condition is termed user equilibrium (UE) (Bar-Gera 1999). The origin, destination, and capacities in each used path are fixed under same UE condition. For a more accurate traffic analysis, TSTT is used and calculated by EMME4 software in the further developed method and numerical example. TSTT is one of the widely used performance measures based on the system optimum (SO) condition, which exists if all drivers acted to minimize total TSTT rather than their own individual TSTT. In the SO condition, users choose routes based on the marginal travel time.

The proposed network performance uses may allow additional performing tasks, as difficulties arise in the application of a mathematical model and also require knowledge. Moreover, only temporal or partial data exist as function of input data. Therefore, technical methods are required to perform network reliability more efficiently. To identify the TSTT values instead of studying their detailed knowledge or function, the concept of a *surrogate model* is considered with the ANN model.

The surrogate model is a method to substitute black-box models either when a result of interest cannot be easily measured, or when difficulties are found in the original model. This can be constructed to provide approximate results through a function using only some input data, not requiring detailed knowledge of the dynamic parameters of the system. Of the many techniques available for surrogate modeling, the ANN has been successfully applied in many researches. Assuming that there is a total X_o damage scenarios observed, (in this example, $o = 1, \ldots, 100000$), the ANN-based surrogate models can be expressed as following equation suggested by Pina et al. (2013)

$$\mathrm{Q}(\ldots) = f(\mathbf{W}, \mathbf{X_o}\left(q_{n_b,(n_d)}\right)) \tag{22}$$

where $Q(\ldots)$ denotes the performance quantity of the system, $f(\ldots)$ denotes the particular surrogate model employed the ANN, $\mathbf{W}$ is the parameter of the model, which depicts the set of synaptic weights w_i. This will be automatically adjusted during the training of the ANN, and X_o is the input of the surrogate model with 100000 observed system events with j^{th} damage states of the ith bridge. For example, $X_{3(2,1,\ldots,1)}$ means that all of the components are in the first damage state except for the first component, which is in the second damage state, at the 3rd system event as one input value. Then, using the surrogate model and Equation (22), the quantities in Equation (9) are changed to

$$\mathbf{q}_s = \begin{bmatrix} Q_{(1,1,\ldots,1)} \\ Q_{(2,1,\ldots,1)} \\ \vdots \\ Q_{\left(d_1,d_2,\ldots d_{n_b}\right)} \\ \vdots \\ Q_{(n_d,n_d,\ldots n_d)} \end{bmatrix} = \begin{bmatrix} f(w_1, x_1(q_{1,(1)}, q_{2(1)}, \ldots, q_{n_b,(1)})) \\ f\left(w_2, x_2(q_{1,(2)}, q_{2,(1)}, \ldots, q_{n_b,(1)})\right) \\ \vdots \\ f\left(w_{d_{n_b}}, x_{d_{n_b}}(q_{1,(d_1)}, q_{2,(d_2)}, \ldots, q_{n_b,\left(d_{n_b}\right)})\right) \\ \vdots \\ f\left(w_{n_d}, x_{n_d}(q_{1,(n_d)}, q_{2,(n_d)}, \ldots, q_{n_b,(n_d)})\right) \end{bmatrix} \tag{23}$$

where $\mathbf{q}_s$ denotes the quantity vector estimated by ANN-surrogated model.

Second, the TSTT increment factor (TIF), a new version of IM, is proposed in this method. TIF can compute the increment of the expected TSTT by the observed event E_{obs}, e.g., the failure of a bridge, which can quantify the relative importance of component bridges. The computation of the proposed TIF is as follows:

$$\text{TIF} = \frac{\text{TSTT}_{\mu_{Q|E_i}} - \text{TSTT}_{No\ damage}}{\text{TSTT}_{full} - \text{TSTT}_{No\ damage}} \tag{24}$$

where $\mu_{Q|Eobs}$ represents the conditional mean of the TSTT given an observed event, $E_{obs.}$ $\text{TSTT}_{No\ damage}$ depicts the minimum TSTT value, given that all of the bridges experience no damage. In turn, TSTT_{full} denotes the maximum TSTT value where of the bridges experience collapse damage.

4.2 Numerical example

In this section, the target bridge transportation network which was described in Section 3 is introduced again as a developed numerical example of the matrix-based seismic risk assessment employing the ANN-based surrogate model. This is because 1) the maximum flow capacity as a measure of network performance is a simple node-to-node analysis; and 2) to improve the accuracy of the estimation of network performance, a new performance measure is used to this example, which requires more time for estimating the network performance. Therefore, TSTT is used as a measure of flow capacity compared to connectivity and the maximum flow capacity to consider the accuracy. The ANN-based surrogate model with a matrix-based framework is also introduced to reduce the computational time costs.

The same five damage states of no, slight, moderate, extensive, and complete damage are used for the input data in the ANN. The input value in ANN is the set of five damage states for each component failure scenario, and they need to be normalized to span values between 0 and 1. This is because normalization or scaling significantly helps, as it transposes the input variables into the data range of the sigmoid activation functions (i.e., sigmoid functions), which are bounded between 0 and 1. This process is useful in preparing the data, making it appropriate for the training step (Meloa et al. 2014). The five normalized damage states for each considered bridge are composed of a 100000×10 matrix, representing static data as 100000 samples of 10 elements, which were randomly selected from 100000 original TSTTs data. Table 8 presents five damage states of the considered bridge and the associated input value bounded between 0 and 1. To account for uncertainty in the seismic damage states of bridges, seismic fragility curves are introduced (as discussed Section 3.2.). Similarly, the seismic fragility curves of the ten bridges are determined based on the structural information given in Table 3. To identify the earthquake uncertainty in the target region, the same earthquake data and the bounded PDF of the earthquake magnitude are used again (as detailed in Figure 7). In the ANN training 70% of the 70000 samples were selected and 15% of the samples were used for the validation set. Another 15% of the rest

were used to test the performance of the network. All samples were randomly selected; also continuous sigmoid function was used as an activation function using Equation (13).

Damage states	Discrete values	Normalized input value in ANN model
No	5	1
Slight	4	0.75
Moderate	3	0.50
Extensive	2	0.25
Complete	1	0

Table 8. Damage states of bridge and associated input value in ANN model

For the application considered in this section, the ANN has been implemented in the MathWorks MATLAB® language. The structure of the neural network was set as a feed-forward with two layers between static input and target data. The neural network is mapped with seven neurons in the hidden layers and one neuron in the output layer, corresponding to the target value, which in the network performance measure depicts the TSTT. The number of neurons in hidden layer, N_h, is based on preliminary methods, as discussed Section 2.3.

Three configurations of the ANN model were constructed in order to fine the best approximation of number of hidden layers. Table 9 shows a comparison between the target TSTT and output in ANN prediction which has the maximum error, where three cases are determined by methods in Table 1. The maximum error is relatively small when seven neurons compared to three and four hidden neurons. Note that the use of more neurons could increase computation times resulting reduced efficiency of such configuration, so appropriate determination of the number of hidden neuron is necessary (Pina et al. 2013). In addition, the mean error and the standard deviation for the cases were also calculated. Figure 16 represents regression values, R, which shows model outputs compared to the target values of TSTT. As a result, method 2 (*rules of thumb*) in Table 1 shows the highest regression values $R = 0.99684$ (*all* case). This demonstrates that the ANN can represent the relationship between the input and output data with two layers and seven neurons in the hidden layer.

ANN models	Number of hidden neurons (method in Table 1)	TSTT [min]		Difference [min]
		target	ANN output	
Model 1	3 (Shibata and Ikeda, and Hunter et al.)	5015893	5105658	120997 (+2.37%)
Model 2	4 (Li et al., and Sheela and Deepa)	5102052	5195505	93453 (+1.83%)

| Model 3 | 7 (Rules of Thumb) | 5102052 | 5194032 | 91980 (+1.80%) |

Table 9. Maximum error analysis in ANN predictions for three ANN models

ANN models	Statistical moments (min)	
	Mean error	the standard deviation
Model 1	6677.475	9581.826
Model 2	20.92964	6611.59
Model 3	-7.58947	2758.394

Table 10. The mean error and the standard deviation for three ANN models

Figure 16. Regression values, R using *Rules of Thumb* method (N_h = 7)

4.3 Analysis results

In this case, the network performance considered the value of TSTT nearby 10 bridges regions for distinct changes in numerical results. In total, 399 links are selected out of 3490 links in target transportation network. The average of TSTT is constant, 4140000 (min) and the value was left out from quantity vector in Equation (23). Figure 17 shows the mean TSTTs of the twenty earthquake

scenarios and their average (colored blue), which depicts the mean TSTT for the uncertain earthquake location (L). Compared to Figure 10, the mean TSTT clearly increases with increasing earthquake magnitude. Because the earthquake may cause disconnections in a transportation network, leading to traffic jams and requiring more time from origin to destination. Moreover, EQ 8 is considered as the most critical one followed by EQ 13, among the twenty earthquake scenarios.

The standard deviation and the c.o.v. of TSTT in the twenty earthquake scenarios, along with their averages (colored blue) for the uncertain earthquake location are estimated and presented in Figures 17 and 18, respectively. Similarly, the standard deviation increases with increasing magnitude, however it has a tendency to decrease after a certain magnitude. Moreover, the c.o.v. increases as the earthquake magnitude increases. This trend is similar to the standard deviation depicted in Figure 12, which means the stronger earthquake events is, the more uncertainty the network performance has in this case.

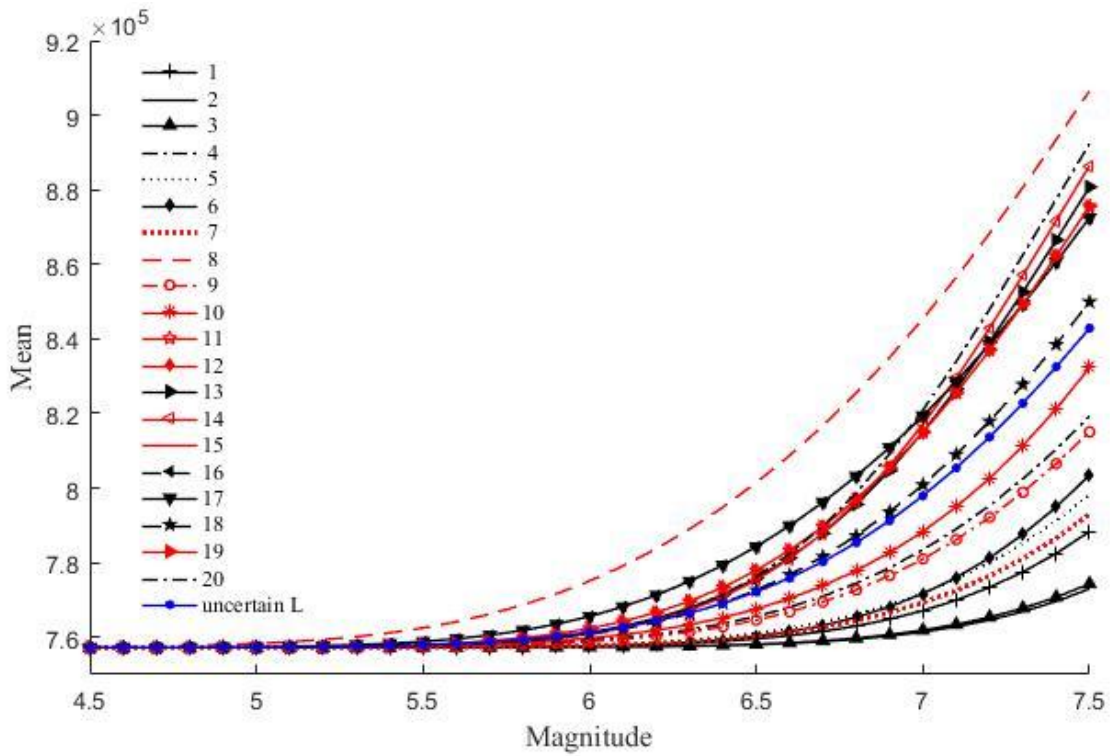Figure 17. Collected mean (min) of TSTT and their mean values (colored blue) with varying magnitudes
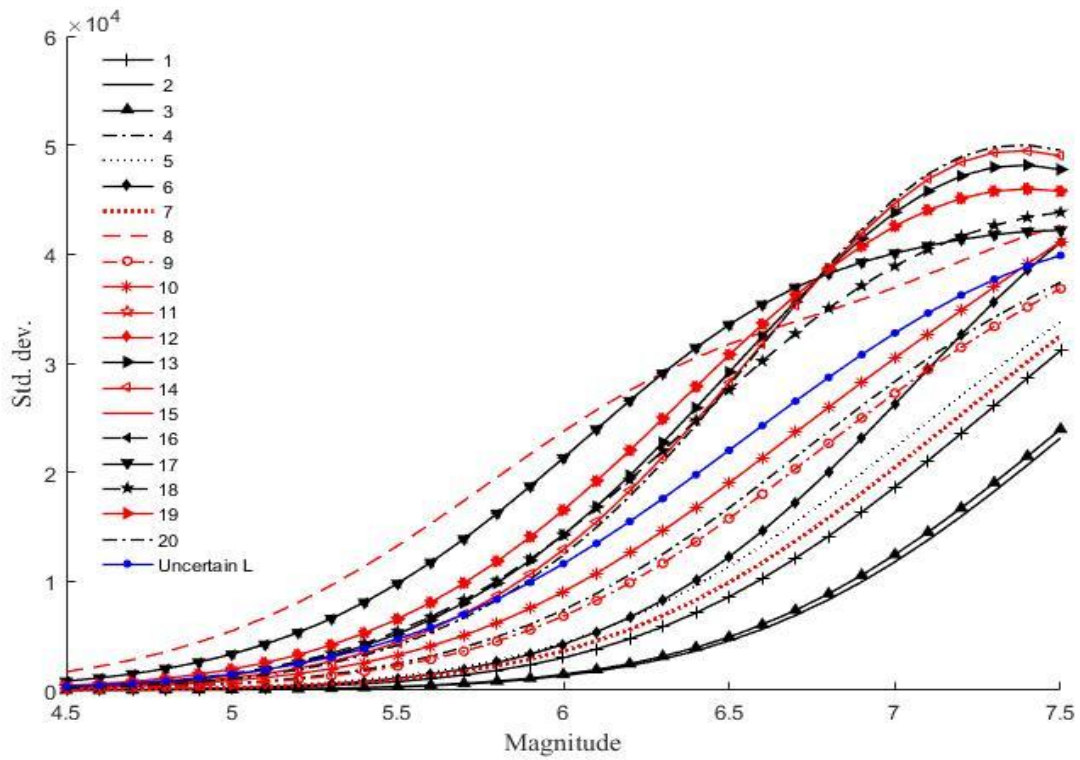
Figure 18. Collected standard deviations (min) of TSTT and their mean values (colored blue) with varying magnitudes
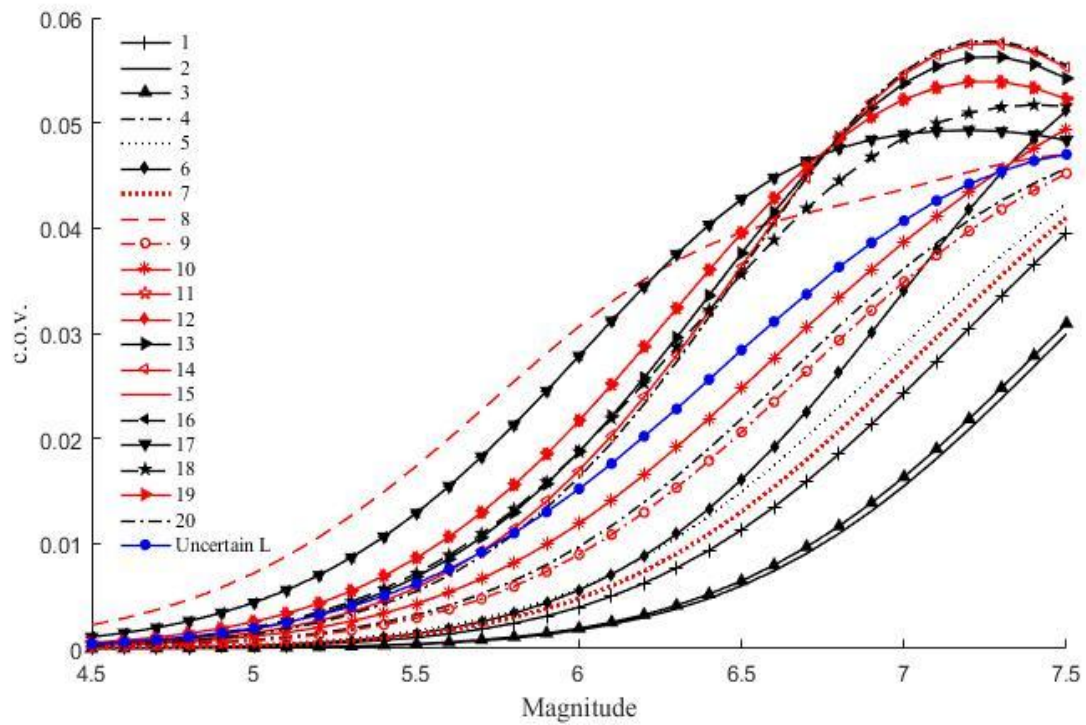

Figure 19. Collected c.o.v.s of TSTT and their mean values (colored blue) with varying magnitudes

Table 11 shows the mean, standard deviation, and c.o.v. of the network travel time for the uncertain

3 5

earthquake calculated by Equation (19). The matrix-based framework based on the total probability theorem enables to calculate these statistical moments efficiently.

Statistical moments	Results
Mean (μ_Q, min)	702114.977
Standard deviation (σ_Q, min)	3338.714
c.o.v (δ_Q)	0.00433

Table 11. Statistical moments of TSTT for uncertain earthquake

The further developed method identified the mean of TSTT for the twenty earthquake scenarios. The computation used the joint PDF of the considered earthquake epicenter when $L = l$, applying the total probability theorem, and the mean values were calculated with respect magnitude. In this case, EQ 8 shows critical increasing in the travel time of the network.

Figure 20. Mean of TSTT from the twenty earthquake scenarios for uncertain magnitude

Furthermore, the proposed method also computes a new importance measure, the TSTT increasing factor TIF, using Equation (24). TIF contains the performance measure; hence, the results can be used to investigate the relative importance of bridges in the network, similarly to RF, as shown in Equation (20). Figure 21 shows the TIFs of ten bridges for the two severe earthquake scenarios with increasing TSTT obtained Figure 17 (i.e., EQ 8 and EQ 13) and one earthquake scenario located near the east coast

(i.e., EQ 9). Bridges 1, 3, and 8 are found to be relatively important, which implies that these are located along the main routes for the given origin and destination of each traveler and their chosen routes in the region. The disconnection of these bridges will cause an increase in the TSTT under this condition.

Figure 21. TSTT increasing factors for EQ 8, EQ 9, and EQ 13

However, the proposed method has the a few limitations. First, it only covers ten relatively bridges in the numerical example. It may cause slight impacts on post-hazard network performance, so it is necessary to apply to more realistic transportation network by increasing the number of bridge or choose bridge lying on the main locations. Second, seismic attenuation law and fragility parameter of bridge may be replaced by finding related researches in this field. This is because fragility of bridges is one of the input data for vulnerability and main source to construction of the probability vector. Therefore, seismic attenuation equation and fragility curve are determined based on adequate for domestic bridge and seismic hazard circumstances in Korea. Lastly, there are other characteristics of performance measure in traffic flow analysis. Currently, traffic capacity and flow measure are being conducted to address more complex and practical traffic scenarios in this field. Based on an improved and high-resolution performance measure, it may contribute to increasing accuracy for estimation of transportation network.

5.   Conclusion

This thesis has proposed a new method of system-level seismic risk assessment of bridge transportation network. To test the proposed method, it has been applied to a numerical example of an actual transportation network around Pohang city, South Korea, considering twenty past earthquake records with a range of earthquake magnitude from 4.5 to 7.5, and ten bridges with five damage states. The proposed method has been developed in two steps. In the first step, seismic risk assessment for system reliability is conducted by employing PSHA with the MSR method, which consists of three small steps: 1) component failure probability calculation of bridges based on PSHA; 2) system-level performance estimation of the transportation network using the matrix-based framework of the MSR method; and 3) seismic risk assessment based on the total probability theorem. PSHA enables the seismic fragility estimation of the component bridges considering the uncertainty of earthquake locations and magnitudes, and it is systemically used to carry out the estimation of the post-earthquake performance (e.g., maximum flow capacity and TSTT) of the target bridge network by employing the matrix-based framework. In the second step, the proposed method has been further developed for more accurate assessment of network performance based on the proposed framework and a new approach, Artificial neural network (ANN) model. This model enables estimating target TSTT values corresponding to damage states of considered ten bridge with no detailed information. The further developed approach has been successfully applied to target transportation network again. In both steps, matrix-based framework enables efficient evaluations of the network performance with various magnitudes and locations of earthquake, without performing deterministic flow capacity analyses repeatedly. As a result, the statistical moments of the network, critical earthquake scenarios and bridge significances are obtained. The analysis results for numerical examples are summarized as follows:

1) As the earthquake magnitude increases, the mean flow capacity of the network decreases, while the mean of TSTT increases.

2) In both examples (maximum flow capacity and TSTT), the c.o.v. that is a standardized measure of dispersion increases with the increasing magnitudes, which means the stronger earthquake events is, the more uncertainty the network performance has.

3) Through computation of the importance measure factors for all of the bridges, it is observed that in the first step, Bridges 3, 5, 6, 9, and 10 are relatively important through RF and in the second step, Bridges 1, 3, and 8 affect increasing travel time the most through TIF in the target transportation network.

4) Among the twenty earthquakes scenarios, EQ 8 is the most critical located in the downtown of the city.

Therefore, it has been confirmed that the proposed method is effective for performing the system-

level seismic risk assessment of bridge transportation networks.

References

Applied Technology Council (ATC). (1991). Seismic Vulnerability and Impact of Disruption of Lifelines in the Conterminous United States. no. ATC-25.

Ahuja, R. K., Magnanti, T. L. & Orlin, J. B. (1993). *Network Flow: Theory, Algorithms, and Applications*. Prentice-Hall, Inc. Upper Saddle River, NJ, USA.

Bar-Gera, H. (1999). Origin-based algorithms for transportation network modeling. Technical Report Number 103. National Institute of Statistical Sciences, 19 T. W. Alexander Drive, PO Box14006, Research Triangle Park, NC 27709-4006.

Basheer, I.A., & Hajmeer, M. (2000). Artificial neural networks: fundamentals, computing, design, and application. J. Microbiol. Methods 43, 3–31.

Ben-Nakhi, A.E., & Mahmoud, M.A. (2004). Cooling load prediction for buildings using general regression neural networks. *Energy Convers*ion and Management, 45(13-14), 2127–2141.

Baker, J. W. (2008). An introduction to probabilistic seismic hazard analysis (PSHA), White Paper, Version 1.3.

Boost, *Boost graph library.* (2008). https://www.boost.org/doc/libs/1_37_0/libs/graph/doc/index.html

Cornell, C. A. (1968). Engineering seismic risk analysis. *Bulletin of the Seismological Society of America,* 58(5), 1583-1606.

Chang, L., Elnashai, A., Spencer, B., Song, J., & Ouyang, Y. (2010). Transportation systems modeling and applications in earthquake engineering. *Mid-America Earthquake Center*, 10-03.

Dueñas-Osorio L, Craig, J. I., & Goodno, B. J. (2007). Seismic response of critical interdependent networks. *Earthquake Engineering Structural Dynamics*, 26(2), 285-306.

Ellingwood, B. R., & Kinali, K. (2009). Quantifying and communication uncertainty in seismic risk assessment. *Structural Safety*, 31(2), 179-187.

Emolo, A., Sharma, N., Festa, G., Zollo, A., Convertito, V., Park. J. -H., Chi. H. -C., & Lim. In -S. (2015). Ground-Motion Prediction Equations for South Korea Peninsula. *Bulletin of the Seismological Society of America*, 105(5), 2625–2640.

Eisenberg, D. A., Park, J., & Seager, T. P. (2017). Sociotechnical network analysis for power grid resilience in South Korea. *Complexity*, 2017, 14.

FEMA. (2003). Multi-Hazard Loss Estimation Methodology Earthquake Model, HAZUS-MH MR4 Technical Manual: United States Department of Homeland Security. *Federal Emergency Management Agency*.

Ford, E. B., Moorhead, A.V., & Veras. D. A. (2011). Bayesian surrogate model for rapid time series analysis and application to exoplanet observations. *Bayesian Analysis,* 6(3), 475–500. http://dx.doi.org/10.1214/11-BA619.

Faturechi, R., & Miller-Hooks, E. (2014). A mathematical framework for quantifying and optimizaing pretective actions for civil infrastructure systems, *computer-aided civil and infrastructure engieering,* 29, 572-589.

Furtado, M. N. (2015). Measuring the Resilience of Transportation Networks Subject to Seismic Risk. Masters Theses, https://scholarworks.umass.edu/masters_theses_2/148.

Gutenberg. B., & Richter, C. F. (1994). Frequency of earthquakes in California. *Bulletin of the Seismological Society of America*, 34(4), 185-188.

Gleich, D. (2008). *MATLAB BGL*, MATLAB Central.

https://kr.mathworks.com/matlabcentral/fileexchange/10922-matlabbgl

Goda, K., & Hong, H.-P. (2008). Spatial correlation of peak ground motions and response spectra. *Bulletin of the Seismological Society of America,* 98(1), 354-365.

Goda, K. & Atkinson, G. M. (2009). Probabilistic characterization of spatially correlated response spectra for earthquakes in Japan. *Bulletin of the Seismological Society of America*, 99(5), 3003-3020.

Haykin, S. (1994). Neural Networks: a comprehensive foundation. Upper Saddle River, New Jersey: Prentice Hall.

Heaton, J. (2005). Introduction to Neural Networks with Java, Heaton Research Inc.

Hunter, D., Yu, H. , Pukish III, M. S., Kolbusz, J., & Wilamowski, B. M. (2012). Selection of proper neural network sizes and architectures: a comparative study, *Proceedings of the IEEE Transactions on Industrial Informatics*, 228 – 240.

Joyner, W. B., & Boore, D. M. (1993). Methods for regression analysis of strong-motion data. *Bulletin of the Seismological Society of America*, 83(2), 469–487.

Jensen, J. R., Qiu, F., & Ji, M. (1999). Predictive Modeling of coniferous Forest Age Using Statistical and Artificial Neural network Approaches Applied to Remote Sensing Data. *International Journal of Remote Sensing*, 20(14), 2805-2822.

Kramer, S. L. (1996). Geotechnical Earthquake Engineering. *Pearson Education*, Reprinted 2003, Delhi, India.

Kiremidjian, A., Moore, J., Fan, Y., Yazlali, O., Basoz, N., & Williams, M. (2007). Seismic Risk Assessment of Transportation Network Systems. *Journal of Earthquake Engineering*, 11(3), 371-382.

Kang, W.-H., Song, J., & Gardoni, P. (2008). Matrix-based System Reliability Method and Applications to Bridge Networks. *Reliability Engineering & System Safety*, 93(11), 1584-1593.

Kang W.-H., & Song, J. (2008). Evaluation of multinormal integral and sensitivity by matrix-based system reliability method. *in Proceedings of 10th AIAA Nondeterministic Approaches Conference*, Schaumburg, IL.

Kang, W.-H., Lee, Y.-J., Song, J., & Gencturk, B. (2012). Further development of matrix-based system reliability method and applications to structural systems. *Structure and Infrastructure Engineering*, 8(5), 441-457.

Konsuk, H. & Aktas, S. (2013). Estimating the recurrence periods of earthquakes data in Turkey. *Open Journal of Earthquake Research*, 2, 21-25.

Kang, W.-H., Lee, Y.-J., & Zhang, C. (2017). Computer-aided analysis of flow in water pipe networks after a seismic event. *Mathematical Problems in Engineering*, 2017, 14.

Korea Meteorological Administration (KMA). (2019). Available online: http://kma.go.kr/ (accessed on 28 August 2017).

Lee, W. H. K., Wu, F. T., & Jacobsen, C. (1976). A catalog of historical earthquakes in China compiled from recent Chinese publication, *Bulletin of the Seismological Society of America*, 66(6), 2003-2016.

Li, J. Y., Chow, T. W. S., & Yu, Y. L. (1995). Estimation theory and optimization algorithm for the number of hidden units in the higher-order feedforward neural network. *Proceedings of the IEEE International Conference on Neural Networks,* 1229 - 1233.

Li, J. & He, J. (2002). A recursive decomposition algorithm for network seismic reliability evaluation. *Earthquake Engineering and Structural Dynamics*, 31, 1525–1539.

Lee, K., & Yang W.-S. (2006). Historical seismicity of Korea. *Bulletin of the Seismological Society of America,* 96(3), 846–855.

Lee, S. M., Kim, T. J., & Kang, S. L. (2007). Development of fragility curves for bridges in Korea. *KSCE Journal of Civil Engineering*, 11(3), 165-174.

Lee, Y.-J., Song, J., Gardoni, P., & Lim, H.-W. (2011). Post-hazard flow capacity of bridge transportation network considering structural deterioration of bridges. *Structure and Infrastructure Engineering*, 7(7-8), 509-521.

Lee Y.-J. & Moon, D. S. (2014). A new methodology of the development of seismic fragility curves. *Smart Structures and Systems*, 14(5), 847-867.

McGuire, R. K. (2004). Seismic Hazard and Risk Analysis, Earthquake Engineering Research Institute, Berkeley

Murray-Tuite, P. M. (2006). A comparison of transportation network resilience under simulated system optimum and user equilibrium conditions. *In Proceedings of the 2006 Winter Simulation Conference,* Monterey, CA.

McGuire, R. K. (2007). Probabilistic seismic hazard analysis: Early history. *Earthquake Engineering & Structural Dynamics* (in press).

Melo, A. P., Cóstola, D., Lambertsa, R., & Hensenb, J. L. M. (2014). Development of surrogate models using artificial neural network for building shell energy labelling. *Energy Policy*, 69, 457-466.

Moon, D.-S., Lee, Y.-J. & Lee, S. (2018). Fragility analysis of space reinforced concrete frame structures with structural irregularity in plan. *Journal of Structural Engineering*, 144(8), 04018096.

Nojima, N. (1998). Prioritization in upgrading seismic performance of road network based on system reliability analysis. *Proceedings of the 3rd China-Japan-US trilateral symposium on lifeline earthquake engineering*, Kunming, China, 323-330.

Nicholson, A. J., & Dalziell, E. (2003). Risk evaluation and management: A road network reliability study. *The Network Reliability of Transport*, Emerald Group Publishing Limited, Bingley, 45-60.

Nuti, C., Rasulo, A., & Vanzi, I. (2010). Seismic safety of network structures and infrastructures. *Structure and Infrastructure Engineering,* 6(1-2), 95–110.

Nguyen, D.-D., & Lee, T.-H. (2018). Seismic fragility curves of bridge piers accounting for ground motions in Korea. *In IOP Conference Series: Earth and Environmental Science*, 143(1), 012029.

Oregon Department of Transportation. (2018). The analysis procedures manual (APM) version 2, chapter 9: transportation analysis performance mesaures.
Available online: https://www.oregon.gov/ODOT/Planning/Pages/APM.aspx

Poirier, J. P., & Taher, M. A. (1980). Historical seismicity in the near and Middle East, North Africa, and Spain from Arabic documents (VIIth–XVIIIth century). *Bulletin of the Seismological Society of America*, 70, 2185–2201.

Peeta S., & Mahmassani H. S. (1995). System optimal and user equilibrium time-dependent traffic assignment in congested networks. *Annals of Operations Research,* 60, 81 - 113.

Pina, A.C., & Zaverucha, G. (2008). Applying REC analysis to ensembles of particle filters. *Neural Computing and Applications,* 18(1), 25-35.

Poljanšek, K., Bono, F., & Gutièrrez, E. (2012). Seismic risk assessment of interdependent critical infrastructure systems: The case of European gas and electricity networks. *Earthquake Engineering and Structural Dynamics*, 41(1), 61–79.

Pina, A. C., Pina, A.A., Carl, H. A., Lima, B. S. L. P, & Jacob. B. P. (2013). ANN-based surrogate models for the analysis of morring lines and risers. *Applied Ocean Research*. 41, 76-86.

Park, S. H., Jang, K., Kim, D. K., Kho, S. Y., & Kang, S. (2015). Spatial analysis methods for identifying hazardous locations on expressways in Korea. *Scientia Iranica*, 22(4), 1594-1603.

Rahat Rahman, S. M., & Mamun, M.S. (2015). Comparison of User Equilibrium (UE) and System Optimum (SO) Traffic Assignment Methods for Auto Trips. *International Conference on Recent Innovation in Civil Engineering for Sustainable Development* (IICSD-2015).

Sung, A.H. (1998). Ranking importance of input parameters of neural networks. *Expert Systems with Application*, 15(3-4), 405-411.

Shibata K., & Ikeda, Y. (2009). Effect of number of hidden neurons on learning in large-scale layered neural networks. *In Proceedings of the ICROS-SICE International Joint Conference*, 5008-5013.

Sokolov, V., Wenzel, F., Jean, W.-Y., & Wen, K.-L. (2010). Uncertainty and spatial correlation of earthquake ground motion in Taiwan. *Terrestrial, Atmospheric and Oceanic sciences journal*, 22(6), 905-921.

Sheela, K., & Deepa, S. N. (2013). Review on Methods to Fix Number of Hidden Neurons in Neural Networks, *Mathematical Problems in Engineering,* 2013, 11.

Sánchez-Silva, M., Daniels, M., Lleras, G., & Patiño, D. (2005). A transport network reliability model for the efficient assignment of resources. *Transportation Research Part B: Methodological*, 39(1), 47-63.

Tijanana V., Tripo M., Jelena L., Adis B., & Zoran, Š. (2016). Comparative analysis of methods for determining number of hidden neurons in artificial neural network. *Central European Conference on Information and Intelligent Systems*, 219-223.

Usami, T. (1979). Study of historical earthquakes on Japan, *Bulletin of the Earthquake Research Institute, University of Tokyo,* 54, 399–439.

Widrow, B., Rumelhar, D. E., Lehr, M. A. (1994). Neural networks: applications in industry, business and science. *Communications of the ACM*, 37(3), 93-105.

Master's Thesis

System-Level Seismic Risk Assessment of Bridge Transportation Networks

Hye-Young Tak

Department of Urban and Environmental Engineering
(Disaster Management Engineering)

Graduate School of UNIST

2019

System-Level Seismic Risk Assessment of Bridge Transportation Networks

Hye-Young Tak

Department of Urban and Environmental Engineering

(Disaster Management Engineering)

Graduate School of UNIST

System-Level Seismic Risk Assessment of Bridge Transportation Networks

A thesis submitted to the Graduate School of UNIST
in partial fulfillment of the requirements for the degree of
Master of Science

Hye-Young Tak

07. 09. 2019

Approved by

_____

Advisor

Young Joo Lee

System-Level Seismic Risk Assessment of Bridge Transportation Networks

Hye-Young Tak

This certifies that the thesis of Hye-Young Tak is approved.

07/09/2019

_____

Advisor: Young Joo Lee

Department of Urban and Environmental Engineering

Ulsan National Institute of Science and Technology (UNIST)

_____

Thesis Committee Member: Sung-Han Sim

Department of Urban and Environmental Engineering

Ulsan National Institute of Science and Technology (UNIST)

_____

Thesis Committee Member: Byungmin Kim

Department of Urban and Environmental Engineering

Ulsan National Institute of Science and Technology (UNIST)

ABSTRACT

Seismic risk assessment has recently emerged as an important issue for infrastructure systems because of their vulnerability to seismic hazards. Earthquakes can have significant impacts on transportation networks such as bridge collapse and the resulting disconnections in a network. One of the main concerns is the accurate estimation of the seismic risk caused by the physical damage of bridges and the reduced performance of the associated transportation network. This requires estimating the performance of a bridge transportation network at the system level. Moreover, it is necessary to deal with various possible earthquake scenarios and the associated damage states of component bridges considering the uncertainty of earthquake locations and magnitudes.

To perform the seismic risk assessment of a bridge transportation network, system reliability is required. It is a challenging task for several reasons. First, the seismic risk itself contains a great deal of uncertainty, which comprises location, magnitude, and the resulting intensity of possible earthquakes in a target network. Second, the system performance of a bridge transportation network after the seismic event needs to be estimated accurately, especially for realistic and complex networks. Third, the seismic risk assessment employing system reliability may increase the computational costs and can be time-consuming tasks, because it requires dealing with various possible earthquake scenarios and the resulting seismic fragility of component bridges. Fourth, a precise performance measure of the system needs to be introduced.

In this study, a new method is proposed to assess the system-level seismic risk of bridge transportation networks considering earthquake uncertainty. In addition, a new performance measure is developed to help risk-informed decision-making regarding seismic hazard mitigation and disaster management. For the tasks, first of all, a matrix-based system reliability framework is developed, which performs the estimation of a bridge transportation network subjected to earthquakes. Probabilistic seismic hazard analysis (PSHA) is introduced to enable the seismic fragility estimation of the component bridges, considering the uncertainty of earthquake locations and magnitudes. This is systemically used to carry out a post-hazard bridge network flow analysis by employing the matrix-based framework. Secondly, two different network performance measures are used to quantify the network performance after a seismic event. Maximum flow capacity was originally used for a bridge transportation network, however the numerical example using this measure is further developed for applications to more accurate system performance analysis using total system travel time (TSTT). Finally, a new method for system-level seismic risk assessment is proposed to carry out a bridge network flow analysis based on TSTT by employing the matrix-based system reliability (MSR) method. In the proposed method, the artificial neuron network (ANN) is introduced to approximate the network performance, which can reduce the computational cost of network analysis.

The proposed method can provide statistical moments of the network performance and component importance measures, which can be used by decision-makers to reduce the seismic risk of a target area. The proposed method is tested by application to a numerical example of an actual transportation network in South Korea. In the seismic risk assessment of the example, PSHA is successfully integrated with the matrix-based framework to perform system reliability analysis in a computationally efficient manner.

Keywords: seismic risk, bridge transportation network, system reliability, probabilistic seismic hazard analysis, artificial neural network

TABLE OF CONTENTS

List of Figures

List of Tables

1. Introduction

Natural disasters have serious impacts on infrastructure systems, including transportation, electricity, gas and water distribution networks, etc., causing structural damage and massive economic losses in both commercial and residential activities. Because these systems are structurally complicated, interdependent and interconnected, the damage to any component infrastructure will cascade into another resulting in widespread failure or disruption of human activities. In particular, earthquakes are one of the natural disasters that can cause significant physical damage and disconnection of transportation networks. Damage to transportation system is a major concern, as it imposes an extra burden on other lifelines (Applied Technology Council 2004, Nicholson and Dalziell 2003). One of the most significant impacts of earthquakes is the disconnection of bridge transportation networks, which can impede post-hazard emergency responses, such as the movement of emergency vehicles. This is because bridges are one of the most critical components of transportation networks, acting as "bottlenecks": the structural failure of a bridge can interfere with traffic flow and decrease network performance (Furtado 2015). Hence, it is essential to assess the seismic risk of a bridge transportation system and accurately predict the post-hazard performance.

The objective of seismic risk assessment is to obtain useful information for risk-informed decision-making regarding seismic hazard mitigation and disaster management. Seismic risk assessment of critical infrastructure systems has been conducted extensively. Nuti et al. (2010) proposed a methodology for the reliability assessment of electric power, water and road systems, not considering the interdependence between the networks, whereas Poljnašek et al. (2012) proposed a method for gas and electricity transmission networks considering the increased vulnerability due to interdependency. Dueñas-Osorio et al. (2007) evaluated seismic responses considering the interdependency of the water and power networks in Shelby County, Tennessee 56 area, and proposed a method to apply mitigation action efficiently. With regard to transportation networks, Kiremidjian et al. (2007) evaluated the risk posed by earthquakes to a transportation system in terms of direct loss caused by damage to bridges in the San Francisco Bay area. Moreover, various studies have proposed post-earthquake flow models for evaluating the impact of seismic events and the functionality of the networks (Chang et al. 2010, Eisenberg et al. 2017)

Most infrastructure systems are composed of a number of components, and their reliability is predicted by overall system states or the probability that the system does not fail. Therefore, to perform the seismic risk assessment of a bridge transportation network, system reliability analysis is required to predict the post-hazard flow capacity of the network after a seismic event. However, predicting both the disconnection probabilities in the network and the uncertain traffic flow capacity are challenging tasks due to the following reasons. First, the seismic risk itself contains a great deal of uncertainty, namely, location, magnitude, and the resulting intensity of possible earthquakes in target networks. Second, conceptualizing and quantifying system performance measures in uncertain events is not easy, because

their determination depends on various specifications of the system under different situations. An appropriate performance measure can quantify the ability of the network more accurately, especially for realistic and complex bridge transportation networks. While numerous performance measures have been proposed for such quantification, these definitions are sometimes inconsistent and few attempts to review all literature (Faturechi and Miller-Hooks 2014). Third, quantifying these uncertainties and accurately estimating the performance of system reliability may increase computational costs and can be time-consuming tasks to deal with in possible earthquake scenarios and the resulting seismic fragility of the component bridges.

The characterization of uncertainty, accuracy, and efficiency motivated the research reported in this thesis, which focuses on proposing a new method of system-level seismic risk assessment. First, to assess the seismic hazard, the uncertainty of earthquake locations and magnitudes is analyzed probabilistically, which is also referred to as probabilistic seismic hazard analysis (PSHA) (Kramer 1996). Cornell (1968) firstly introduced the concept of PSHA, and McGuire (2004, 2007) summarized the early development of PSHA and provided probabilistic estimation of losses from earthquakes along with information on practical estimation of the input parameters. PSHA aims to quantify the uncertainties and produce a desired description of them as explicit probability distributions (Baker 2008). This mathematical analysis helps to quantify the uncertainties in an earthquake event.

Post-hazard network performance analysis is also important because the analysis results are necessary to make effective plans for emergency evacuations, rescue, and recovery. Performance measure typically have target value which defines the acceptable conditions for a network. For example, Murray-Tuite (2006) proposed quantitative measures for transportation system adaptability, mobility, and recovery based on simulation method for computation. Faturechi and Miller-Hooks (2014) provided a comprehensive framework for conceptualizing, categorizing and quantifying system performance measures, especially numerical-transportation-related example. Moreover, The Analysis Procedures Manual (Oregon department of transportation 2018), or APM, provides the current methodologies, and procedures for conducting analysis of transportation plans and projects. In this manual, transportation analysis performance measure, as also referred to as measures of effectiveness (MOEs), are quantitative estimates on the performance of a transportation network. In traffic engineering, there are commonly used performance measures such as volume to capacity ratio, level of service, vehicle delay, travel time, and capacity.

To deal with the uncertainties associated with earthquakes and infrastructure response, a few sampling-based approaches was often used (Ellingwood and Kinali 2009). However, this may increase the computational costs and can be time-consuming tasks to deal with in possible component failure scenarios. To overcome these challenges, a few non-sampling-based approaches have been developed. Li and He (2002) proposed a recursive decomposition algorithm for seismic reliability evaluation to compute the probabilities of disconnections in a network, while Kang et al. (2008) and Kang and Song

(2008) proposed a new non-sampling-based system reliability analysis method, namely the matrix-based system reliability (MSR) method. The matrix-based framework of the MSR method enables rapid calculation of multiple probability scenarios and separation of network and vulnerability analyses. Employing the MSR method, Lee et al. (2011) estimated the post-hazard flow capacity of a bridge transportation network considering ten seismically vulnerable bridge. The MSR method was successfully applied for evaluating the system reliability within a network. Lastly, this thesis further develops original numerical example such that it can account for network performance capacity more accurately according to change in maximum flow capacity into total system travel time (TSTT). Since the evaluation of TSTT requires function to calculate this measure and thousands of network states as input data, a different approach based on a *surrogate model* or *meta-model* is used. Numerous engineering problems have benefited from such models, particularly when difficulties are found in the construction or application of a mathematical model, and likewise when considering optimization procedures (Pina et al. 2013). Surrogate models can be constructed to provide approximate results through function using only some of the input data, thus not requiring detailed knowledge of the dynamic parameters of the system (Pina et al 2008 and Ford et al. 2011). The ANN is one of the widely used as surrogate model and advantages of learning algorithms to approximate discrete or continuous target values. The merit of this model is useful to several applications such as classification, clustering, pattern recognition, function approximation, optimization, signal processing, and robotics (Widrow et al. 1993). For example, among many approaches and attempts available for surrogate model, the ANN has been successfully applied in many fields (Basheer and Hajmeer 2000, Ben-Nakhi and Mahmoud 2004, Sung 1998, Pina et al. 2013, and Melo et al. 2014).

This thesis is organized into two steps. In the first step, a new framework for seismic risk assessment is proposed by employing PSHA with the MSR method, which consists of three small steps as follows: 1) seismic fragility estimation of the bridges based on PSHA; 2) system-level performance estimation using the matrix-based framework of the MSR method; and 3) seismic risk assessment based on the total probability theorem. PSHA enables the seismic fragility estimation of the components considering the uncertainty of earthquake events. Moreover, MSR method helps to conduct efficient calculations for seismic risk assessment and system reliability. In the second step, the proposed framework is further developed for more accurate assessment of network performance by introducing an advanced performance measure of bridge transportation networks and ANN-based surrogated model. In the further developed method, the matrix-based seismic risk assessment using ANN model enables the system performance estimation with only partial real data. The method in both steps is systemically used to carry out a post-hazard bridge network flow analysis employing the matrix-based framework.

The proposed method offers insights into seismic risk assessment and system reliability and provides statistical moments of the network performance, critical earthquake scenarios and component importance measures, which can be useful for decision-makers to reduce the seismic risk of a target

area. In summary, the seismic risk assessment employing PSHA are successfully integrated with the matrix-based framework to perform system reliability analysis in a computationally efficient manner.

2. Theoretical Background

2.1. Probabilistic seismic hazard analysis (PSHA)

The main concern of seismic hazard analysis is to ensure that structural damage is assigned a desired level of performance and intensity. However, the estimation of ground motion intensity corresponding to hazards is a challenging task due to the uncertainty in seismic hazards and structural damage, as well as the complex nature of the network performance in the area. PSHA aims to consider the uncertainties with respect to the size, location, and resulting intensity of the earthquake, and combine them to produce the description of a possible earthquake event that may occur in an area of interest. In PSHA, a seismic hazard is defined as a physical phenomenon, such as ground shaking or failure caused by an earthquake, which can have serious effects on human activities (Kramer 1996).

The main goal of seismic hazard analysis is to refine the understanding of earthquake magnitudes and the corresponding intensity of ground shaking. Particularly, PSHA allows a better insight into earthquake generation and seismic effects on a region by quantifying the uncertainties and estimating the distribution of earthquake occurrences (Sánchez-Silva et al. 2005). The resulting intensity is calculated by the ground motion prediction model (GMPE), also referred to as the *seismic attenuation model*. This prediction model is generally developed using statistical regression on the observation from various data of observed and cumulated ground motion intensities. For the precise estimation of the risk caused by a seismic event in a particular area, the seismic hazard should be analyzed probabilistically, by considering uncertainties in earthquake locations and magnitudes. The approach presented in this thesis is based on the concepts as exemplified in the study of Baker (2008). PSHA comprises five steps as follows:

1. Identification of all earthquake sources through means of observation of past locations and geological evidence
2. Quantification of the distribution of earthquake magnitudes (the rates at which earthquakes of various magnitudes are expected to occur)
3. Characterization of the source-to-site distances corresponding to possible earthquake events
4. Calculation of the resulting intensity using ground motion prediction model as a function of earthquake magnitude, distance, etc.
5. Combination of uncertainties in earthquake magnitude, location, and ground motion intensity, using the total probability theorem.

In the proposed method, the uncertainties of earthquake locations and magnitudes are determined using PSHA based on past earthquake records. The locations in cities with the most severe damage were assumed to be the epicenters of past earthquakes in related studies (Lee et al. 1976, Usami 1979, Poirier and Taher, 1980, and Lee and Yang, 2006). Rather than considering all earthquake sources capable of producing damages to the structure, for the sake of simplicity, this thesis focuses uniquely on the

epicenters of past earthquakes at sites of interest for the seismic risk assessment. Meanwhile, to account for the uncertainty in earthquake magnitudes, a series of modeling procedures is required. In this study, one such modeling procedure is briefly introduced, whereas more details on PSHA are provided in Baker (2008).

2.1.1. Earthquake magnitude uncertainty modeling

To account for the uncertainty in earthquake magnitudes, as the first step, the occurrence rate of earthquakes in a target region is assumed to follow the Gutenberg-Richter (G-R) recurrence law (Gutenberg and Richter 1944) given by

$$\log \lambda_m = a - bm \tag{1}$$

where m is the specific earthquake magnitude of interest, λ_m is the occurrence rate of earthquakes with magnitudes greater than m, and a and b are the constants which are referred to as G-R recurrence parameters and can be determined from past earthquake records. When the minimum and maximum magnitudes are determined using Equation (1), the cumulative distribution function (CDF) of the earthquake magnitude can be derived as (Baker 2008)

$$F_M(m) = P(M \leq m | m_{min} \leq M \leq m_{max}) = \frac{1 - 10^{-b(m-m_{min})}}{1 - 10^{-b(m_{max}-m_{min})}} \tag{2}$$

where $F(\cdot)$ denotes the CDF of a random variable, M is the earthquake magnitude, and m_{min} and m_{max} are the minimum and maximum of the earthquake magnitude, respectively. By differentiating Equation (2), the probability density function (PDF) can be obtained as

$$f_M(m) = \frac{b\ln(10)10^{-b(m-m_{min})}}{1 - 10^{-b(m_{max}-m_{min})}} \tag{3}$$

where $f(\cdot)$ denotes the PDF of a random variable. This bounded PDF is termed the *bounded Gutenberg-Richter recurrence law* (Baker 2008), and it can be obtained based on the frequency of past earthquakes with varying magnitudes.

Once the bounded PDF is obtained, to generate possible earthquake scenarios with varying magnitudes as an input of seismic risk assessment, the continuous distribution of earthquake magnitudes needs to be converted into a discrete set of magnitudes of interest. The probabilities of occurrence, according to this discrete set of magnitudes, represent only a partial distribution of the magnitude at a site. Subsequently, a normalizing process that divides all of the cumulated values by their sum is required so that the sum of the probability distribution in the partial magnitudes amounts to 1.0.

2.1.2. Seismic attenuation model

After modeling the probability distribution of earthquake magnitudes, the associated distances from the earthquake source to the bridges (i.e., source-to-site distances) of the target transportation network and

the ground motion intensities need to be analyzed. Given the earthquake magnitude and location, the ground motion intensities at different bridges must be analyzed based on a seismic attenuation model. One such representative model is the ground motion prediction equation (GMPE). In this equation, the ground motion intensity is expressed as a function of several parameters including earthquake magnitude, distance, and local site effects (Joyner and Boore 1993). For seismic event i recorded at the site j, the general form of GMPE considering the total variability of the ground motion is given as Emolo et al. (2015)

$$Y_{ij} = \overline{Y_{ij}(M_i, R_{ij}, \xi_{ij})} + \eta_i + \varepsilon_{ij} \tag{4}$$

where Y_{ij} represents the response variable, such as peak ground acceleration (PGA), peak ground velocity (PGV), and spectral acceleration (SA), which often corresponds to the logarithm (natural or common), M_i is the earthquake magnitude of the event, R_{ij} is the distance between the epicenter of event i and the site j, ξ_{ij} is the geomorphic factor affecting the ground motion, $\overline{Y_{ij}(M_i, R_{ij}, \xi_{ij})}$ is the mean of the response variable, and η_i and ε_{ij} are the inter- and intra-event parameters representing the uncertainty of the ground motion. The parameter η_i represents the uncertainty of the ground motion inherent to the earthquake itself, termed the *Earthquake-to-Earthquake* variability, whereas the parameter ε_{ij} denotes the uncertainty of the ground motion because of the energy paths and geological characteristics, termed the *Site-to-Site* variability (Emolo et al. 2015).

In this study, as in HAZUS-MH (FEMA 2003), the structural vulnerabilities of a bridge are described by the probability conditioned to the ground motion intensity which is expressed in terms of SA. In addition, the GMPE proposed by Emolo et al. (2015) is introduced. The GMPE was derived using statistics of 222 earthquakes recorded at 132 stations in South Korea, employing the nonlinear mixed effects regression analysis. Moreover, the equation includes both fixed and random effects accounting for inter- and intra-event residual values. Using this equation, the mean of the response variable in Equation (4) can be given as

$$\overline{Y_{ij}(M_i, R_{ij}, \xi_{ij})} = \ln \left(SA_{ij} \right)$$
$$= c_1 + c_2 M_i + c_3 \ln \left[\sqrt{R_{ij}^2 + h^2} \right] + c_4 R_{ij} + c_5 s \tag{5}$$

where SA_{ij} is the spectral acceleration caused by an earthquake event i at site j, h is the focal depth, c_k ($k = 1, \ldots, 5$) are the regression coefficients, and s is the station dummy variable, which assumes a value of -1, 0, or 1. The dummy variable depends on the sign of the mean residual (negative, zero, or positive, respectively), and it is generally chosen by the seismological observatory.

In addition, the inter- and intra-events parameters in Equation (4) can be expressed by the following equations (Goda and Hong 2008, Goda and Arkinson 2009, Sokolov et al., 2010):

$$\eta_i = \frac{\sigma_\eta^2}{\sigma_\eta^2 + \sigma_\varepsilon^2}, \qquad \varepsilon_{ij} = \frac{\sigma_\varepsilon^2}{\sigma_\eta^2 + \sigma_\varepsilon^2}\rho(\Delta_{ij}) \tag{6}$$

where σ_η^2 and σ_ε^2 are the inter- and intra-standard residuals, respectively, Δ_{ij} is the distance between the epicenter of event i and the site j, and $\rho(\Delta_{ij})$ is the spatial correlation equation. For the special correlation equation, in this study, the following equation suggested by Goda and Hong (2008) is introduced:

$$\rho(\Delta_{ij}) = e^{(-0.509\sqrt{\Delta_{ij}})} \tag{7}$$

As described above, PSHA enables the consideration of earthquake uncertainty. For the given location and magnitude of an earthquake, the ground shaking intensity of individual bridges is expressed in terms of SA using the GMPE in Equation (4). Then, the probabilities of several damage states of bridges can be provided by fragility curves. Subsequently, it becomes possible to estimate the performance of the bridge transportation network, which requires system reliability analysis.

2.2. Matrix-based system reliability (MSR) method

The MSR method was recently proposed and successfully applied to evaluate the post-earthquake performance of a bridge transportation network in terms of the disconnection probability (Kang et al. 2008) and maximum flow capacity (Lee et al. 2011). The MSR method conducts a matrix-based framework of system reliability analysis in which two tasks of "system event description" and "probability calculation" are performed separately. This enables efficient evaluations of the post-hazard capacity under possible component scenarios of the system without repeatedly performing deterministic flow capacity analyses.

In this study, a bridge transportation network is considered, consisting of n_b bridges, each of which has n_d distinct damage states. Under the assumption that component bridges are statistically independent, there is a total of $(n_d)^{n_b}$ damage scenarios, which are mutually exclusive and collectively exhaustive (MECE) events. Due to their mutual exclusiveness, the probability of the system event E_{sys}, i.e., $P(E_{sys})$ is the sum of the probabilities that belong to the system event. Therefore, $P(E_{sys})$ can be easily computed by the inner product of the two vectors, namely the probability and event vectors (Kang et al. 2008 and Lee et al. 2011)

Let $P_{i(j)}$, $i = 1, \ldots, n_b$, $j = 1, \ldots, n_d$, indicate the probability that the ith bridge enters the jth damage state. Then, the probability of dealing with multiple damage states can be expressed by the following sequential matrix calculations,

$$\mathbf{p} = \begin{bmatrix} P_{(1,1,\ldots,1)} \\ P_{(2,1,\ldots,1)} \\ \vdots \\ P_{(d_1,d_2,\ldots d_{n_b})} \\ \vdots \\ P_{(n_d,n_d,\ldots n_d)} \end{bmatrix} = \begin{bmatrix} P_{1,(1)} \times P_{2,(1)} \times \ldots \times P_{n_b,(1)} \\ P_{1,(2)} \times P_{2,(1)} \times \ldots \times P_{n_b,(1)} \\ \vdots \\ P_{1,(d_1)} \times P_{2,(d_2)} \times \ldots \times P_{n_b,(d_{n_b})} \\ \vdots \\ P_{1,(n_d)} \times P_{2,(n_d)} \times \ldots \times P_{n_b,(n_d)} \end{bmatrix} \tag{8}$$

where $\mathbf{p}$ denotes the probability vector for all possible damage scenario of the system, d_i is the damage state of the ith bridge (where $i = 1, \ldots, n_b$), and $P(\ldots)$ denotes the probability of a damage state system with the numbers in the subscript. The subscript signifies the component damage states. For example the second row, $P_{(2,1,\ldots,1)}$ depicts that all of the components are in the first damage state, except for the first component, which is in the second damage state.

To carry out a post-hazard flow analysis employing the MSR method, a certain corresponding quantity can be estimated using the matrix-based framework. Therefore, a new column vector $\mathbf{q}$, termed the "quantity vector", is constructed, which has same size as $\mathbf{p}$ in Equation (8). For all damage states of the system, the quantities are generalized to

$$\mathbf{q} = \begin{bmatrix} Q_{(1,1,\ldots,1)} \\ Q_{(2,1,\ldots,1)} \\ \vdots \\ Q_{(d_1,d_2,\ldots d_{n_b})} \\ \vdots \\ Q_{(n_d,n_d,\ldots n_d)} \end{bmatrix} = \begin{bmatrix} f\big(q_{1,(1)}, q_{2(1)}, \ldots, q_{n_b,(1)}\big) \\ f\big(q_{1,(2)}, q_{2,(1)}, \ldots, q_{n_b,(1)}\big) \\ \vdots \\ f\big(q_{1,(d_1)}, q_{2,(d_2)}, \ldots, q_{n_b,(d_{n_b})}\big) \\ \vdots \\ f\big(q_{1,(n_d)}, q_{2,(n_d)}, \ldots, q_{n_b,(n_d)}\big) \end{bmatrix} \quad (9)$$

where $\mathbf{q}$ denotes the quantity vector, $Q(\ldots)$ denotes the performance quantity of the system with damage states as the subscript, and $f(\cdot)$ is the post-earthquake capacity of the network. In this study, the maximum flow capacity, i.e., the maximum number of vehicles that can pass per unit time, is considered as a measure of the network flow capacity (Ahuja et al 1993 and Nojima 1998). For each maximum flow capacity corresponding to the damage states of the network, the MATLAB® version of Boost Graph Library (Boost 2008 and Gleich 2008) is employed.

As results of the probability vector $\mathbf{p}$ in Equation (8) and the quantity vector $\mathbf{q}$ in Equation (9), the statistical parameters such as the mean, variance, and coefficient of variation (c.o.v.) can be obtained as follows:

$$\mu_Q = \mathbf{q}^{\mathbf{T}}\mathbf{p}$$
$$\sigma^2{}_Q = \mathbf{p}^T(\mathbf{q}.*\mathbf{q}) - \mu_Q{}^2 \quad (10)$$
$$\delta_Q = \sigma_Q/|\mu_Q|$$

where μ_Q, $\sigma^2{}_Q$ and δ_Q are the mean, variance, and c.o.v. of the network flow capacity Q, respectively. In Equation (10), '.*' denotes the element-by-element multiplication.

Furthermore, an importance measure (IM) of components can also be evaluated using a matrix-based formulation. For regional authorities who need to make decisions regarding the allocation of budgets and other resources, it is important to identify the important locations of a transportation network (Park et al. 2015). To evaluate the relative importance of these components, several IMs have been developed in system engineering. In this study, the reduction factor (RF) proposed by Lee et al. (2011) is adopted as a new IM. RF computes the reduction of the expected mean flow capacity by the observed event E_{obs}, e.g., the failure of a bridge, which can quantify the relative importance of

component bridges. The computation of the proposed RF is as follows:

$$RF = 1 - \mu_{Q|E_{obs}} / \mu_Q = 1 - (\mathbf{q}^\mathbf{T}\tilde{\mathbf{p}})/(\mathbf{q}^\mathbf{T}\mathbf{p}) \qquad (11)$$

where $\mu_{Q|Eobs}$ represents the conditional mean of the flow capacity given an observed event, E_{obs}, and

$\tilde{\mathbf{p}}$ is the probability vector constructed using the conditional probabilities of components given by E_{obs}.

2.3. Artificial neural network (ANN)

The artificial neural network (ANN) has been developed extensively during the past three decades. An ANN is a branch of artificial intelligence techniques, and it represents a computing model whose layered structure is similar to the networked structure of neurons in the human brain with layers of inter-connected nodes.

The ANN is defined by the neurons, topological structure, and learning rules. Analogous to the neurons in the human brain, an artificial neuron consists of inputs, weights, processing units, and outputs (Haykin 1994). A typical ANN is composed three of more layers: one input layer, one output layers, and one or two hidden layers. The input layer consists of a data set, which represents the problem of interest, and the output layer indicates a related response or function result regarding each problem. This approach has the ability to learn from data, and it can be trained to recognize patterns, classify data, and forecast future events. The goal of learning is to achieve a set of weights that will produce an output most resembling the target (Jensen et al. 1999). Therefore, it is important for input layers to match each input to the output.

For the best configuration of the ANN, *training* processes are carried out, to enable the trained network to provide a good approximation of the desired response. During the training process, the constructed ANN iteratively minimizes the mean square error of the data set, adjusting a set of known input-output pairs until the output error falls below an acceptable value.

2.3.1. Artificial neuron and activation function

The neuron is the cell responsible for reception of external inputs, processing of signals, and transmission. Figure 1 shows a simplified artificial model of a neuron, also referred to as the McCulloch-Pitts neuron (Widrow et al. 1994)

Figure 1. Simplified artificial model of a neuron

Each neuron receives a designated number of inputs x_i (where $i = 1, \ldots, N$) and calculates a linear combination of these inputs using weights w_i to produce the w*eighted input z*, that can be expressed by

$$z = \sum_{i=1}^{N} w_i x_i \tag{12}$$

Next, it produces an output y through an activation function $f(z)$, which serves for increasing monotonic behavior over a range of values for z, assuming a constant value outside this range (Pina et al. 2013). Several configurations of adjusting z values were tested, and the continuous log *sigmoid function*, illustrated in Figure 2, is widely used in ANN applications. As the sigmoid function is bounded between 0 and 1, the input data needs to be normalized within the same range. This is because the normalization or scaling process aids in the appropriate preparation for the training data set. This function is expressed by the following equation:

$$y = f(z) = \frac{1}{1 + e^{-z}} \tag{13}$$

Figure 2. Typical sigmoid function

2.3.2. Layers and methods for determining number of hidden neurons

Neural networks consist of several neurons in layers, which can be simply illustrated as in Figure 3. The structure of the network comprises one or more layers between the input and output layers. If the neurons are arranged into layers, then all neurons in the same layer send or receive signals through the specified learning process. In further detail, the input layer receives data, which represents the problem of interest from the user. The output layer represents the targeted response or desired performance of an unknown function. This layer sends the data to the user. The intermediate layer is also referred to as the *hidden layer* that can contain zero or more 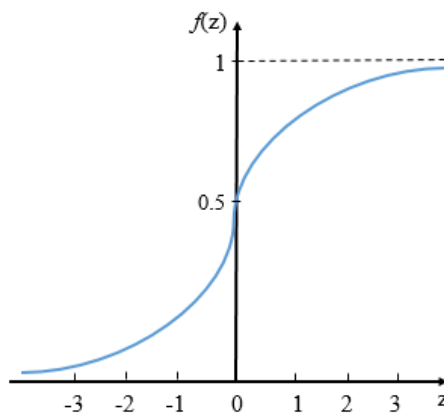layers. Figure 3(b) illustrates two-layer networks that are widely used in most ANN applications, with only one hidden layer.

Figure 3. Topology of typical layered neural networks: (a) single layer neural network and (b) multilayer neural network

Here, the determination of the number of neurons in the hidden layer, N_h, is one of the major difficulties in the process of creating the ANNs topology. If N_h is too small, then the network may not be strong enough to fulfill desired requirements. In contrast, too large N_h may cause long training steps and recalling time (Tijanana et al. 2016). In this study, five different methods were applied to choose the number of hidden neurons, as shown in Table 1. N_i and N_o depict the number of input neurons and the number of output neurons, respectively.

Method 1	Li, Chow and Yu, 1995
Equation	$$N_h = \frac{\sqrt{1 + 8N_i} - 1}{2}$$
Method 2	Rules of Thumb by Heaton, 2005
Equation	$$(N_i + N_o) \cdot \frac{2}{3}$$
Method 3	Shibata and Ikeda, 2009
Equation	$$N_h = \sqrt{N_i \cdot N_o}$$
Method 4	Hunter, Yu, Pukisi Ⅲ, Kolbusz and Wilamowski, 2012
Equation	$$N_h = \log_2(N_i + 1) - N_o$$

Method 5	Sheela and Deepa, 2013
Equation	$N_h = \dfrac{(4N_i^2 + 3)}{N_i^2 - 8}$

Table 1. Methods for determining number of hidden neurons

Finally, the network output y_j of the jth hidden neuron can be expressed by combining Equations (12) and (13):

$$y_j = \frac{1}{1 + \exp(-\sum_{i=1}^{N} w_{ij} x_i)} \tag{14}$$

where w_{ij} is the weight of the input x_i for the jth neuron. The network output y_o can be derived when the optimal N_h are determined through comparison of those methods, similarly to Equation (14):

$$y_o = \sum_{j=1}^{N_h} w_{jo} \frac{1}{1 + \exp(-\sum_{i=1}^{N} w_{ij} x_i)} \tag{15}$$

where w_{jo} denotes the weight of the contribution of the jth hidden neuron to the network output.

3. Proposed Method

3.1 Matrix-based seismic risk assessment employing PSHA

The objective of a seismic risk assessment is to obtain useful information for risk-informed decision-making regarding seismic hazard mitigation. Seismic risk assessment of critical infrastructure has been conducted extensively, addressing water distribution, electric power, and transportation networks. Various studies have proposed the direct loss of components from the networks based on sampling-based approaches. However, dealing with possible component failure scenarios may a time-consuming task. To overcome this problem, a few non-sampling-based system reliability analysis methods have been developed. The MSR method is one of the approaches proposed by Kang et al. (2008) and Kang and Song (2008).

Most previous studies conducted seismic risk assessments without probabilistic seismic hazard analysis (PSHA). At a fundamental level of seismic risk assessments, there is a consensus regarding a great degree of uncertainty regarding the location, magnitude, and resulting intensity of possible earthquakes, such that a mathematical approach for considering uncertainty in the form of PSHA is necessary. PSHA has the merit of considering earthquake uncertainty, as it is useful for determining the uncertainty of earthquake locations and magnitudes in a target region (Baker 2008). However, employing PSHA in seismic risk assessment is not easy, as it requires dealing with a large number of possible earthquake scenarios and quantifying the performance of a bridge transportation network. This

section proposes a new method that is a matrix-based system-level seismic risk assessment for bridge transportation networks employing PSHA. The MSR method is successfully applied to perform system-level seismic risk assessment. It enables rapid calculation of multiple probability scenarios corresponding to the number of potential earthquake sources.

The main goal of the proposed method is to estimate the performance of a bridge transportation network after a seismic event, considering earthquake uncertainty. For this purpose, PSHA is employed to deal with the uncertainty of earthquake magnitudes and locations in the proposed method. The proposed method introduces the matrix-based framework of the MSR method to evaluate the uncertainty of the performance of a bridge transportation network at the system level, due to uncertain earthquakes.

The MSR method was originally developed to perform system reliability analyses of various structures (Kang et al. 2008, 2012). However, its matrix-based framework provides efficient calculation for the system reliability analysis of lifelines, and it was successfully applied to evaluate the system-level performance of bridge transportation networks (Lee et al. 2011 and Kang et al. 2017). Lee et al. (2011) derived the post-hazard flow capacity considering the structural deterioration of bridges within a network. In previous research, the time-dependent bridge fragilities could be computed efficiently using the MSR method, while the corresponding flow capacities were evaluated using a maximum flow capacity analysis algorithm. The matrix-based framework allowed the separate probability calculation and network flow analysis, which enabled performing extensive parametric studies and time-varying post-hazard flow analyses without repeated network flow analyses. Similarly, in this research, the matrix-based framework of the MSR method is introduced to deal with the earthquake uncertainty.

As mentioned above, by assuming that all components are statistically independent, basic MECE events can be simply computed by use of the matrix calculation proposed in Equation (8). However, many reliability problems of network systems are composed of various components that are statistically inter-dependent. Nevertheless, applying the concept of a *common source random variable* (CSRV), a system event can be described by the combination of component MECE events, which are conditionally independent.

In the proposed method, the earthquake magnitude and various locations are introduced as CSRVs that influence the damage states of individual bridges within the network. When the uncertainty of earthquake magnitudes and locations is characterized by PSHA and defined as CSRVs, applying the total probability theorem, the probability of a system can be expressed as

$$P(E_{sys}) = \iint P(E_{sys}|m,l) f_{M,L}(m,l) \, dm \, dl \qquad (16)$$

where E_{sys} is the system event of interest, M is the earthquake magnitude, L is the earthquake location, and $f_{M,L}(m,l)$ is the joint PDF of the earthquake magnitude and location when $M = m$ and $L = l$. With the conditional PDF, the joint PDF in Equation (16) can be changed to

$$f_{M,L}(m,l) = f_{M|L}(m|l)f_L(l) \tag{17}$$

where $f_L(l)$ is the marginal PDF of the earthquake location and $f_{M|L}(m|l)$ is the marginal PDF of the earthquake magnitude conditioned to $L = l$.

Since the damage states of individual bridges become conditionally statistically independent given the earthquake magnitude and location, the conditional probability vector $\mathbf{p}|(m,l)$ can be constructed using Equations (8), (16), and (17):

$$
\mathbf{p}|(m,l) = \begin{bmatrix}
P_{(1,1,\dots,1)}|(m,l) \\
P_{(2,1,\dots,1)}|(m,l) \\
\vdots \\
P_{\left(d_1,d_2,\dots d_{n_b}\right)}|(m,l) \\
\vdots \\
P_{(n_d,n_d,\dots n_d)}|(m,l)
\end{bmatrix}
\tag{18}
$$

$$
= \begin{bmatrix}
\left(P_{1,(1)}|(m,l)\right) \times \left(P_{2,(1)}|(m,l)\right) \times \dots \times \left(P_{n_b,(1)}|(m,l)\right) \\
\left(P_{1,(2)}|(m,l)\right) \times \left(P_{2,(1)}|(m,l)\right) \times \dots \times \left(P_{n_b,(1)}|(m,l)\right) \\
\vdots \\
\left(P_{1,(d_1)}|(m,l)\right) \times \left(P_{2,(d_2)}|(m,l)\right) \times \dots \times \left(P_{n_b,\left(d_{n_b}\right)}|(m,l)\right) \\
\vdots \\
\left(P_{1,(n_d)}|(m,l)\right) \times \left(P_{2,(n_d)}|(m,l)\right) \times \dots \times \left(P_{n_b,(n_d)}|(m,l)\right)
\end{bmatrix}
$$

where $P_{(\dots)}|(m,l)$ represents the conditional probability of a component's damage state with the numbers in the subscript. Unlike the probability vector, the quantity vector $\mathbf{q}$ can remain the same as in Equation (9), because the matrix-based framework of the MSR method enables the separate construction of the probability and quantity vectors.

Hence, applying the total probability theorem, the statistical parameters can be obtained as

$$
\mu_Q = \iint \mu_Q(m,l)f_{M,L}(m,l)dmdl = \iint \mathbf{q}^{\mathbf{T}}(\mathbf{p}|(m,l))dmdl
$$

$$
\sigma_Q{}^2 = \iint (\mathbf{p}|(m,l))^{\mathbf{T}}(\mathbf{q}.*\mathbf{q})dmdl - \mu_Q{}^2 \tag{19}
$$

$$
\delta_Q = \sigma_Q/|\mu_Q|
$$

Similarly, the reduction factor RF can be calculated as

$$
\text{RF} = \iint \{1 - (\mathbf{q}^{\mathbf{T}}\tilde{\mathbf{p}}|(m,l))/(\mathbf{q}^{\mathbf{T}}\mathbf{p}|(m,l))\}dmdl \tag{20}
$$

where $\tilde{\mathbf{p}}|(m,l)$ is the conditional probability vector which can be constructed using Equation (11).

The proposed method consists of three steps: 1) seismic fragility estimation of the bridges based on PSHA, 2) system-level performance estimation using the matrix-based framework of the MSR method, and 3) seismic risk assessment based on the total probability theorem. In the proposed method, PSHA enables the seismic fragility estimation of the component bridges considering the uncertainty of earthquake locations and magnitudes, and it is systemically used to carry out a post-earthquake bridge

network flow analysis employing the MSR method.

The MSR method provides an efficient framework for seismic risk assessment, which performs separate calculations for the seismic hazard and network flow analyses. PSHA contains the investigation of earthquake generation using several proposed relations provided in Equations (1)–(7), with the aim to obtain the probabilities of structural damage scenarios considering bridge fragilities, given the earthquake magnitude and location. When the corresponding network flow capacities are identified, and the probability vector and quantity vector are constructed, the MSR method enables the calculation of various risk-informed measures and statistical use of the total probability theorem. Figure 4 shows a flow chart of the seismic risk assessment proposed in this research.

Figure 4. Flow chart of proposed seismic risk assessment employing PSHA and MSR method

To initiate the analysis employing the proposed method, it is first necessary to collect input data in the form of information related to the study area. The input data can be classified into three groups: exposure data, hazard data, and structural vulnerability data. The exposure data contains the topology information of the target transportation network, such as the number of nodes and links in the target region. Past earthquake data are likewise necessary to identify the earthquake uncertainty using PSHA. The hazard data contain the mean occurrence rate of earthquakes with varying magnitudes and the seismic attenuation law (i.e., GMPE) with the spatial correlations described in Equations (4)–(7). Lastly, the structural vulnerability data include the determination of damage states in individual bridges. For this task, the fragility curve parameters provided in HAZUS-MH (FEMA 2003) are adopted in this study.

The next step is to perform seismic risk assessment employing PSHA and the matrix-based framework of the MSR method. First, using past earthquake data, earthquake sources are analyzed using the G-R relation law. The purpose of PSHA is to identify uncertainties related to the earthquake itself and calculate the resulting intensity of the ground motion. Therefore, final results comprise the PDF of earthquake magnitude and the probability of the different damage states of the component bridges. After performing the seismic hazard analysis, the proposed approach predicts the post-hazard flow capacity of a transportation network for given magnitudes and locations of earthquake. In this process, the quantity vector **q** is constructed for all possible combinations of bridge damage states using the maximum flow capacity analysis. Next, the conditional probability vector $\mathbf{p}|(m,l)$ in Equation (18) is constructed based on the probabilities of bridge damage states.

Lastly, the conditional probability vector construction is repeated for various earthquake scenarios with different earthquake magnitudes (M) and locations (L). Subsequently, the performance of the transportation network can be estimated in terms of the statistical moments of the maximum flow capacity using Equation (19). Moreover, the importance measure of RF can be estimated for all component bridges using Equation (20). Only the tasks marked by the dotted boxes in Figure 4 need to be repeated, whereas the computationally expensive maximum flow capacity analysis does not.

3.2. Numerical example

The proposed method is tested by applying it to an actual transportation network around Pohang city, South Korea. The study area is located in the southeast of the Korean Peninsula, which experienced a 5.4-magnitude earthquake in 2017 (Kang et al. 2019). Although South Korea is known to have relatively low seismic risk, this earthquake and its aftershocks raised lasting concerns, which this study aims to help address.

Figure 5 illustrates the topology of the target network, consisting of 37 nodes (red solid circles) and 46 links (blue lines). It is a network of expressways and national routes in and around Pohang city and includes ten (i.e., $n_b = 10$) relatively long bridges (illustrated in black) in the area. In this example, the objective is to measure the network capability to accommodate an emergency evacuation. Nodes 3 and 30 represent an evacuation area and a downtown area, respectively. Table 2 depicts the locations (i.e., connecting nodes) of the ten bridges, and Table 3 shows their structural information. Table 4 lists the maximum flow capacities of the links (given as the number of passing vehicles per hour). These assumptions enable the performance assessment of this network in terms of the maximum flow capacity using a node-to-node flow analysis.

Figure 5. Network map of the Pohang bridge transportation network

Bridge no.	Connecting nodes
1	(14,16)
2	(19,20)
3	(25,26)
4	(20,21)
5	(29,30)
6	(33,36)
7	(15,23)
8	(28,29)
9	(4,7)
10	(10,12)

Table 2. Locations of the bridges

Bridge no.	Total length (m)	Width (m)	Maximum span length (m)	Type	Year of construction	Design
1	169.7	20.5	25.7	PSCI	1992	Conventional
2	345	7.5	60	Steel box	2006	Seismic
3	455	28	35	PSCI	2009	Seismic
4	300	21	40	PSCI	2011	Seismic
5	25	8	12.5	RC slab	1990	Conventional
6	140	20	50	Steel box	2012	Seismic
7	102	9.5	14.6	RC slab	1992	Conventional
8	125.2	24	26	Steel plate	1975	Conventional
9	480	12.1	60	Steel box	2004	Seismic
10	115	8.3	45	Steel box	2004	Seismic

Table 3. Structural information on the bridges

Flow capacity (number of vehicles per hour)	Link numbers
2200	(2,5), (4,5), (5,6), (6,11), (10,11), (11,14), (14,15), (15,23), (22,23), (23,25), (22,28), (28,29), (29,30), (30,32)
4400	(1,2), (2,3), (2,4), (4,7), (7,10), (13,14), (14,16), (16,17), (17,18), (17,21), (18,19), (19,20), (19,24), (20,21), (21,22), (24,25), (25,26), (26,27), (27,35), (29,31), (31,32), (31,33), (32,34), (33,34), (33,36), (35,36), (35,37)
6520	(8,9), (9,10), (10,12), (12,18), (27,37)

Table 4. Maximum flow capacity of links in the Pohang transportation network

To account for the uncertainty in the seismic damage states of bridges, seismic fragility curves are introduced. Seismic fragility is defined as the conditional probability that the demand of a structure exceeds a specified threshold for a given earthquake intensity (Lee and Moon 2014, Moon et al. 2018, Nguyen and Lee 2018), and seismic fragility curves are often used for setting retrofit and repair priorities of bridges after an unexpected and disastrous event (Lee et al. 2007). In this study, SA, which can be calculated by the GMPE provided in Equation (4), is introduced as the earthquake intensity. In

addition, seismic fragility curves are obtained from HAZUS-MH (FEMA 2003), where bridges are classified by several factors including their length, type, and seismic design methods, and the corresponding seismic fragility curves are provided. Similarly, the seismic fragility curves of the ten bridges considered are determined based on the structural information presented in Table 3.

In this example, five damage states of slight, moderate, extensive, and complete damage are assumed (i.e., $n_d = 5$). The maximum flow capacities of a bridge are assumed to be related to its damage state, as described in Table 4. In the table, 100%, 75%, 50%, 25%, and 0% of original flow capacities represent the remaining traffic capacity of the five damage states. For each combination of bridge damage states in the probability vector, in the MSR method, these flow capacity values are assigned to the corresponding bridges during the maximum flow capacity analysis, so that the quantity vector can be constructed.

Damage states	Description	Flow capacities
No	–	100%
Slight	Any column experiencing minor cracking	75%
Moderate	Any column experiencing moderate cracking	50%
Extensive	Any column degrading without collapse	25%
Complete	Any column collapsing and connection	0%

Table 5. Damage states and associated flow capacities

To identify earthquake uncertainty in the target region, past earthquake data (with magnitude, M_L, greater than or equal to 3.0) was collected from the Korea Meteorological Association (KMA) website (KMA 2019), in the period from January 1st, 1918 to August 22nd, 2018. In total, twenty earthquake records were collected. Table 6 presents the earthquake information, and Figure 6 shows the locations of the twenty earthquakes (named EQ1, EQ2, …, EQ20) and ten bridges (named Bridge 1, Bridge 2, …, Bridge 10). In this example, it is assumed that all past earthquake epicenters have the same likelihood of a repeated earthquake occurrence, and the distances between the epicenters and the bridge locations are calculated based on their location information.

No.	Date	Origin time	Latitude	Longitude	Depth (km)	M_L
1	14 Apr. 1981	11:47	35.90	130.10	7	4.8
2	27 Aug. 1981	21:35	35.80	129.80	7	3.5
3	10 Dec. 1985	21:42	35.80	129.70	7	3.2
4	17 Mar. 1986	11:52	35.90	129.50	7	3.2
5	6 Oct. 1987	7:04	35.90	129.90	7	3.1

6	6 Oct. 1987	23:36	36.20	130.10	7	3.5
7	22 Oct. 1990	18:09	35.90	130.00	7	3.4
8	24 Apr. 1999	1:35	36.00	129.30	7	3.2
9	9 Jul. 2002	4:01	35.90	129.60	7	3.8
10	28 Mar. 2011	13:50	35.97	129.95	7	3.2
11	15 Apr. 2017	11:31	36.11	129.36	7	3.1
12	15 Nov. 2017	14:29	36.11	129.37	7	5.4
13	15 Nov. 2017	14:32	36.10	129.36	8	3.6
14	15 Nov. 2017	15:09	36.09	129.34	8	3.5
15	15 Nov. 2017	16:49	36.12	129.36	10	4.3
16	16 Nov. 2017	9:02	36.12	129.37	8	3.6
17	19 Nov. 2017	23:45	36.12	129.36	9	3.5
18	20 Nov. 2017	6:05	36.14	129.36	12	3.6
19	25 Dec. 2017	16:19	36.11	129.36	10	3.5
20	11 Feb. 2018	5:03	36.08	129.33	9	4.6

Table 6. Earthquake events of magnitude 3.0 and above in the study area
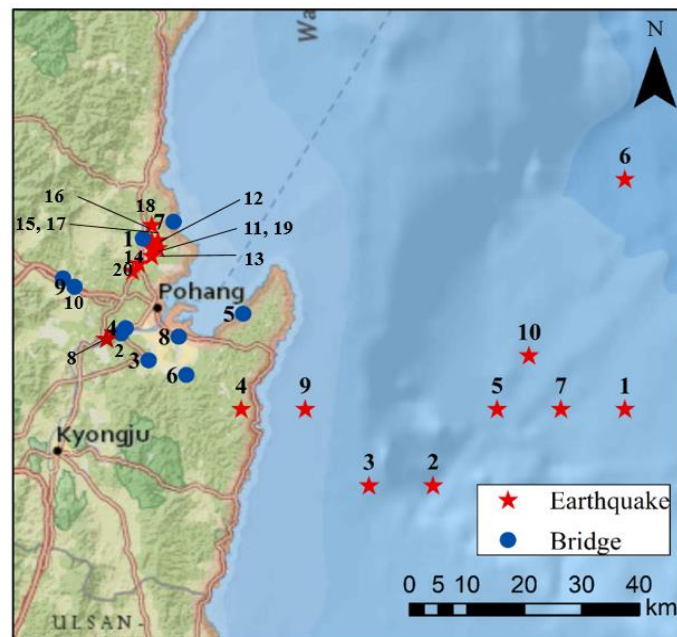

Figure 6. Locations of earthquake epicenters and bridges around Pohang, South Korea

Based on these earthquake records, the earthquake uncertainty is identified using the G-R law given in Equation (1), and the parameters of a and b are obtained as 2.167 and 0.699, respectively, from the regression analysis. The bounded PDF of the earthquake magnitude can be constructed by Equation (3).

The observations of earthquake magnitudes are shown in Figure 7 (a), along with Gutenberg-Richter recurrence laws fit to the data and Figure 7(b) shows the corresponding discrete occurrence probabilities with varying earthquake magnitudes in the range from 4.5 to 7.5.

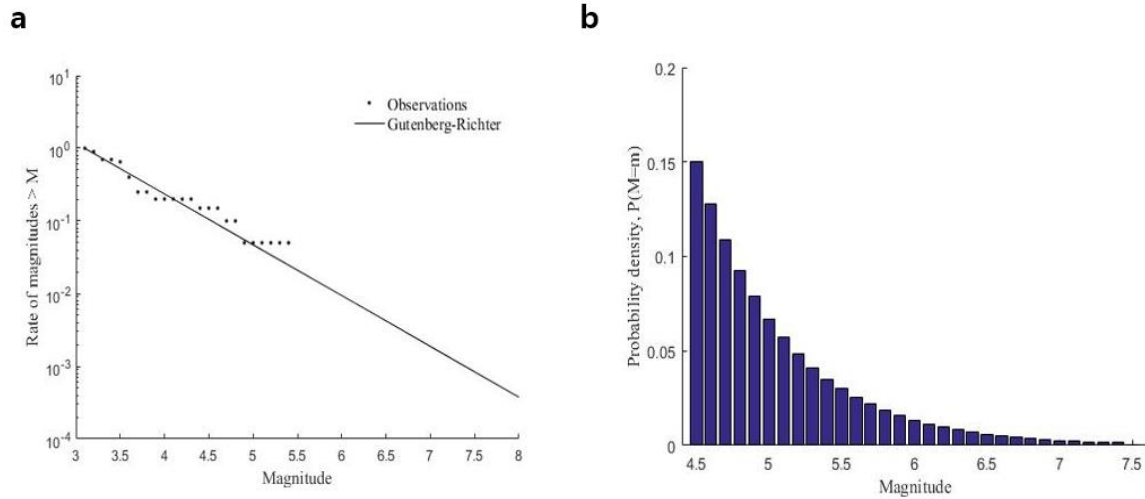**a**   **b**

Figure 7. (a) Distribution of observed earthquake magnitude along with G-R recurrence laws fit to the observations and (b) the corresponding occurrence probability

Once the PDF of the earthquake magnitude is constructed, the earthquake intensities at the ten bridge locations are calculated using Equation (4). Primarily, the mean of the response variable can be calculated using Equation (5). For the calculation, the regression coefficients c_k ($k = 1, …, 5$) are assumed to be −5.15, 0.95, −0.92, 6.8, −0.0003, and 0.208, respectively (Emolo et al. 2015), and the station dummy variable s is assumed to be −1, which was recommended by the seismological observatory (station code: PHA2) of the region.

3.3. Analysis results

3.3.1. Annual expected earthquake frequency (AEEF)

PSHA results are formulated in terms of return periods, which are defined as the reciprocal of the rate of occurrence (Sánchez-Silva et al. 2005). Based on H. Konsuk et al. (2013), the return periods of earthquakes are estimated annually. Consequently, the average recurrence time of given magnitudes can be defined as the number of years between the occurrences of an earthquake in the region. The annual expected earthquake frequency (AEEF) is simply obtained by multiplying each probability, $f_M(m)$ by the ratio of the number of observed earthquake frequencies to the entire time considered. In this study, the number of earthquake frequencies is 20 and the total time is 100 years. The average recurrence period can likewise be calculated using the following equation:

$$Recurrence\ period\ (year) = \frac{1}{AEEF\ (a\ year)} \qquad (21)$$

where *AEEF (a year)* denotes the expected annual earthquake frequencies, given particular probabilities of earthquake magnitudes. For example, the AEEF of a 5.4 magnitude earthquake is 0.001532, and resulting average recurrence period is 653 years. Figure 8 plots the AEEF (left blue y-axis) and return period (right red y-axis) corresponding to the earthquake magnitudes.
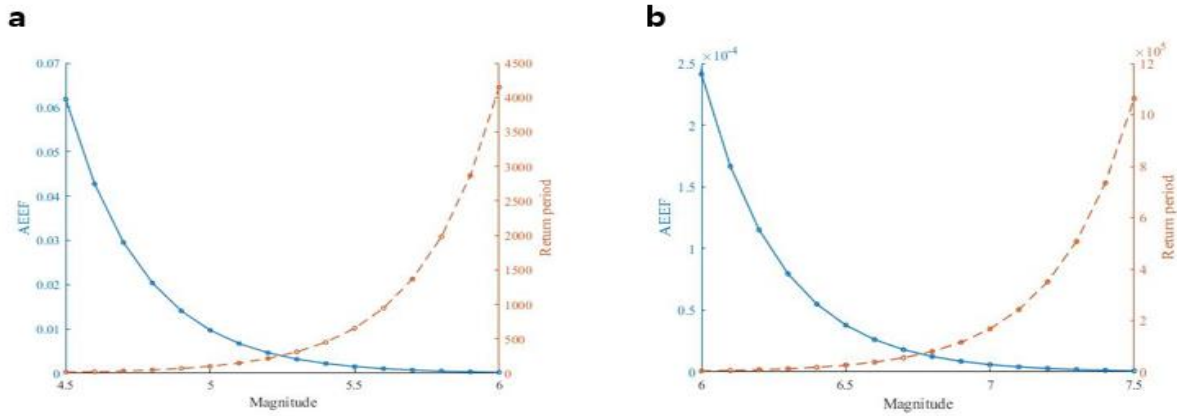

Figure 8. Return periods obtained from annual expected earthquake frequencies (a) Magnitude distribution, given $4.5 \leq M \leq 6.0$ (b) Magnitude distribution, given $6.0 \leq M \leq 7.5$

3.3.2. Evaluation of network performance

For earthquake magnitudes between 4.5 and 7.5, the statistical moments of the flow capacity according to the twenty earthquake sources are obtained by the proposed method. Figure 9 shows the mean of the maximum flow capacity with varying earthquake magnitudes for the twenty earthquake locations presented in Table 6. Results show that the mean flow decreases with increasing earthquake magnitude. When the earthquake magnitudes are relatively small, the mean flow capacity is close to the original maximum flow capacity of the network, 4440, however it decreases with increasing earthquake magnitude. In addition, the rates of decrease are different among the twenty earthquake sources, since the associated site-source distances and focal depths are different.
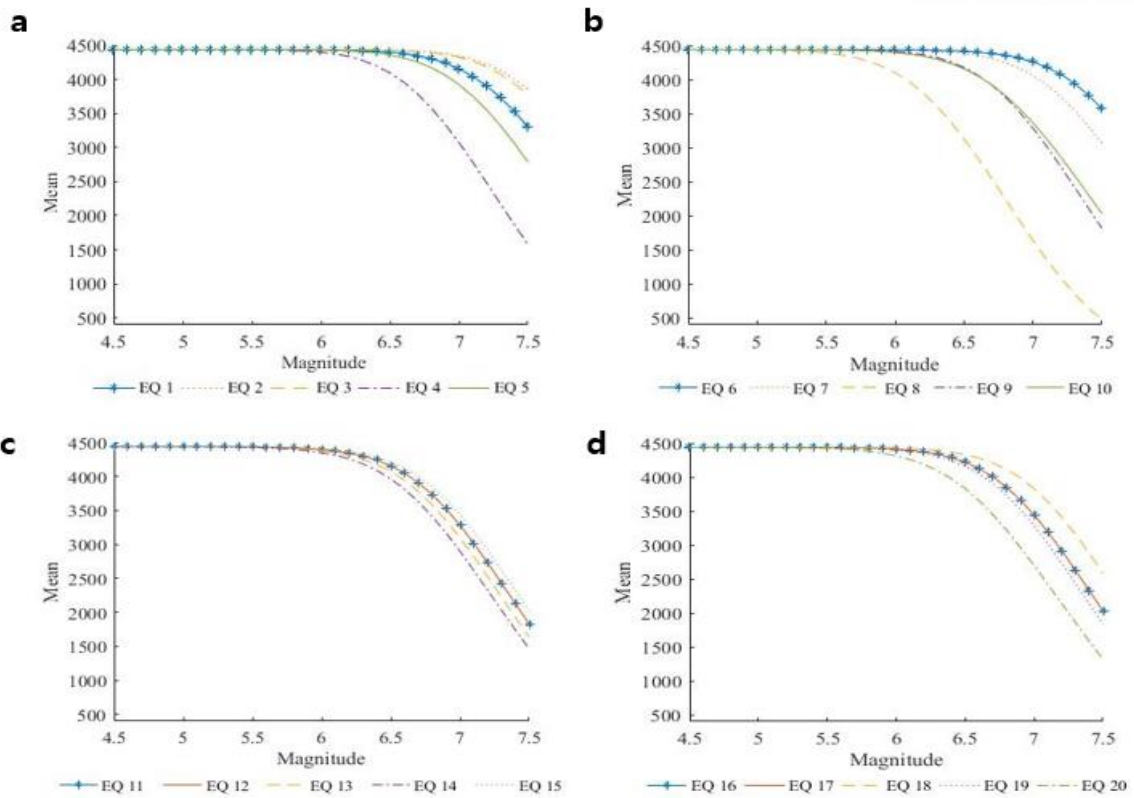
Figure 9. Mean flow capacity for all earthquake scenarios with varying earthquake magnitudes for (a) EQ 1-5 (b) EQ 6-10 (c) EQ 11-15 (d) EQ 16-20

For a better comparison, Figure 10 presents the mean flow capacities of the twenty earthquake scenarios and their average (colored blue) which depicts the mean flow capacity for uncertain earthquake location (L). The mean flow capacity for uncertain location also decreases as the earthquake magnitude increases. In addition, it is found that, among the twenty earthquake scenarios, EQ 8 is the most critical, followed by EQ 20.
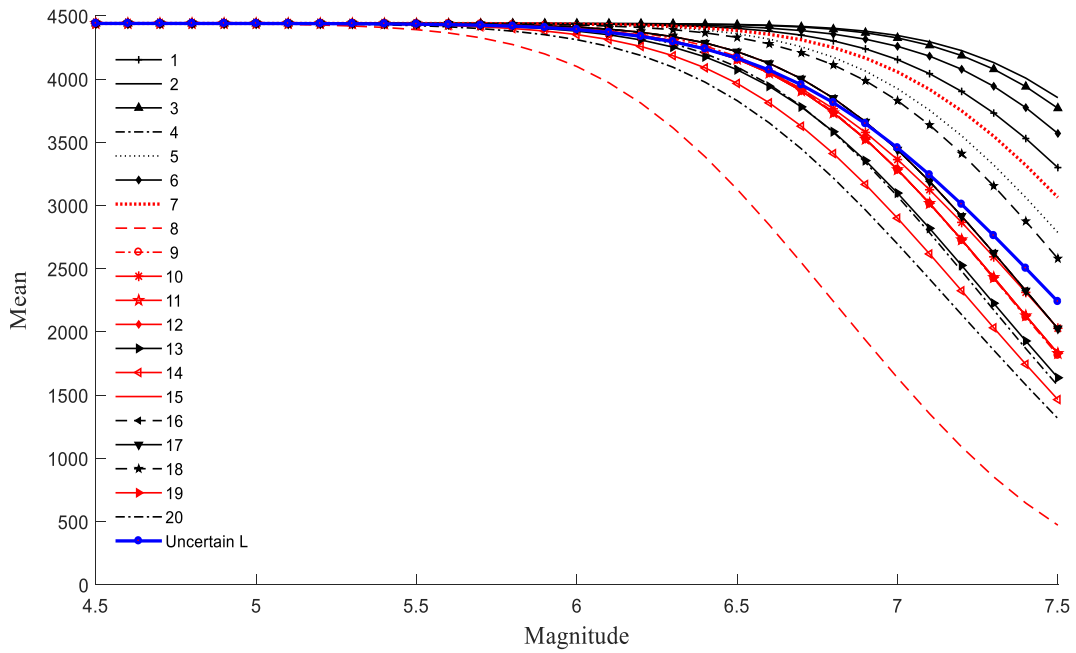
Figure 10. Collected mean flow capacities and their mean values (colored blue) with varying
magnitudes

Similarly, the standard deviation and the c.o.v. of the flow capacities of the twenty earthquake scenarios and their average (illustrated in blue) for uncertain earthquake location can be calculated and are presented in Figures 11 and 12, respectively. Generally, the standard deviation increases with increasing earthquake magnitude. In some scenarios, however, the standard deviation decreases after certain magnitude. Figure 12 shows that the c.o.v., i.e., a standardized measure of dispersion, increases with increasing magnitude. This means that a stronger seismic event gives rise to more uncertainty regarding the network flow capacity. Furthermore, the mean, standard deviation, and c.o.v. of the network flow capacity for uncertain earthquakes (i.e., uncertain magnitudes and locations of earthquake) can be calculated using Equation (19), the results of which are shown in Table 7.

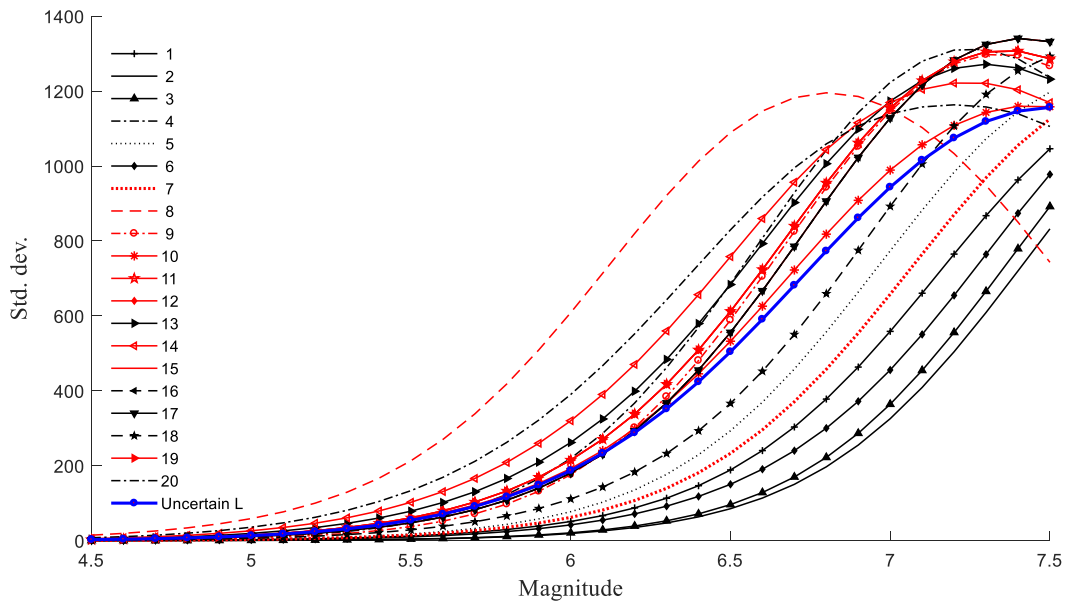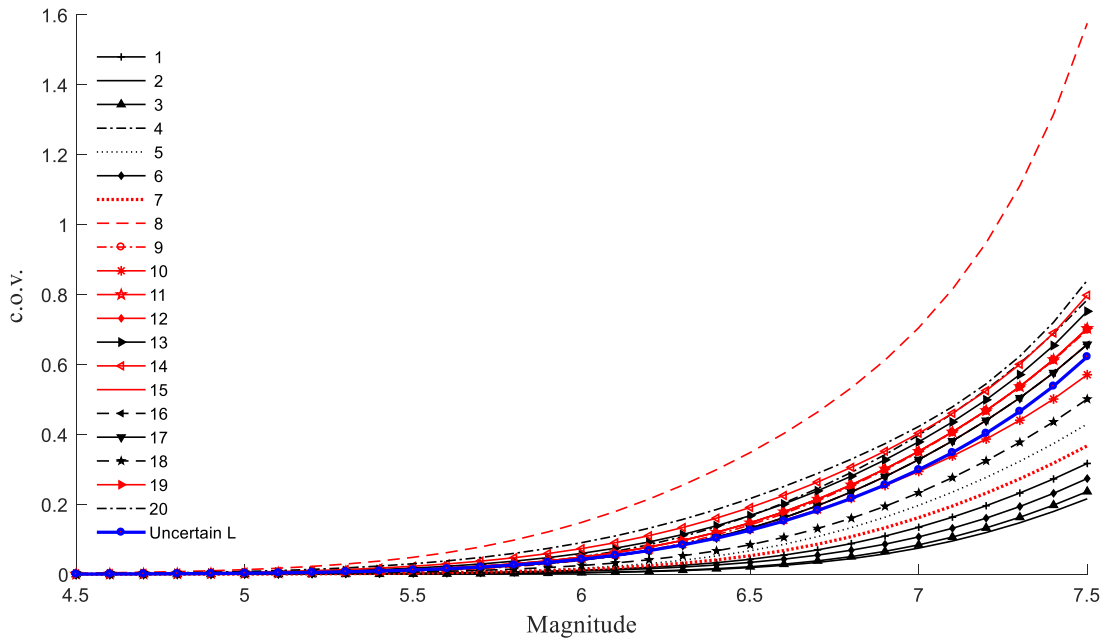Figure 11. Collected standard deviations of flow capacities and their mean values (colored blue) with varying magnitudes

Figure 12. Collected c.o.v.s of flow capacities and their mean values (colored blue) with varying magnitudes

Statistical moments	Results
Mean (μ_Q, number of vehicles per hour)	4076.077
Standard deviation (σ_Q, number of vehicles per hour)	57.263

c.o.v (δ_Q)	0.015

Table 7. Statistical moments of the network flow capacity for uncertain earthquake

It is noteworthy that sampling-based approaches would be inefficient for this sort of parametric study, because network flow analysis should be conducted for all of the individual magnitude values and locations of earthquake. On the contrary, the proposed method makes it possible to perform this parametric study efficiently.

3.3.3. Evaluation of component risk and importance

The first evaluation of component risks involves the construction of the hazard curve shown in Figures 13 and 14. The overall curve has a higher rate of exceedance with smaller-magnitude earthquakes. The hazard curve for SA shows the rates of exceedance with varying of SA levels. In this study, the rate of exceedance is defined as AEEF, for the range of earthquake magnitudes from 4.5 to 7.5. Further, the location of the earthquake is set to the location of EQ 8 (as shown in Figure 6). Subsequently, the earthquake intensities for the magnitudes are computed by the seismic attenuation model in Equation (5). In Figures 13 and 14, Bridge 2 and Bridge 4 have a higher annual rate of exceedance with respect to SA levels than the other bridges, in the case where the earthquake occurs near the location of EQ 8.

In the second evaluation of component risks, the proposed method moreover enables the computation of the reduction factor RF using Equation (20). RF contains the performance measure; hence, the results can be used to investigate the relative importance of bridges in the network. Figure 9 shows RFs of all bridges for the two severe earthquake scenarios (i.e., EQ 8 and EQ 20) and for the uncertain earthquake. Consequently, Bridges 3, 5, 6, 9, and 10 are relatively important in the region under the assumed emergency evacuation scenario from Node 30 to Node 3. For example, $RF_{6, avg.}$, $RF_{6, EQ8}$, and $RF_{6, EQ20}$ for Bridge 6 are 0.5031, 0.5322, and 0.5034, respectively. The values depict that the mean of passing vehicles per hour is reduced by 50.31%, 53.22%, and 50.34%, respectively, if Bridge 6 fails. Bridges 3, 5, 6, 9, and 10 are located at the most critical sites under the assumed emergency evacuation scenario from Node 30 to Node 3.
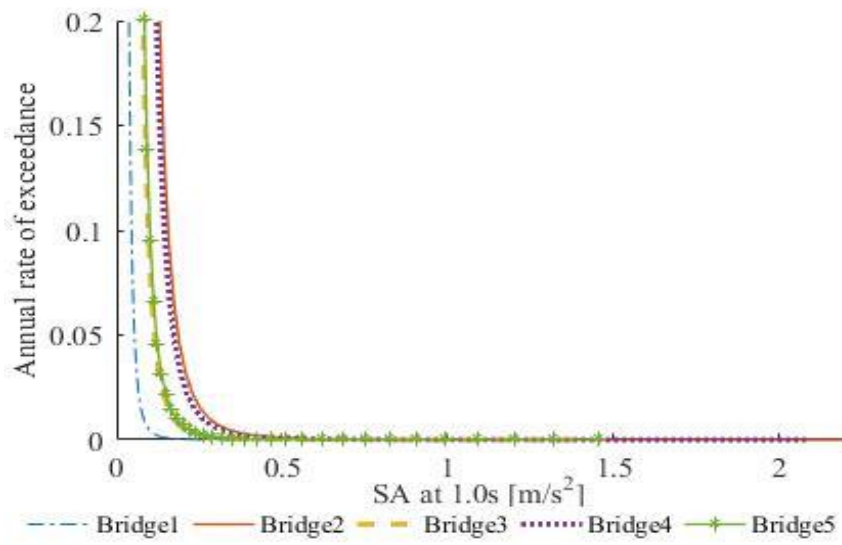
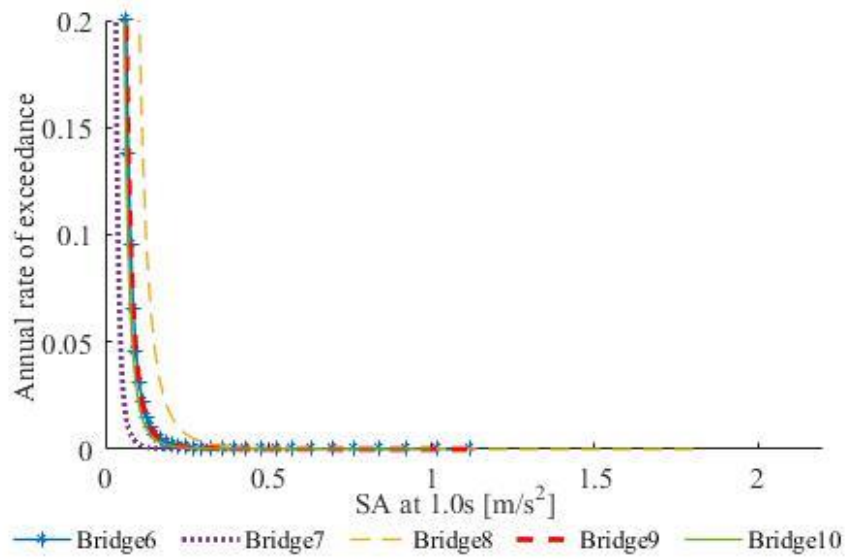Figure 13. Hazard curves for uncertain magnitudes from Bridge 1 to Bridge 5

Figure 14. Hazard curves for uncertain magnitudes from Bridge 6 to Bridge 10
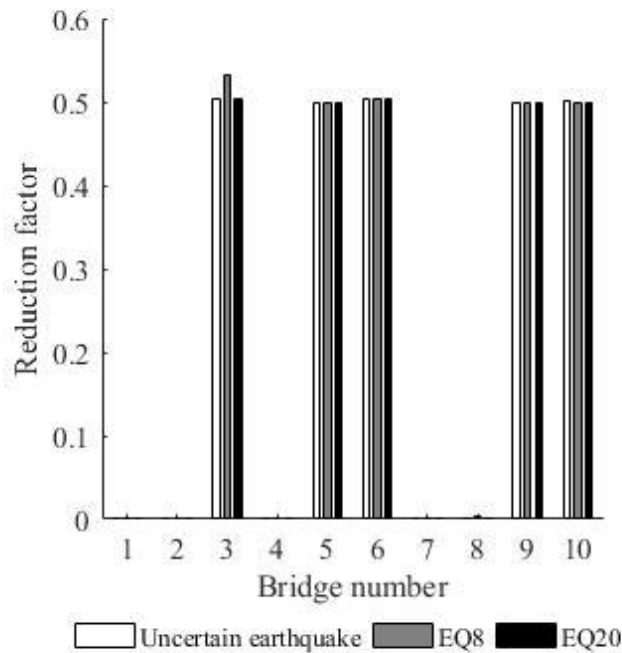
2 8

Figure 15. Reduction factors for EQ 8, EQ 20, and uncertain earthquake

4. Further Development of the Proposed Method

4.1 Matrix-based seismic risk assessment employing ANN-based surrogate model

The goal of further developing the method is to increase accuracy to estimate the performance of a bridge transportation network, as illustrated in Figure 6. To this end, the proposed method in this section introduces a new network performance, where TSTT is compared to the maximum flow capacity. Similarly, the performance of a bridge transportation network that is subjected to earthquakes becomes uncertain, and the further developed method employs the matrix-based framework of the MSR method to evaluate this uncertainty at the system level. Moreover, the ANN model is used for the approximation of TSTT in a partial earthquake scenario and corresponding TSTT values.

As stated in Section 3, all the components are statistically independent as the concept of CSRV events applies. This assumption enables the use of the more efficient matrix calculation. The calculations of the probability of a system and the three statistical parameters are obtained from Equation (16) to (19). The development of the method is two-fold: (1) the performance quantity of the system with damage states is changed from the maximum flow capacity to TSTT, and it is supplied to the quantity vector **q** as a dataset using the ANN model; and (2) a new importance measure is suggested that can account for the relative importance of components under the new performance quantity.

In this thesis, the maximum flow capacity was originally used for a bridge transportation network, but the numerical example using this measure is further developed for applications to achieve more

accurate system performance analysis using TSTT. Under the system condition of maximum flow capacity, no driver can reduce travel costs by shifting to another route, and this condition is termed user equilibrium (UE) (Bar-Gera 1999). The origin, destination, and capacities in each used path are fixed under same UE condition. For a more accurate traffic analysis, TSTT is used and calculated by EMME4 software in the further developed method and numerical example. TSTT is one of the widely used performance measures based on the system optimum (SO) condition, which exists if all drivers acted to minimize total TSTT rather than their own individual TSTT. In the SO condition, users choose routes based on the marginal travel time.

The proposed network performance uses may allow additional performing tasks, as difficulties arise in the application of a mathematical model and also require knowledge. Moreover, only temporal or partial data exist as function of input data. Therefore, technical methods are required to perform network reliability more efficiently. To identify the TSTT values instead of studying their detailed knowledge or function, the concept of a *surrogate model* is considered with the ANN model.

The surrogate model is a method to substitute black-box models either when a result of interest cannot be easily measured, or when difficulties are found in the original model. This can be constructed to provide approximate results through a function using only some input data, not requiring detailed knowledge of the dynamic parameters of the system. Of the many techniques available for surrogate modeling, the ANN has been successfully applied in many researches. Assuming that there is a total X_o damage scenarios observed, (in this example, $o = 1, …, 100000$), the ANN-based surrogate models can be expressed as following equation suggested by Pina et al. (2013)

$$Q(…) = f(\mathbf{W}, \mathbf{X_o}\left(q_{n_b,(n_d)}\right)) \tag{22}$$

where $Q(…)$ denotes the performance quantity of the system, $f(…)$ denotes the particular surrogate model employed the ANN, $\mathbf{W}$ is the parameter of the model, which depicts the set of synaptic weights w_i. This will be automatically adjusted during the training of the ANN, and X_o is the input of the surrogate model with 100000 observed system events with j^{th} damage states of the ith bridge. For example, $X_{3(2,1,…,1)}$ means that all of the components are in the first damage state except for the first component, which is in the second damage state, at the 3rd system event as one input value. Then, using the surrogate model and Equation (22), the quantities in Equation (9) are changed to

$$\mathbf{q}_s = \begin{bmatrix} Q_{(1,1,…,1)} \\ Q_{(2,1,…,1)} \\ \vdots \\ Q_{\left(d_1,d_2,…d_{n_b}\right)} \\ \vdots \\ Q_{(n_d,n_d,…n_d)} \end{bmatrix} = \begin{bmatrix} f(w_1, x_1(q_{1,(1)}, q_{2(1)}, …, q_{n_b,(1)})) \\ f\left(w_2, x_2(q_{1,(2)}, q_{2,(1)}, …, q_{n_b,(1)})\right) \\ \vdots \\ f\left(w_{d_{n_b}}, x_{d_{n_b}}(q_{1,(d_1)}, q_{2,(d_2)}, …, q_{n_b,\left(d_{n_b}\right)})\right) \\ \vdots \\ f\left(w_{n_d}, x_{n_d}(q_{1,(n_d)}, q_{2,(n_d)}, …, q_{n_b,(n_d)})\right) \end{bmatrix} \tag{23}$$

where $\mathbf{q}_s$ denotes the quantity vector estimated by ANN-surrogated model.

Second, the TSTT increment factor (TIF), a new version of IM, is proposed in this method. TIF can compute the increment of the expected TSTT by the observed event E_{obs}, e.g., the failure of a bridge, which can quantify the relative importance of component bridges. The computation of the proposed TIF is as follows:

$$\text{TIF} = \frac{\text{TSTT}_{\mu_{Q|E_i}} - \text{TSTT}_{No\ damage}}{\text{TSTT}_{full} - \text{TSTT}_{No\ damage}} \tag{24}$$

where $\mu_{Q|Eobs}$ represents the conditional mean of the TSTT given an observed event, $E_{obs.}$ $\text{TSTT}_{No\ damage}$ depicts the minimum TSTT value, given that all of the bridges experience no damage. In turn, TSTT_{full} denotes the maximum TSTT value where of the bridges experience collapse damage.

4.2 Numerical example

In this section, the target bridge transportation network which was described in Section 3 is introduced again as a developed numerical example of the matrix-based seismic risk assessment employing the ANN-based surrogate model. This is because 1) the maximum flow capacity as a measure of network performance is a simple node-to-node analysis; and 2) to improve the accuracy of the estimation of network performance, a new performance measure is used to this example, which requires more time for estimating the network performance. Therefore, TSTT is used as a measure of flow capacity compared to connectivity and the maximum flow capacity to consider the accuracy. The ANN-based surrogate model with a matrix-based framework is also introduced to reduce the computational time costs.

The same five damage states of no, slight, moderate, extensive, and complete damage are used for the input data in the ANN. The input value in ANN is the set of five damage states for each component failure scenario, and they need to be normalized to span values between 0 and 1. This is because normalization or scaling significantly helps, as it transposes the input variables into the data range of the sigmoid activation functions (i.e., sigmoid functions), which are bounded between 0 and 1. This process is useful in preparing the data, making it appropriate for the training step (Meloa et al. 2014). The five normalized damage states for each considered bridge are composed of a 100000 × 10 matrix, representing static data as 100000 samples of 10 elements, which were randomly selected from 100000 original TSTTs data. Table 8 presents five damage states of the considered bridge and the associated input value bounded between 0 and 1. To account for uncertainty in the seismic damage states of bridges, seismic fragility curves are introduced (as discussed Section 3.2.). Similarly, the seismic fragility curves of the ten bridges are determined based on the structural information given in Table 3. To identify the earthquake uncertainty in the target region, the same earthquake data and the bounded PDF of the earthquake magnitude are used again (as detailed in Figure 7). In the ANN training 70% of the 70000 samples were selected and 15% of the samples were used for the validation set. Another 15% of the rest

were used to test the performance of the network. All samples were randomly selected; also continuous sigmoid function was used as an activation function using Equation (13).

Damage states	Discrete values	Normalized input value in ANN model
No	5	1
Slight	4	0.75
Moderate	3	0.50
Extensive	2	0.25
Complete	1	0

Table 8. Damage states of bridge and associated input value in ANN model

For the application considered in this section, the ANN has been implemented in the MathWorks MATLAB® language. The structure of the neural network was set as a feed-forward with two layers between static input and target data. The neural network is mapped with seven neurons in the hidden layers and one neuron in the output layer, corresponding to the target value, which in the network performance measure depicts the TSTT. The number of neurons in hidden layer, N_h, is based on preliminary methods, as discussed Section 2.3.

Three configurations of the ANN model were constructed in order to fine the best approximation of number of hidden layers. Table 9 shows a comparison between the target TSTT and output in ANN prediction which has the maximum error, where three cases are determined by methods in Table 1. The maximum error is relatively small when seven neurons compared to three and four hidden neurons. Note that the use of more neurons could increase computation times resulting reduced efficiency of such configuration, so appropriate determination of the number of hidden neuron is necessary (Pina et al. 2013). In addition, the mean error and the standard deviation for the cases were also calculated. Figure 16 represents regression values, R, which shows model outputs compared to the target values of TSTT. As a result, method 2 (*rules of thumb*) in Table 1 shows the highest regression values $R = 0.99684$ (*all* case). This demonstrates that the ANN can represent the relationship between the input and output data with two layers and seven neurons in the hidden layer.

ANN models	Number of hidden neurons (method in Table 1)	TSTT [min]		Difference [min]
		target	ANN output	
Model 1	3 (Shibata and Ikeda, and Hunter et al.)	5015893	5105658	120997 (+2.37%)
Model 2	4 (Li et al., and Sheela and Deepa)	5102052	5195505	93453 (+1.83%)

Model 3	7 (Rules of Thumb)	5102052	5194032	91980 (+1.80%)

Table 9. Maximum error analysis in ANN predictions for three ANN models

ANN models	Statistical moments (min)	
	Mean error	the standard deviation
Model 1	6677.475	9581.826
Model 2	20.92964	6611.59
Model 3	-7.58947	2758.394

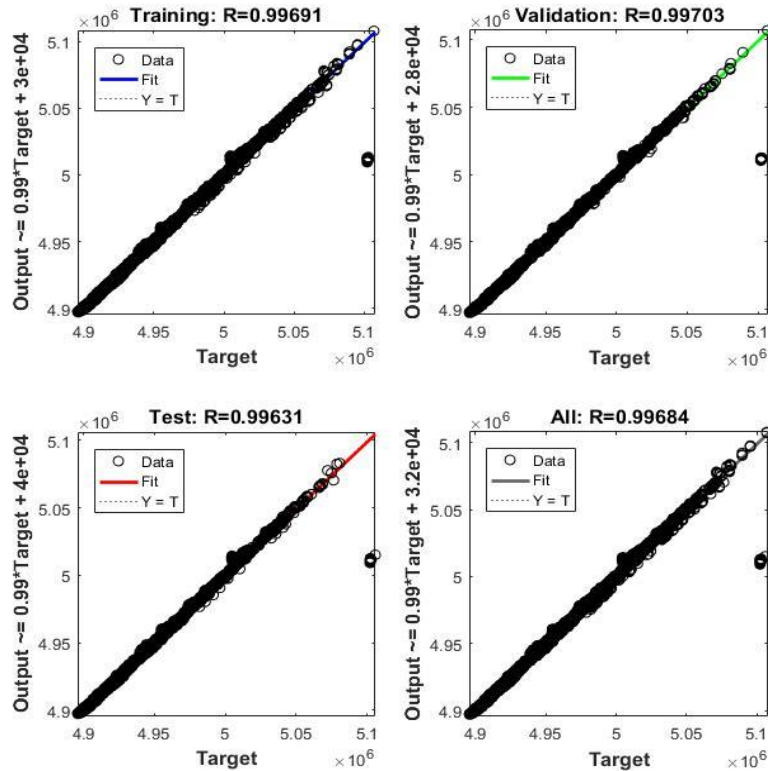Table 10. The mean error and the standard deviation for three ANN models

Figure 16. Regression values, R using *Rules of Thumb* method ($N_h = 7$)

4.3 Analysis results

In this case, the network performance considered the value of TSTT nearby 10 bridges regions for distinct changes in numerical results. In total, 399 links are selected out of 3490 links in target transportation network. The average of TSTT is constant, 4140000 (min) and the value was left out from quantity vector in Equation (23). Figure 17 shows the mean TSTTs of the twenty earthquake

scenarios and their average (colored blue), which depicts the mean TSTT for the uncertain earthquake location (*L*). Compared to Figure 10, the mean TSTT clearly increases with increasing earthquake magnitude. Because the earthquake may cause disconnections in a transportation network, leading to traffic jams and requiring more time from origin to destination. Moreover, EQ 8 is considered as the most critical one followed by EQ 13, among the twenty earthquake scenarios.

The standard deviation and the c.o.v. of TSTT in the twenty earthquake scenarios, along with their averages (colored blue) for the uncertain earthquake location are estimated and presented in Figures 17 and 18, respectively. Similarly, the standard deviation increases with increasing magnitude, however it has a tendency to decrease after a certain magnitude. Moreover, the c.o.v. increases as the earthquake magnitude increases. This trend is similar to the standard deviation depicted in Figure 12, which means the stronger earthquake events is, the more uncertainty the network performance has in this case.
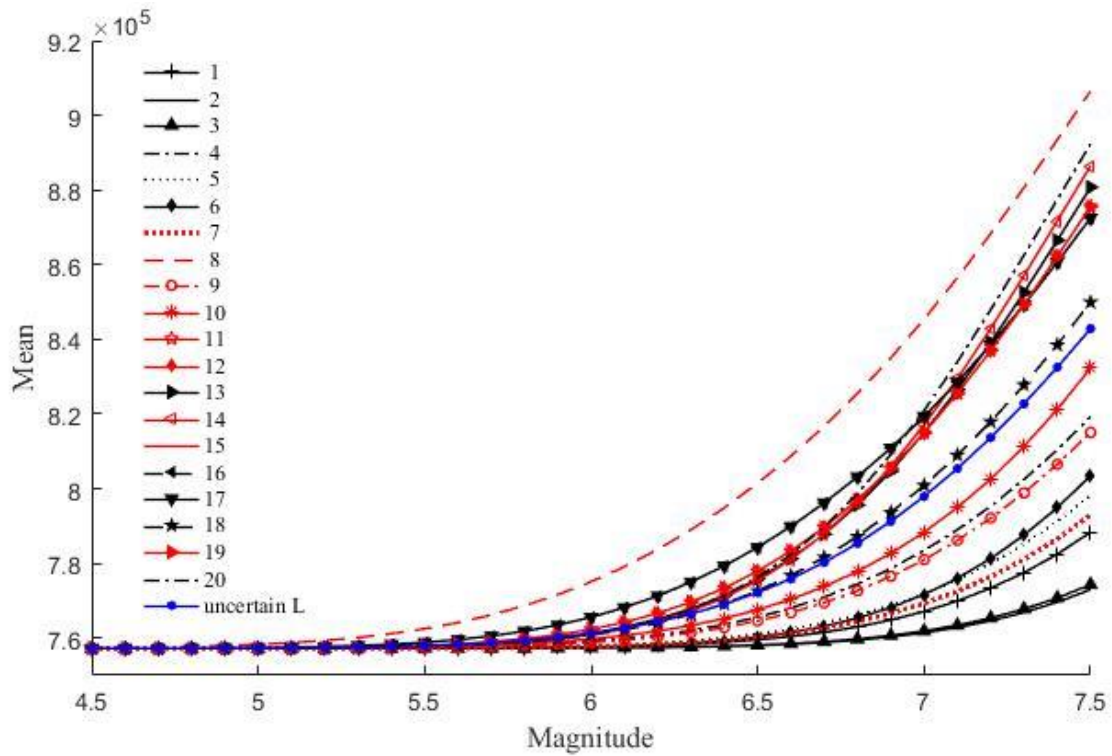

Figure 17. Collected mean (min) of TSTT and their mean values (colored blue) with varying magnitudes
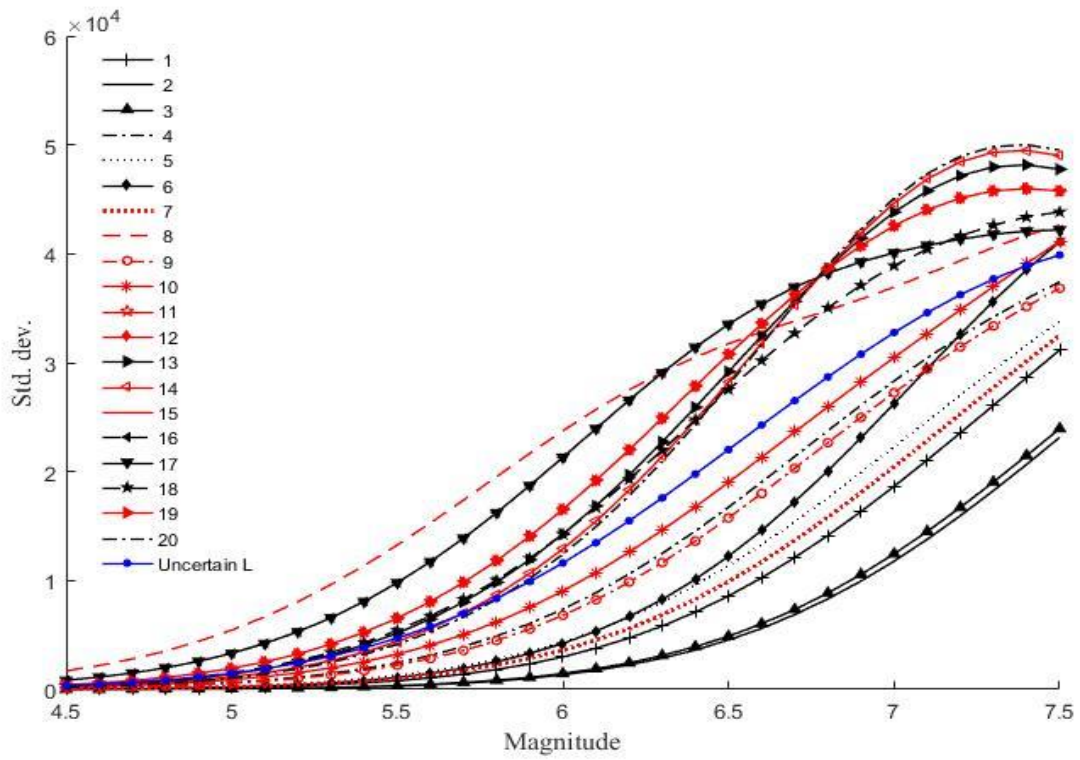
Figure 18. Collected standard deviations (min) of TSTT and their mean values (colored blue) with varying magnitudes
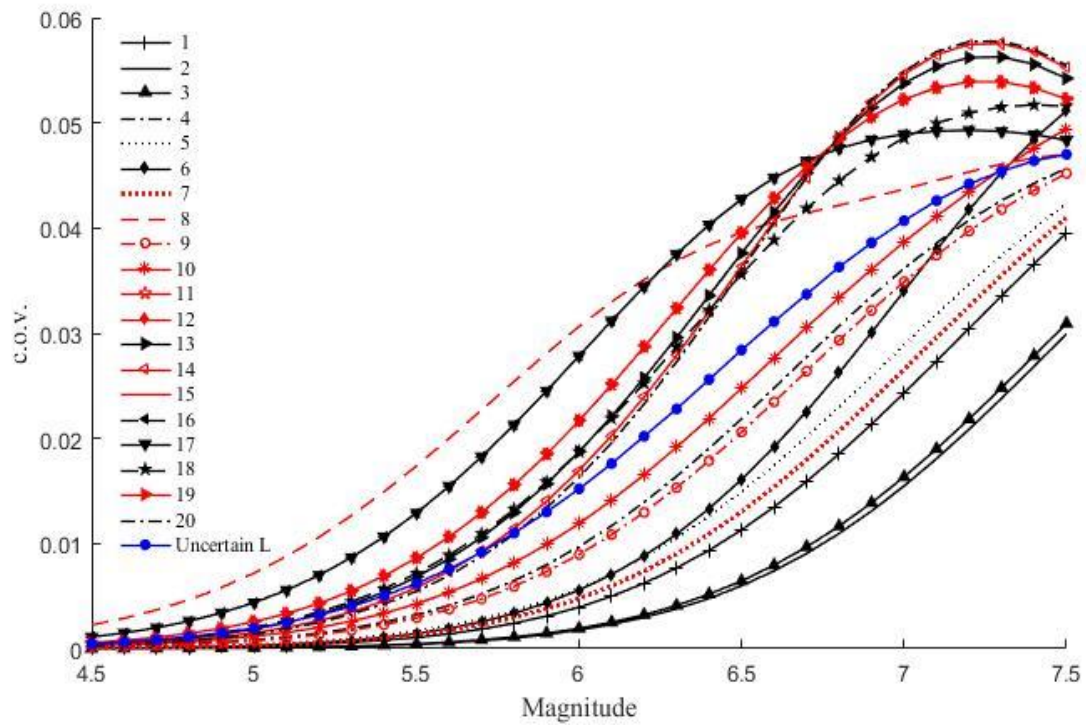

Figure 19. Collected c.o.v.s of TSTT and their mean values (colored blue) with varying magnitudes

Table 11 shows the mean, standard deviation, and c.o.v. of the network travel time for the uncertain

earthquake calculated by Equation (19). The matrix-based framework based on the total probability theorem enables to calculate these statistical moments efficiently.

Statistical moments	Results
Mean (μ_Q, min)	702114.977
Standard deviation (σ_Q, min)	3338.714
c.o.v (δ_Q)	0.00433

Table 11. Statistical moments of TSTT for uncertain earthquake

The further developed method identified the mean of TSTT for the twenty earthquake scenarios. The computation used the joint PDF of the considered earthquake epicenter when L = l, applying the total probability theorem, and the mean values were calculated with respect magnitude. In this case, EQ 8 shows critical increasing in the travel time of the network.

Figure 20. Mean of TSTT from the twenty earthquake scenarios for uncertain magnitude

Furthermore, the proposed method also computes a new importance measure, the TSTT increasing factor TIF, using Equation (24). TIF contains the performance measure; hence, the results can be used to investigate the relative importance of bridges in the network, similarly to RF, as shown in Equation (20). Figure 21 shows the TIFs of ten bridges for the two severe earthquake scenarios with increasing TSTT obtained Figure 17 (i.e., EQ 8 and EQ 13) and one earthquake scenario located near the east coast

(i.e., EQ 9). Bridges 1, 3, and 8 are found to be relatively important, which implies that these are located along the main routes for the given origin and destination of each traveler and their chosen routes in the region. The disconnection of these bridges will cause an increase in the TSTT under this condition.
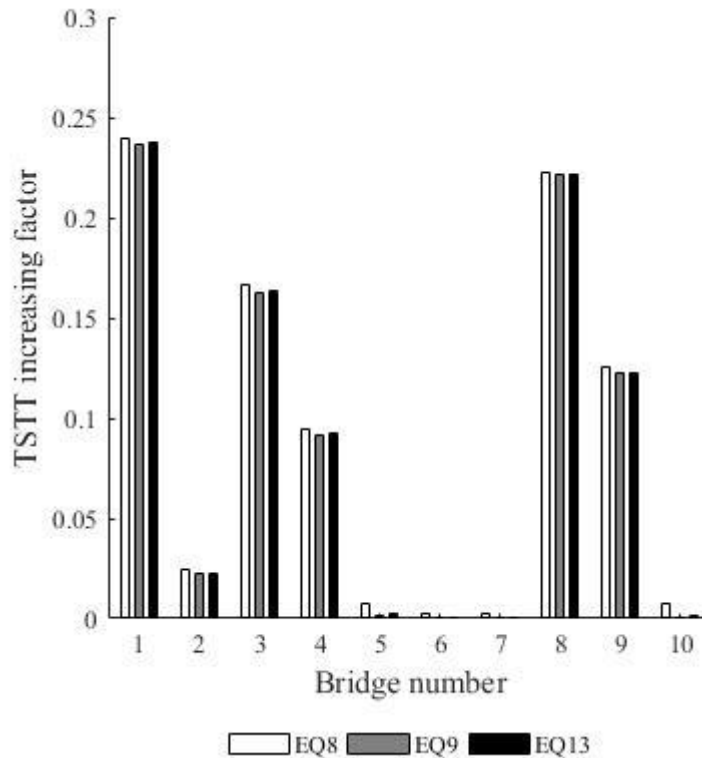

Figure 21. TSTT increasing factors for EQ 8, EQ 9, and EQ 13

However, the proposed method has the a few limitations. First, it only covers ten relatively bridges in the numerical example. It may cause slight impacts on post-hazard network performance, so it is necessary to apply to more realistic transportation network by increasing the number of bridge or choose bridge lying on the main locations. Second, seismic attenuation law and fragility parameter of bridge may be replaced by finding related researches in this field. This is because fragility of bridges is one of the input data for vulnerability and main source to construction of the probability vector. Therefore, seismic attenuation equation and fragility curve are determined based on adequate for domestic bridge and seismic hazard circumstances in Korea. Lastly, there are other characteristics of performance measure in traffic flow analysis. Currently, traffic capacity and flow measure are being conducted to address more complex and practical traffic scenarios in this field. Based on an improved and high-resolution performance measure, it may contribute to increasing accuracy for estimation of transportation network.

5. Conclusion

This thesis has proposed a new method of system-level seismic risk assessment of bridge transportation network. To test the proposed method, it has been applied to a numerical example of an actual transportation network around Pohang city, South Korea, considering twenty past earthquake records with a range of earthquake magnitude from 4.5 to 7.5, and ten bridges with five damage states. The proposed method has been developed in two steps. In the first step, seismic risk assessment for system reliability is conducted by employing PSHA with the MSR method, which consists of three small steps: 1) component failure probability calculation of bridges based on PSHA; 2) system-level performance estimation of the transportation network using the matrix-based framework of the MSR method; and 3) seismic risk assessment based on the total probability theorem. PSHA enables the seismic fragility estimation of the component bridges considering the uncertainty of earthquake locations and magnitudes, and it is systemically used to carry out the estimation of the post-earthquake performance (e.g., maximum flow capacity and TSTT) of the target bridge network by employing the matrix-based framework. In the second step, the proposed method has been further developed for more accurate assessment of network performance based on the proposed framework and a new approach, Artificial neural network (ANN) model. This model enables estimating target TSTT values corresponding to damage states of considered ten bridge with no detailed information. The further developed approach has been successfully applied to target transportation network again. In both steps, matrix-based framework enables efficient evaluations of the network performance with various magnitudes and locations of earthquake, without performing deterministic flow capacity analyses repeatedly. As a result, the statistical moments of the network, critical earthquake scenarios and bridge significances are obtained. The analysis results for numerical examples are summarized as follows:

1) As the earthquake magnitude increases, the mean flow capacity of the network decreases, while the mean of TSTT increases.

2) In both examples (maximum flow capacity and TSTT), the c.o.v. that is a standardized measure of dispersion increases with the increasing magnitudes, which means the stronger earthquake events is, the more uncertainty the network performance has.

3) Through computation of the importance measure factors for all of the bridges, it is observed that in the first step, Bridges 3, 5, 6, 9, and 10 are relatively important through RF and in the second step, Bridges 1, 3, and 8 affect increasing travel time the most through TIF in the target transportation network.

4) Among the twenty earthquakes scenarios, EQ 8 is the most critical located in the downtown of the city.

Therefore, it has been confirmed that the proposed method is effective for performing the system-

level seismic risk assessment of bridge transportation networks.

References

Applied Technology Council (ATC). (1991). Seismic Vulnerability and Impact of Disruption of Lifelines in the Conterminous United States. no. ATC-25.

Ahuja, R. K., Magnanti, T. L. & Orlin, J. B. (1993). *Network Flow: Theory, Algorithms, and Applications*. Prentice-Hall, Inc. Upper Saddle River, NJ, USA.

Bar-Gera, H. (1999). Origin-based algorithms for transportation network modeling. Technical Report Number 103. National Institute of Statistical Sciences, 19 T. W. Alexander Drive, PO Box14006, Research Triangle Park, NC 27709-4006.

Basheer, I.A., & Hajmeer, M. (2000). Artificial neural networks: fundamentals, computing, design, and application. J. Microbiol. Methods 43, 3–31.

Ben-Nakhi, A.E., & Mahmoud, M.A. (2004). Cooling load prediction for buildings using general regression neural networks. *Energy Convers*ion and Management, 45(13-14), 2127–2141.

Baker, J. W. (2008). An introduction to probabilistic seismic hazard analysis (PSHA), White Paper, Version 1.3.

Boost, *Boost graph library.* (2008). https://www.boost.org/doc/libs/1_37_0/libs/graph/doc/index.html

Cornell, C. A. (1968). Engineering seismic risk analysis. *Bulletin of the Seismological Society of America,* 58(5), 1583-1606.

Chang, L., Elnashai, A., Spencer, B., Song, J., & Ouyang, Y. (2010). Transportation systems modeling and applications in earthquake engineering. *Mid-America Earthquake Center*, 10-03.

Dueñas-Osorio L, Craig, J. I., & Goodno, B. J. (2007). Seismic response of critical interdependent networks. *Earthquake Engineering Structural Dynamics*, 26(2), 285-306.

Ellingwood, B. R., & Kinali, K. (2009). Quantifying and communication uncertainty in seismic risk assessment. *Structural Safety*, 31(2), 179-187.

Emolo, A., Sharma, N., Festa, G., Zollo, A., Convertito, V., Park. J. -H., Chi. H. -C., & Lim. In -S. (2015). Ground-Motion Prediction Equations for South Korea Peninsula. *Bulletin of the Seismological Society of America*, 105(5), 2625–2640.

Eisenberg, D. A., Park, J., & Seager, T. P. (2017). Sociotechnical network analysis for power grid resilience in South Korea. *Complexity*, 2017, 14.

FEMA. (2003). Multi-Hazard Loss Estimation Methodology Earthquake Model, HAZUS-MH MR4 Technical Manual: United States Department of Homeland Security. *Federal Emergency Management Agency*.

Ford, E. B., Moorhead, A.V., & Veras. D. A. (2011). Bayesian surrogate model for rapid time series analysis and application to exoplanet observations. *Bayesian Analysis,* 6(3), 475–500. http://dx.doi.org/10.1214/11-BA619.

Faturechi, R., & Miller-Hooks, E. (2014). A mathematical framework for quantifying and optimizaing pretective actions for civil infrastructure systems, *computer-aided civil and infrastructure engieering,* 29, 572-589.

Furtado, M. N. (2015). Measuring the Resilience of Transportation Networks Subject to Seismic Risk. Masters Theses, https://scholarworks.umass.edu/masters_theses_2/148.

Gutenberg. B., & Richter, C. F. (1994). Frequency of earthquakes in California. *Bulletin of the Seismological Society of America*, 34(4), 185-188.

Gleich, D. (2008). *MATLAB BGL*, MATLAB Central.
https://kr.mathworks.com/matlabcentral/fileexchange/10922-matlabbgl

Goda, K., & Hong, H.-P. (2008). Spatial correlation of peak ground motions and response spectra. *Bulletin of the Seismological Society of America,* 98(1), 354-365.

Goda, K. & Atkinson, G. M. (2009). Probabilistic characterization of spatially correlated response spectra for earthquakes in Japan. *Bulletin of the Seismological Society of America*, 99(5), 3003-3020.

Haykin, S. (1994). Neural Networks: a comprehensive foundation. Upper Saddle River, New Jersey: Prentice Hall.

Heaton, J. (2005). Introduction to Neural Networks with Java, Heaton Research Inc.

Hunter, D., Yu, H. , Pukish III, M. S., Kolbusz, J., & Wilamowski, B. M. (2012). Selection of proper neural network sizes and architectures: a comparative study, *Proceedings of the IEEE Transactions on Industrial Informatics*, 228 – 240.

Joyner, W. B., & Boore, D. M. (1993). Methods for regression analysis of strong-motion data. *Bulletin of the Seismological Society of America*, 83(2), 469–487.

Jensen, J. R., Qiu, F., & Ji, M. (1999). Predictive Modeling of coniferous Forest Age Using Statistical and Artificial Neural network Approaches Applied to Remote Sensing Data. *International Journal of Remote Sensing*, 20(14), 2805-2822.

Kramer, S. L. (1996). Geotechnical Earthquake Engineering. *Pearson Education*, Reprinted 2003, Delhi, India.

Kiremidjian, A., Moore, J., Fan, Y., Yazlali, O., Basoz, N., & Williams, M. (2007). Seismic Risk Assessment of Transportation Network Systems. *Journal of Earthquake Engineering*, 11(3), 371-382.

Kang, W.-H., Song, J., & Gardoni, P. (2008). Matrix-based System Reliability Method and Applications to Bridge Networks. *Reliability Engineering & System Safety*, 93(11), 1584-1593.

Kang W.-H., & Song, J. (2008). Evaluation of multinormal integral and sensitivity by matrix-based system reliability method. *in Proceedings of 10th AIAA Nondeterministic Approaches Conference*, Schaumburg, IL.

Kang, W.-H., Lee, Y.-J., Song, J., & Gencturk, B. (2012). Further development of matrix-based system reliability method and applications to structural systems. *Structure and Infrastructure Engineering*, 8(5), 441-457.

Konsuk, H. & Aktas, S. (2013). Estimating the recurrence periods of earthquakes data in Turkey. *Open Journal of Earthquake Research*, 2, 21-25.

Kang, W.-H., Lee, Y.-J., & Zhang, C. (2017). Computer-aided analysis of flow in water pipe networks after a seismic event. *Mathematical Problems in Engineering*, 2017, 14.

Korea Meteorological Administration (KMA). (2019). Available online: http://kma.go.kr/ (accessed on 28 August 2017).

Lee, W. H. K., Wu, F. T., & Jacobsen, C. (1976). A catalog of historical earthquakes in China compiled from recent Chinese publication, *Bulletin of the Seismological Society of America*, 66(6), 2003-2016.

Li, J. Y., Chow, T. W. S., & Yu, Y. L. (1995). Estimation theory and optimization algorithm for the number of hidden units in the higher-order feedforward neural network. *Proceedings of the IEEE International Conference on Neural Networks,* 1229 - 1233.

Li, J. & He, J. (2002). A recursive decomposition algorithm for network seismic reliability evaluation. *Earthquake Engineering and Structural Dynamics*, 31, 1525–1539.

Lee, K., & Yang W.-S. (2006). Historical seismicity of Korea. *Bulletin of the Seismological Society of America,* 96(3), 846–855.

Lee, S. M., Kim, T. J., & Kang, S. L. (2007). Development of fragility curves for bridges in Korea. *KSCE Journal of Civil Engineering*, 11(3), 165-174.

Lee, Y.-J., Song, J., Gardoni, P., & Lim, H.-W. (2011). Post-hazard flow capacity of bridge transportation network considering structural deterioration of bridges. *Structure and Infrastructure Engineering*, 7(7-8), 509-521.

Lee Y.-J. & Moon, D. S. (2014). A new methodology of the development of seismic fragility curves. *Smart Structures and Systems*, 14(5), 847-867.

McGuire, R. K. (2004). Seismic Hazard and Risk Analysis, Earthquake Engineering Research Institute, Berkeley

Murray-Tuite, P. M. (2006). A comparison of transportation network resilience under simulated system optimum and user equilibrium conditions. *In Proceedings of the 2006 Winter Simulation Conference,* Monterey, CA.

McGuire, R. K. (2007). Probabilistic seismic hazard analysis: Early history. *Earthquake Engineering & Structural Dynamics* (in press).

Melo, A. P., Cóstola, D., Lambertsa, R., & Hensenb, J. L. M. (2014). Development of surrogate models using artificial neural network for building shell energy labelling. *Energy Policy*, 69, 457-466.

Moon, D.-S., Lee, Y.-J. & Lee, S. (2018). Fragility analysis of space reinforced concrete frame structures with structural irregularity in plan. *Journal of Structural Engineering*, 144(8), 04018096.

Nojima, N. (1998). Prioritization in upgrading seismic performance of road network based on system reliability analysis. *Proceedings of the 3rd China-Japan-US trilateral symposium on lifeline earthquake engineering*, Kunming, China, 323-330.

Nicholson, A. J., & Dalziell, E. (2003). Risk evaluation and management: A road network reliability study. *The Network Reliability of Transport*, Emerald Group Publishing Limited, Bingley, 45-60.

Nuti, C., Rasulo, A., & Vanzi, I. (2010). Seismic safety of network structures and infrastructures. *Structure and Infrastructure Engineering,* 6(1-2), 95–110.

Nguyen, D.-D., & Lee, T.-H. (2018). Seismic fragility curves of bridge piers accounting for ground motions in Korea. *In IOP Conference Series: Earth and Environmental Science*, 143(1), 012029.

Oregon Department of Transportation. (2018). The analysis procedures manual (APM) version 2, chapter 9: transportation analysis performance mesaures.
Available online: https://www.oregon.gov/ODOT/Planning/Pages/APM.aspx

Poirier, J. P., & Taher, M. A. (1980). Historical seismicity in the near and Middle East, North Africa, and Spain from Arabic documents (VIIth–XVIIIth century). *Bulletin of the Seismological Society of America*, 70, 2185–2201.

Peeta S., & Mahmassani H. S. (1995). System optimal and user equilibrium time-dependent traffic assignment in congested networks. *Annals of Operations Research,* 60, 81 - 113.

Pina, A.C., & Zaverucha, G. (2008). Applying REC analysis to ensembles of particle filters. *Neural Computing and Applications,* 18(1), 25-35.

Poljanšek, K., Bono, F., & Gutièrrez, E. (2012). Seismic risk assessment of interdependent critical infrastructure systems: The case of European gas and electricity networks. *Earthquake Engineering and Structural Dynamics*, 41(1), 61–79.

Pina, A. C., Pina, A.A., Carl, H. A., Lima, B. S. L. P, & Jacob. B. P. (2013). ANN-based surrogate models for the analysis of morring lines and risers. *Applied Ocean Research*. 41, 76-86.

Park, S. H., Jang, K., Kim, D. K., Kho, S. Y., & Kang, S. (2015). Spatial analysis methods for identifying hazardous locations on expressways in Korea. *Scientia Iranica*, 22(4), 1594-1603.

Rahat Rahman, S. M., & Mamun, M.S. (2015). Comparison of User Equilibrium (UE) and System Optimum (SO) Traffic Assignment Methods for Auto Trips. *International Conference on Recent Innovation in Civil Engineering for Sustainable Development* (IICSD-2015).

Sung, A.H. (1998). Ranking importance of input parameters of neural networks. *Expert Systems with Application*, 15(3-4), 405-411.

Shibata K., & Ikeda, Y. (2009). Effect of number of hidden neurons on learning in large-scale layered neural networks. *In Proceedings of the ICROS-SICE International Joint Conference*, 5008-5013.

Sokolov, V., Wenzel, F., Jean, W.-Y., & Wen, K.-L. (2010). Uncertainty and spatial correlation of earthquake ground motion in Taiwan. *Terrestrial, Atmospheric and Oceanic sciences journal*, 22(6), 905-921.

Sheela, K., & Deepa, S. N. (2013). Review on Methods to Fix Number of Hidden Neurons in Neural Networks, *Mathematical Problems in Engineering,* 2013, 11.

Sánchez-Silva, M., Daniels, M., Lleras, G., & Patiño, D. (2005). A transport network reliability model for the efficient assignment of resources. *Transportation Research Part B: Methodological*, 39(1), 47-63.

Tijanana V., Tripo M., Jelena L., Adis B., & Zoran, Š. (2016). Comparative analysis of methods for determining number of hidden neurons in artificial neural network. *Central European Conference on Information and Intelligent Systems*, 219-223.

Usami, T. (1979). Study of historical earthquakes on Japan, *Bulletin of the Earthquake Research Institute, University of Tokyo,* 54, 399–439.

Widrow, B., Rumelhar, D. E., Lehr, M. A. (1994). Neural networks: applications in industry, business and science. *Communications of the ACM*, 37(3), 93-105.